

HIGH-ENERGY PHOTOPRODUCTION*

R. Diebold

Argonne National Laboratory
Argonne, Illinois, 60439

and

Stanford Linear Accelerator Center
Stanford University, Stanford, California 94305

Review Talk Presented at
High Energy Physics Conference

Boulder, Colorado

August 18-23, 1969

Much interesting experimental data on high energy photoproduction has become available in the past two years and I regrettably have had to make an arbitrary lower limit of 2 or 3 GeV. Although many new results are included, the following is more in the nature of a general review of the subject, and thus includes many things discussed at previous conferences.¹⁻³ See the review of Rollnick⁴ for a discussion of the low energy results.

*Work supported by the U. S. Atomic Energy Commission.

I. GENERAL REMARKS

Photoproduction is traditionally lumped into "Electromagnetic Interactions," primarily because the experiments are done at electron machines. These reactions tell us very little about electromagnetism, however, because the theory of quantum electrodynamics (QED) appears to work as well as the initials imply. Rather, the theoretical uncertainty in the photoproduction of hadrons lies with the word "hadrons," and in fact the theoretical interest in these reactions is mainly the same as for reactions studied at proton machines. Among the models used to interpret photoproduction at high energies are diffraction, elementary one-pion exchange with and without absorption, coherent droplet, Regge poles, Regge cuts, and dispersion relations such as continuous moment sum rules. At low energies, as for hadronic induced reactions, phase-shift analyses⁵ have been useful and, in fact, some of the early photoproduction work was instrumental in the analysis of low-lying N^* 's.

Photon beams can be compared with pion beams; both γp and πp have s -channel quantum numbers of an N^* : $S = 0$, $B = 1$. The γ rays, of course, have a much smaller cross section than π 's; e. g., at 10 GeV

$$\frac{\sigma_{\text{tot}}(\gamma p)}{\sigma_{\text{tot}}(\pi p)} \approx \frac{120 \mu\text{b}}{26 \text{ mb}} = \frac{1}{220} = \alpha/1.6 \quad .$$

Compared with spin parity 0^- for pions, photons are somewhat more complicated, having spin parity 1^- but, because they have zero mass, photons can have helicity = ± 1 only. It is generally assumed that the photon has both isoscalar and isovector components; as we shall see later, charged pion photoproduction data demonstrate the simultaneous presence of both components very dramatically. Some evidence substantiates the theoretical prejudice that

the photon has no isotensor component; an analysis of pion photoproduction near the first resonance has shown that the isotensor-photon amplitude is at most a few percent of the isovector-photon amplitude.⁶ Since the photon has negative charge conjugation C, the G parity of the two isotopic components is given by

$$\begin{aligned}
 G &= C(-1)^I \\
 &= -1 \text{ for isoscalar } (I = 0), \\
 &= +1 \text{ for isovector } (I = 1).
 \end{aligned}$$

Both the isospin mixing and nonzero spin lead to a richness in photoproduction reactions not possible in pion reactions. Unfortunately, with the present state of strong-interaction theory cynics may claim that the word "complexity" better describes the situation than "richness."

Photons are also more complicated experimentally: they are neutral and can neither be momentum-analyzed nor focused like a π^\pm beam. Although methods exist for obtaining monochromatic photon beams, the simplest beam is simply bremsstrahlung giving a $1/k$ spectrum. Further, the small hadronic cross sections often get lost in the electromagnetic background.

The Vector Dominance Model (VDM)^{7,8} directly relates photoproduction to hadronic processes. This model suggests that a γ -ray beam may be thought of as a coherent beam of vector mesons, the known ones being ρ (isovector photon), ω and ϕ (isoscalar photon). The beam is coherent in the sense that the amplitude for a ρ -like photon can interfere with that for an ω -like photon, etc. Assuming the photon to belong to an SU(3) octet and taking the $\omega\phi$ mixing angle from SU(6) (substantiated by the mass formula), the γV couplings are predicted to be in the ratio

$$g_{\gamma\rho}^2 / g_{\gamma\omega}^2 / g_{\gamma\phi}^2 = 9/1/2$$

in substantial agreement with the Orsay⁹ storage-ring results $9/(1.28 \pm 0.26)/(1.72 \pm 0.27)$. Since the ρ coupling is considerably larger than the ω or ϕ couplings, a photon beam can be crudely thought of as a beam of ρ^0 mesons having zero mass and helicity of ± 1 . Interference effects often turn out to be important, however, in which case the most reliable predictions are those for which the isovector-isoscalar interference terms drop out. Since the ω and ϕ frequently have smaller cross sections, the isoscalar terms in the cross section are usually only a few percent of the ρ term and the comparisons discussed below are mainly tests of ρ dominance. In general, ρ dominance works to within about a factor of two. Closer agreement may be possible with further theoretical and/or experimental refinements but, as we shall see, the situation is rather murky.

II. TOTAL PHOTON CROSS SECTIONS

The total γp hadronic cross section has been measured by several methods, with results shown in Fig. 1. The inelastic electron scattering group at SLAC has large quantities of data¹⁰ extending from threshold up to an equivalent photon energy of 15 GeV. They obtain an estimate of the total photon cross section by extrapolating the inelastic electron scattering data to $t = 0$. At low energies their results are in good agreement with the counter experiments indicated by the dashed curve. At higher energies their results appear to be slightly higher than the directly measured cross sections. Although their extrapolation method is rather straightforward at low virtual photon energies, it does become more and more difficult with increasing energy.

The other measurements of the total cross section have all been made with special photon beams. A tagged photon beam has been used at DESY for experiments with both the bubble chamber¹⁴ and with counters.¹² At SLAC the e^+e^- annihilation beam was used for

the 40-inch bubble chamber measurement,¹⁵ the backscattered laser beam for the 82-inch bubble chamber measurements,¹³ and a tagged photon beam for the counter experiment.¹⁶

From 5 to 15 GeV the γp total cross section¹⁶ falls from 125 to 113 μb , a 10% drop similar to that seen for πp . This similarity is quite natural from the vector dominance point of view but is not easily explained by Regge theory. Since the total cross section is related through the optical theorem to the forward Compton scattering cross section, slowly-varying high-energy cross sections imply a diffraction mechanism, i. e., Pomeron exchange, for Compton scattering. However, at $t = 0$ we have

$$\alpha_P = 1$$

and the Pomeron should not couple to two photons since two units of helicity are exchanged in the t channel giving a nonsense zero for the spin-1 Pomeron.¹⁷ The Regge theorists must then either introduce a fixed pole at $J = 0$ or resort to a singular residue to cancel the vanishing coupling.¹⁸ The total cross section measurements are also useful for evaluating certain dispersion relations for Compton scattering.¹⁹ In particular, the finite energy sum rule integral may be unable to cancel the low-energy Compton term, leaving a real part to the forward Compton scattering amplitude which behaves like a fixed pole with $J = 0$.

The DESY counter¹² group quotes a fit to their data from 1.5 to 6.3 GeV,

$$\sigma_{\gamma p} = (110 \pm 5) + (72 \pm 13)/k \text{ } \mu\text{barns}$$

for k , the laboratory photon energy in GeV. After making Glauber corrections (3% at 6 GeV) they quote

$$\sigma_{\gamma n} = (114 \pm 7) + (31 \pm 18)/k \text{ } \mu\text{barns}$$

implying $\sigma_{\gamma n} = \sigma_{\gamma p}$ asymptotically, but that $\sigma_{\gamma n}$ may be less than $\sigma_{\gamma p}$ by a few percent in the region measured (this result, of course, depends on the accuracy

of the Glauber correction). The above parameterizations are consistent with the Santa Barbara-SLAC¹⁶ data which show $\sigma_{\gamma d}/\sigma_{\gamma p} = 1.89$, but with no significant energy dependence.

III. VECTOR MESONS

1. Photoproduction of Vector Mesons From Hydrogen

Since vector mesons have spin, parity, and charge conjugation identical to the photon, photoproduction of ρ^0 , ω , or ϕ can be accomplished by the exchange of a Pomeron. Hence, one would expect that at high energies both the s and t dependence of these processes would look much like that for π or K elastic scattering. As shown in Fig. 2, the ρ^0 cross section is rather constant above 2 GeV, a typical value being $16 \mu\text{b}$ at 6 GeV. There does appear to be some fall-off as the energy increases, however, and we shall come back to this later. The ω photoproduction has a rather steep fall-off between 2 and 5 GeV which has been explained with absorbed OPE plus a residual cross section from diffraction scattering.²⁶ Above 2 GeV the ω data seem to fall rather well along the line $1.5 + \frac{25}{k^2} \mu\text{b}$ (for k in GeV) with the constant term representative of diffraction scattering and the $1/k^2$ dependence typical of high energy photoproduction involving one-pion exchange. The importance of OPE in ω production relative to ρ^0 production is consistent with the SU(3) predictions for the relative coupling constants. The data on ϕ photoproduction are much more sparse but seem to be consistent with a rather flat cross section, perhaps with a maximum between $1/2$ and $1 \mu\text{b}$ in the 5 to 10 GeV region.

Figure 3 shows the differential cross sections for ρ photoproduction as obtained by Anderson et al., with the 1.6 GeV/c spectrometer.²⁵ They observed only the recoiling proton and fit the mass distribution with steps corresponding to

the photoproduction of neutral particles. A 10% correction to the ρ step was made for contamination from ω production. Because of the method used, they were unable to go to values of t less than about 0.2 GeV^2 . They obtained good agreement with the DESY²⁰ and Cornell²⁷ data near 6 GeV. The lines drawn in the figure show the predictions of VDM combined with a broken-SU(3) quark model,²⁸ the only free parameter being the over-all normalization constant C_ρ . The good agreement with the data indicates that the ρ^0 cross section has the same s and t dependence as that for πp elastic scattering. Note that the energy dependence is non-negligible, the forward cross section going from about $135 \mu\text{b}/\text{GeV}^2$ at 6.5 GeV down to $102 \mu\text{b}/\text{GeV}^2$ at 17 GeV. The best value obtained for the normalization constant corresponds to $\gamma_\rho^2/4\pi = 0.61$.

The $\pi\pi$ mass distribution obtained by the SLAC streamer chamber group²⁴ is shown in Fig. 4a. The distribution is not symmetric about the ρ mass but has a long low-mass tail, typical of photoproduced ρ 's. Two formulations have been used to give this asymmetry. The first by Ross and Stodolsky²⁹ involves multiplying the Breit-Wigner by a factor $(M_\rho/M_{\pi\pi})^4$ to take into account the variation of the ρ propagator squared in the vector dominance model. A similar ratio, $(M_\rho/M_{\pi\pi})^2$, has been recently obtained in a detailed dynamical model.³⁰ The second is the so-called Söding interference model³¹ and is the model used to fit the distribution shown in Fig. 4a. It assumes that in addition to ρ^0 production there is a nonresonant two-pion background coming from the second diagram shown in the figure, a diagram much like that used by Deck³² to discuss A_1 production by pions. By choosing the sign properly, the interference term between these two diagrams can shift the ρ peak in the appropriate direction.

The momentum transfer dependence of the two-pion system depends very much upon the effective $\pi\pi$ mass as shown in Fig. 4b. Parameterizing the cross section as

$$\frac{d\sigma}{dt} = Ae^{Bt},$$

the value of B drops from about $10/\text{GeV}^2$ to $5/\text{GeV}^2$ over the mass range 0.5 to 1 GeV. Much of the dependence can be accounted for by the Söding interference model as shown in the figure. Incidentally, this rapid variation means that care must be taken in choosing the same mass range when comparing the slopes found by different experiments.

The ρ^0 polarization can be used to study the production mechanism. In the diffraction model the ρ is expected to have the same polarization as the incident γ ray, namely, $m = \pm 1$. This would give a $\sin^2\theta$ decay distribution in the Jackson frame. At very small momentum transfers this seems to be the case, but averaging over the diffraction peak gives isotropy in the Jackson system. The helicity frame does have $\sin^2\theta$, however, implying that it is helicity which tends to be conserved rather than spin component along the beam direction.²⁰ In the forward direction the Jackson and helicity frames are identical and one might have thought that at the small production angles typical of diffraction the difference would be negligible. But kinematics show that for a typical momentum transfer, 0.1 GeV^2 , the angle between the two frames is already 45° .

Experiments with linearly polarized photons can also give information on the production mechanism. A wire-spark-chamber group at DESY has studied ρ^0 production, using coherent bremsstrahlung from a diamond target.³³ They look only at decay pions perpendicular to the production plane, i. e., at events with ρ polarization along the production normal. They study the asymmetry

$$\Sigma = \frac{\sigma_{\parallel} - \sigma_{\perp}}{\sigma_{\parallel} + \sigma_{\perp}},$$

where σ_{\parallel} (σ_{\perp}) refers to photon polarization parallel (perpendicular) to the ρ polarization. Diffraction production contributes only to σ_{\parallel} and one-pion exchange only to σ_{\perp} . The experimental results shown in Fig. 5 are consistent with production proceeding entirely via diffraction. The Cornell spectrometer group has also measured ρ^0 production from a coherent bremsstrahlung beam. At 3.5 GeV they get preliminary results of $\sigma_{\perp}/\sigma_{\parallel} = 0.11 \pm 0.04$ and 0.05 ± 0.03 for hydrogen and carbon, respectively.³⁴

The SLAC backscattered laser beam has been recently used to produce ρ^0 and ω in the 82-inch bubble chamber with $\sim 95\%$ linearly polarized photons. Unlike the spark chamber experiments, the full decay angular distributions can be observed. At both 2.8 and 4.7 GeV the ρ^0 results show that contributions from unnatural parity exchanges are small, $\lesssim 10\%$, with no significant variation with momentum transfer.³⁵ Unnatural parity exchange represents $(52 \pm 12)\%$ and $(42 \pm 17)\%$ of the ω cross section at 2.8 and 4.7 GeV, respectively, in agreement with the expectation that both OPE and diffraction are important at these energies.³⁶

Figure 6 shows the momentum transfer dependence for ϕ photoproduction at energies from 6 to 18 GeV. The data of Anderson *et al.*,²⁵ appear to be in good agreement with previous data^{2,37} at 6 GeV. Although the momentum transfer dependence of the cross sections is in agreement with that predicted by the quark model, there is more energy dependence in the photoproduction cross section than in the corresponding strong interactions.

2. Photoproduction of Vector Mesons From Deuterium

The photoproduction of ρ^0 's has been measured at Cornell from both deuterium and hydrogen.²⁷ At large values of t , the slope of the deuterium cross section is the same as that for hydrogen. At small t values, however, the deuterium cross section shows a marked peak, corresponding to coherent production from the nucleus. The deuterium-to-hydrogen ratio extrapolated to $t = 0$ is found to be 3.26 ± 0.10 , averaged over photon energies from 4 to 9 GeV. If only diffraction amplitudes were present, a value of 3.64 (calculated from Glauber theory) would be expected. The authors interpret this discrepancy as possible evidence for spin or isospin exchange in the t channel. If, for example, isospin exchange is assumed, the discrepancy corresponds to

$$\left| \frac{a_1}{a_1 + a_0} \right| = 0.14 \pm 0.06.$$

where a_0 and a_1 are the amplitudes for $I = 0$ and 1 , in the t channel. While this discrepancy is consistent with being independent of energy, there may be a small decrease of the discrepancy with increasing energy.

Very recent Cornell results³⁸ give the deuterium-to-hydrogen ratio at $-t = 0.004 \text{ GeV}^2$ for ϕ production: 3.05 ± 0.20 at 8.25 GeV , the same to within errors as for ρ^0 production.

3. Vector Dominance Applied to Vector Meson Photoproduction

Many vector dominance games can be played with the vector-meson photoproduction data. In the following examples we shall use the γV coupling constants obtained from the Orsay storage-ring work.⁹ It should be emphasized that other determinations of these constants have given somewhat different answers; the error bars listed in Table 1 do not reflect this, however, and one must beware of taking the answers too seriously. In the vector dominance model, the photoproduction amplitude A_γ is given by

$$A_\gamma = \sum_V g_{\gamma V} A_V$$

where A_V is the amplitude for the process initiated by the vector meson V . In this model the elastic vector-meson scattering can be obtained from the diffractive photoproduction cross sections as

$$\sigma(V^0 p \rightarrow V^0 p) = g_{\gamma V}^{-2} \sigma(\gamma p \rightarrow V^0 p) \quad .$$

The constant $g_{\gamma V}$ is related to the often-used γ_V by

$$g_{\gamma V}^2 = \frac{\pi\alpha}{\gamma_V^2}$$

Values are listed in Table 1; ρp elastic scattering should be about 300 times the photoproduction cross section, for example.

The total $V^0 p$ cross section can be calculated from the optical theorem

$$\left(\frac{d\sigma}{dt}\right)_{0^0} = (1 + \alpha^2) \pi \left(\frac{\sigma_{\text{tot}}}{4\pi\hbar}\right)^2.$$

Neglecting the real part α of the forward scattering amplitude and using practical units, mbarns and GeV,

$$\begin{aligned} \sigma_{\text{tot}}(Vp) &= 4.42 \left[\frac{d\sigma}{dt}(V^0 p \rightarrow V^0 p) \right]_{0^0}^{1/2} \\ &= 4.42 \left[g_{\gamma V}^{-2} \frac{d\sigma}{dt}(\gamma p \rightarrow V^0 p) \right]_{\text{diffractive}}^{1/2} \Big|_{t=0}. \end{aligned}$$

Both the ρ and ω cross sections come out very close to that observed for pions, about 26 mb. The ϕ total cross section, however, comes out low, 9.4 ± 2.4 mb, even slightly lower than had been estimated from the quark model,³⁹ 11 mb.

The optical theorem can also be used to relate $\sigma_{\text{tot}}(\gamma p)$ to forward Compton scattering which in turn can be related by VDM to the forward diffractive photo-production cross sections,^{40,41}

$$\sigma_{\text{tot}}(\gamma p) = 4.42 \sum_V g_{\gamma V} \left[\frac{d\sigma}{dt}(\gamma p \rightarrow V^0 p)_{t=0} \right]^{1/2},$$

where again the units are mb and GeV. Unlike many of the vector dominance relations, this one has no interference terms. The ρ , ω and ϕ contributions are shown in Table 1; as usual, the dominant contribution comes from the ρ meson (the ω and ϕ together contribution less than 20%). If one assumes that each of these contributions have the same phase, the predicted cross section is $109 \pm 8 \mu\text{b}$, in good agreement with the directly measured value¹⁶ $118 \pm 3 \mu\text{b}$ at 10 GeV.

SU(6), however, gives the opposite sign for the ϕ coupling constant, resulting in $97 \pm 8 \mu\text{b}$. A value of $\gamma_\rho^2/4\pi = 0.34$ would change the $97 \mu\text{b}$ to $118 \mu\text{b}$.

4. High-Mass Searches

One might hope to see higher-mass vector mesons lying on the ρ daughter trajectories and several experiments have tried to find them. Shapiro⁴² has used the Veneziano theory to predict a ρ' meson at 1300 MeV and ρ'' at 1670 MeV with partial decay widths into $\pi^+\pi^-$ of 112 and 14 MeV, respectively. Further, one might hope to diffractively produce the ρ Regge recurrence with spin parity 3^- ; for a trajectory slope of 1 GeV^{-2} the recurrence will have a mass of 1600 MeV. Indeed a $\pi\pi$ resonance has been seen in various bubble chamber experiments and a tentative assignment of 3^- given. Note that these heavy mesons may well decay into four pions, as well as two pions, and some of the decay modes, for example, $\rho^+\rho^-$ would be very difficult to observe directly.

The Cornell spectrometer group has studied $\pi^+\pi^-$ photoproduction from carbon in the high-mass ranges.⁴³ The geometry of their spectrometer is fixed so that the effective mass of the two-pion system is proportional to the photon energy, and they observe only production close to 0 degrees and decays close to 90 degrees in the $\pi\pi$ center-of-mass. As shown in Fig. 7, the tail from the ρ Breit-Wigner can account for most or all of their high-mass events but they do see a suggestion of a bump at 1670, the predicted mass of the ρ'' . Assuming spin parity 1^- (so as to give a $\sin^2\theta$ decay distribution) and a full width of 50 MeV (as indicated by the width of their bump) and a partial decay width into 2 π 's of 14 MeV (as predicted by the Veneziano theory) and that all events within this mass region are ρ'' events, and that the elastic scattering of ρ'' from carbon is the same as for the ρ , they find that the coupling of the ρ'' to the photon is 190 times smaller than that for the ρ . This should be considered as a limit since many or all of the events in this region can be ascribed to the ρ tail.

The most significant Cornell bump is at a mass of 1420 MeV and is roughly 60 MeV wide. They see 142 events in the region from 1390 to 1440 MeV, compared

with 98 background events calculated from the event rates in neighboring bins. Although this would be a three-standard-deviation effect, they point out that the probability to get such a bump somewhere in their mass distribution is 10 or 20% and thus independent confirmation must be obtained. Assuming that this bump decays only into 2π 's with a width of about 100 MeV, they set an upper limit on the coupling to the photon of 240 times less than that for the ρ itself.

A spectrometer group⁴⁴ at CEA has also looked for high-mass $\pi^+\pi^-$ bumps with a method similar to that of the Cornell group. They found no significant enhancements.

Davier et al.,⁴⁵ have looked at the process

$$\gamma p \rightarrow \pi^+ \pi^- \pi^+ \pi^- p,$$

using the SLAC streamer chamber with a hydrogen target. They found an enhancement near 1500 MeV in the four-pion mass spectrum. Excluding Δ^{++} events and taking only events having three-pion mass in the A_1 region, they find a bump centered at 1.55 ± 0.04 GeV with a width of 0.26 ± 0.11 GeV as shown in Fig. 8b. They have also combined their $\pi^+\pi^-$ data with DESY²⁰ and SLAC²² bubble chamber data; see Fig. 8a. The compiled data show a bump similar to that found for πA_1 although the statistics are not as good. Assuming that they are, indeed, seeing a new resonance, they find for the branching ratios,

$$\pi^+\pi^-/\pi A_1 \approx 3/2,$$

and a cross section (averaged over photon energies from 4.5 to 18 GeV),

$$\pi^+\pi^- + \pi A_1 = 1.1 \pm 0.5 \mu\text{b}.$$

They hope to improve their statistics in the near future.

Note that both the mass and width of the Cornell bump differ considerably from that found by the streamer chamber group. Further, the Cornell limit seems

considerably below the streamer chamber cross section (about 4% of the ρ cross section), and the null results of the Cornell group would seem to contradict the $\pi^+\pi^-$ results shown in Fig. 8a. One should remember, however, that the Cornell group used carbon rather than hydrogen as a target and that their angular acceptances were quite limited. If the πA_1 bump does not decay into $\pi^+\pi^-$, a Deck-type mechanism (shown schematically in Fig. 8b) might explain the effect.

The SLAC 1.6 GeV spectrometer group has also searched for photoproduction of neutral higher-mass resonances.²⁵ They look only at the recoiling proton; this missing-mass spectrometer technique gives results independent of any worries about decay modes. Near 14 GeV they have 15 missing-mass distributions in the range $-t = 0.3$ to 0.7 GeV^2 . Each of these distributions indicates the presence of an enhancement near $1240 \pm 20 \text{ MeV}$ with a width of about 100 MeV. At higher energies their mass scale was compressed and at lower energies the backgrounds increased, making the signals less clear. The cross section for this enhancement is roughly the same as observed for the ϕ meson, i. e., a few percent of the ρ^0 cross section. They found no evidence for a peak between 1.3 and 2 GeV. With 90% confidence their results show that no particle in this mass range with width $\lesssim 200 \text{ MeV}$ is produced with a cross section $> 5\%$ of the ρ^0 cross section. For 100-MeV widths this upper limit shrinks to 3% of the ρ^0 cross section.

A group from Northeastern University studied the mass spectrum of μ pairs produced at CEA from carbon.⁴⁶ In the range 900 to 1800 MeV they found only the ϕ meson. Under various assumptions they find the upper limit for the coupling of heavy mesons to γ rays to be a few percent of the ρ coupling. A Cornell group⁴⁷ has also studied the $\mu^+\mu^-$ mass spectrum and found only the ϕ .

With the exception of the SLAC missing-mass search, all of the above limits depend upon assumptions concerning the decay modes of the heavy mesons. The 1240-MeV bump seen by the SLAC missing-mass spectrometer may be one of the

known particles such as the B or f^0 ; perhaps one of the bubble chamber exposures in a monochromatic beam will identify the bump. The statistically most compelling object, the broad πA_1 bump at 1550, may not be a vector meson; further study is clearly needed. So far, no heavy vector meson has been found with coupling to the photon similar to the $\gamma\rho$ coupling.

IV. PHOTOPRODUCTION OF PSEUDOSCALAR MESONS

Total cross sections for several pion channels are shown in Fig. 9. At low energies the cross sections were obtained by integrating over all production angles; at high energies the integrations were made over the small- t region and a few-percent correction made for the large- t and backward regions. For each reaction the quantity $k^2\sigma$ [k = laboratory photon energy = $(s-M_p^2)/2M_p$] approaches a constant at high energies. This implies effective Regge spin parameters, $\alpha(t)$, near zero for the small- t region. If anything, the cross sections may be falling slightly faster than $1/k^2$, but not as fast as $k^{-2.2}$; thus, $-0.1 < \alpha_{\text{eff}} \leq 0$.

The asymptotic $1/k^2$ value is approached at a fairly low energy (1 to 3 GeV, depending on the process) and even in the resonance region the deviations from the asymptotic form are relatively small, a phenomenon observed in other processes⁵⁷ and suggested by such theoretical ideas as duality and finite energy sum rules. The $1/k^2$ behavior for these photoproduction processes can be compared with the $1/p \sim 1.6$ dependence found for many similar processes initiated by hadrons.⁵⁸

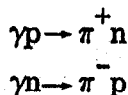
At high energies the cross sections for each channel become very small, making it difficult to get meaningful statistics with devices such as bubble chambers. For example, single π^+ production is only 0.6% of the total γp cross section at 5 GeV; at 16 GeV it drops to 0.06%, one π^+ event every 1600 interactions.

A comparison of the angular distributions for several reactions is shown in Fig. 10. Although somewhat limited, the data beyond $|t| = 1 \text{ GeV}^2$ all go roughly

as e^{3t} with cross sections within a factor of about two of the mean values. At smaller momentum transfers each reaction has its own characteristic signature, discussed below in detail.

1. Single π^\pm Photoproduction

The processes



have been quite extensively studied. The high energy π^+ differential cross sections^{52, 53, 59} are plotted versus $-t$ in Fig. 11. At 16 GeV the e^{3t} form of the cross section still holds at $-t = 3 \text{ GeV}^2$, four and one-half decades down from the forward peak. There seems to be a knee in the curves near $-t = 0.7 \text{ GeV}^2$, the slope changing from 2.0 GeV^{-2} to 3.3 GeV^{-2} . At $-t < 0.02 \text{ GeV}^2$ there is a sharp factor-of-two rise in the cross section, presumably related to one-pion exchange; the slope approaches 100 GeV^{-2} at the steepest point. This forward peak is consistently seen from 0.6 to 16 GeV. The slopes at both large and small t thus differ considerably from the usual $e^{\sim 8t}$ of hadronic interactions.

The energy dependence can be parameterized by an effective $\alpha(t)$:

$$\frac{d\sigma}{dt} = \beta(t) k^{2\alpha(t)-2}$$

As shown by the Fig. 11 inset, the 8 to 16 GeV data give $\alpha \approx 0$ for $-t \lesssim 1 \text{ GeV}^2$. The cross sections appear to fall off somewhat faster at larger t , both the 1967 and 1968 data giving $\alpha \approx -0.4$ at $t = -1.3 \text{ GeV}^2$.

The single π^+ and π^- reactions are charge symmetric and if the photon had definite isospin, the cross sections would be equal. The relative sign of the isoscalar and isovector photon amplitudes changes when going from π^+ to π^- production, however, and any interferences between the two types of amplitudes will appear with

opposite sign in the two reactions. Since isoscalar and isovector photons have opposite G parity, this interference is between t-channel exchanges of opposite G parity.

Several corrections must be made in relating pion production from deuterium to that from free nucleons. These corrections include nucleon-nucleon interactions, Glauber corrections, and exclusion-principle effects, all of which should cancel when taking the π^-/π^+ ratio. The deuterium ratio should thus be a good measure of the ratio from free nucleons. Figure 12 shows the π^- to π^+ ratio^{52,54,60} from deuterium as a function of \sqrt{t} . At small t the ratio is near unity, but then drops rapidly to a minimum of about 1/3 in the region near $t = -0.4 \text{ GeV}^2$, after which it slowly rises. Some energy dependence can be seen, the high energy data falling faster at small t and rising faster at large t.

Beams of linearly polarized photons have been obtained near 3 GeV at both DESY and CEA using coherent bremsstrahlung from oriented crystals. These beams have been used to study π^\pm photoproduction; Fig. 13 shows the results⁶²⁻⁶⁶ in terms of the asymmetry parameter

$$\Sigma = \frac{\sigma_{\perp} - \sigma_{\parallel}}{\sigma_{\perp} + \sigma_{\parallel}}$$

where $\sigma_{\perp}(\sigma_{\parallel})$ is the differential cross section for photons polarized perpendicular (parallel) to the production plane. At $t = 0$, kinematics require $\sigma_{\parallel} = \sigma_{\perp}$. The π^+ asymmetry rises quickly from 0 and remains positive over the range measured. Very recent preliminary data⁶⁷ from CEA (not shown in Fig. 13) give $\Sigma^+ \gtrsim 0.6$ from 0.1 to 1.1 GeV^2 in contradiction to the cut model of Frøylund and Gordon.⁶¹ Recent π^- data⁶³ show that for $-t = 0.05$ to 0.10 GeV^2 the asymmetry Σ^- is large and positive just as for Σ^+ . It then falls to zero at $-t = 0.3 \text{ GeV}^2$ and stays there out to 1.1 GeV^2 , after which it rises to +0.5 and then falls to -0.9 at 90° in the

center-of-mass system.⁶⁶ The oscillations at large t may indicate the importance of s -channel resonances at these energies ($s = 6.3 \text{ GeV}^2$).

2. Comparison of π^\pm Photoproduction with Theory

Two years ago when the small-angle π^+ peak was first observed at high energies, the renaissance of Regge poles was at its height. The Regge-pole people were forced to interpret both the forward π^+ photoproduction peak and a similar peak seen in $n\rho$ charge exchange as a conspiracy between the pion and a pole of opposite parity. This interpretation required that $\alpha_\pi(0) = \alpha_{\pi_c}(0)$ and that the two residues also be related at $t = 0$. As the word "conspiracy" implies, the scheme appeared rather ad hoc, especially since there does not appear to be any particle with $J^P = 0^+$ and mass near m_π . As usual, the Regge pole people had various excuses up their sleeves and there were even Lorentz-symmetry people who fully appreciated the beauties of conspiracy.

The theoretical difficulties in having a finite cross section at $t = 0$ can be superficially understood by the expansion⁶⁸

$$\frac{d\sigma}{dt} = \frac{1}{32\pi} \left\{ \left[|A_1|^2 + |t| |A_4|^2 \right] + \left[|A_1 + tA_2|^2 + |t| |A_3|^2 \right] \right\} .$$

At high energies and small t the terms in the first and second square brackets correspond to t -channel exchanges of $P(-1)^J = +1$ and -1 (natural and unnatural parity), respectively.⁶⁹ At $t = 0$ only the A_1 terms remain, but this implies equal contributions of natural and unnatural parity exchanges. Thus, if one believes only in t -channel exchanges of elementary particles or Regge poles, the amplitudes at $t = 0$ must either go to zero (evasion) or conspire to give equal contributions, e.g., π_c exchange giving the A_1 amplitude in the first square bracket and π exchange giving exactly the same value for A_1 in the second square bracket. Drell and Sullivan⁷⁰ used symmetry arguments for the various possible photon couplings to obtain the result that each exchange amplitude was separately expected to go to zero.

The curve marked "OPE" in Fig. 14 shows the small- t fall-off in cross section expected from one-pion exchange alone (either elementary or Reggeized). The experimental π^+ data clearly go to such small momentum transfers as to exclude any last minute turnover at $t = 0$.

Elementary one-pion exchange by itself is not gauge invariant, and there is an infinity of ways of making the theory gauge invariant. Traditionally, the simplest way is to add the amplitude given by the second diagram of Fig. 15 where the proton is treated as a Dirac particle without anomalous magnetic moment; this gives the curve in Fig. 14 labeled "Electric Born." Surprisingly, this classic calculation reproduces both the π^+ and π^- experimental results to within $\sim 20\%$ for all $k > 1.2$ GeV and $t < 2m_\pi^2$.

As for hadron initiated processes, the simple Born calculation requires a form factor at larger t values. Richter first noted that simply multiplying the Electric Born cross section by $e^{\sim 3t}$ gave fits good to 20 or 30% all the way out to $-t = 2$ or 3 GeV². The π^- Electric Born calculation is nearly identical to that for π^+ , however, and $\pi^-/\pi^+ \neq 1$ clearly indicates the importance of other terms at $-t > 2m_\pi^2$. In fact, any theory which purports to understand π^+ (or π^-) photoproduction at $-t > m_\pi^2$ must include both isoscalar and isovector photon amplitudes.

Both the large and small t data suggest the usefulness of an absorption model. At large t , absorption would cause the Born calculation to fall off and better follow the data; unfortunately, it also reduces the predicted small- t cross section (which was already slightly lower than experiment). One way to increase the small- t prediction is to include terms such as the third one of Fig. 15.

The coherent droplet model, a type of OPE absorption model, has been used to fit the π^+ data with the high partial waves assumed to come from OPE and the low partial waves from empirical fits to other data.⁷³ Although good fits were

obtained up to $-t = 0.2 \text{ GeV}^2$, the model fell off too fast at larger momentum transfers and it did not take into account the π^-/π^+ ratio.

Years ago, Stichel⁷⁴ showed that the cross sections for linearly polarized photons, σ_{\perp} and σ_{\parallel} , have natural and unnatural parity-exchange amplitudes in the t channel, respectively. These cross sections are shown in Fig. 16 for both π^+ and π^- production. The amplitudes are denoted by symbols of the particles exchanged in the t channel. The natural parity-exchange cross section σ_{\perp} falls away smoothly with increasing momentum transfer while σ_{\parallel} has the sharp fall-off responsible for the forward peak in the unpolarized cross sections. In the Regge-conspiracy model^{69,75} this is explained by a smooth variation of the conspirator (π_c) residue function, but a rapid dependence for the pion residue; typically $\beta_{\pi} \propto t + 3/2 m_{\pi}^2$, giving a zero in the pion-exchange amplitude at $-t = 3/2 m_{\pi}^2$. In the Regge cut⁷⁶ and background models⁷⁷ the forward spike can be reproduced without rapid variations of the residues, the cut or background amplitudes giving slowly-varying contributions to both σ_{\parallel} and σ_{\perp} . The evasive π -exchange amplitude starts from zero in the forward direction and rapidly rises, interfering destructively with the cut or background amplitude. When the two amplitudes are equal, but opposite in sign, $\sigma_{\parallel} = 0$, the same end result as given by the conspiracy model.

The sharp forward spike in the unpolarized cross section is well reproduced by calculations⁷¹ with continuous moment sum rules (CMSR) which relate low and high energy data. The phase shift analysis of Walker⁵ was used for the low energy ($k < 1.2 \text{ GeV}$) amplitudes and the high energy amplitudes were assumed to have a conspiracy form. The agreement shown in Fig. 14 was taken as evidence for pion conspiracy. However, the conspiracy and cut models can predict identical amplitudes and the CMSR results cannot in principle distinguish between the two alternatives. As shown by Fig. 14, Jackson and Quigg⁷² obtained a slightly better fit

to the high energy data by simply assuming the amplitudes to be real, as suggested by $\alpha_{\text{eff}} \approx 0$ (their "pseudomodel"). The cut and conspiracy models can be distinguished when comparing several reactions. Factorization should apply for the conspiracy model, giving relations between the residue functions for related processes. It has been pointed out that factorization does not work for the conspiring π model for the reaction $\pi^+ p \rightarrow \rho^0 \Delta^{++}$ nor for ω and Δ photoproduction.⁷⁹

At larger momentum transfers more amplitudes are required to fit the data. Already at $-t = 0.1 \text{ GeV}^2$, $\pi^-/\pi^+ \approx 1/2$ indicating considerable interference between amplitudes corresponding to $G = +1$ and -1 in the t channel. Figure 16 shows that this interference is primarily among the natural-parity exchange amplitudes. In fact, the data are quite consistent with no interference at all in the unnatural-parity amplitudes⁸⁰ and thus no need for exchanges such as the Buddha (nor for a B conspiracy⁸¹); $\chi^2 = 8.4$ for 8 degrees of freedom under the assumption $\sigma_{\parallel}^+ = \sigma_{\parallel}^-$. Large interferences are required, however, for natural-parity amplitudes over the entire t range measured, except $-t \lesssim m_{\pi}^2$. For the Regge pole enthusiasts this is somewhat embarrassing since the ρ trajectory is the only likely $G = +1$ candidate and one would have expected $\sigma_1^+ = \sigma_1^-$ at $-t \approx 0.6 \text{ GeV}^2$ where $\alpha_{\rho} = 0$ (Ref. 80). One must either assume a pole in the ρ residue function, or put in an arbitrary ρ' trajectory, or appeal to cuts.

Having four closely related experimental functions (σ_1^+ , σ_1^- , σ_{\parallel}^+ , σ_{\parallel}^-) has proved rather effective in eliminating various models, especially those which tried to fit only some of the data. The difference $\sigma_1^+ \neq \sigma_1^-$ has proven to be especially effective. Regge theory, both poles and cuts, is still far too ill defined to unambiguously fit the π^{\pm} photoproduction data alone. Rather, a convincing model must assume many parameters, for example trajectories, to be fixed by other experiments. Photoproduction fitting thus becomes part of a larger program.⁸²

3. Vector Meson Dominance and Single-Pion Photoproduction

As discussed above, there is considerable isoscalar-isovector photon interference for π^\pm photoproduction. In the vector dominance model this would imply interferences between ρ -like and ω -like photons. (The ϕ 's will be ignored here because their coupling to nonstrange particles seems small.) A quark model prediction⁸³ for the $\omega\rho$ interference does not agree⁸⁴ with experiment.^{52,60} Since this interference is difficult to calculate, the most reliable method is to take the average of the two cross sections, in which case the interference terms cancel:

$$\frac{1}{2} \left[\frac{d\sigma}{dt} (\gamma n \rightarrow \pi^- p) + \frac{d\sigma}{dt} (\gamma p \rightarrow \pi^+ n) \right] = g_{\gamma\rho}^2 \left(\rho_{11}^{\text{hel}} \frac{d\sigma}{dt} \right)_{\pi^- p \rightarrow \rho^0 n} + g_{\gamma\omega}^2 \left(\rho_{11}^{\text{hel}} \frac{d\sigma}{dt} \right)_{\pi^+ n \rightarrow \omega p} .$$

It turns out that the ω term by itself is only a few percent of the ρ term and can be ignored. Figure 17 shows the good agreement obtained⁸⁵ with the value $\gamma_\rho^2/4\pi = 0.45$. Note that the $\pi \rightarrow \rho^0$ data are not yet sufficient to say whether $\left(\rho_{11}^{\text{hel}} \frac{d\sigma}{dt} \right)_{\pi^- p \rightarrow \rho^0 n}$ has a forward peak similar to photoproduction.

A year ago it thus seemed that vector dominance was doing very well for π^\pm photoproduction and was good to within the uncertainties of 20 or 30%. The polarized-photon data⁶⁴ soon dispelled any complacency on the part of the vector dominance theorists. Components of linear polarization for the ρ mesons can be extracted from the ρ density matrix and compared with the photoproduction asymmetry. Again, taking sums of the π^\pm photoproduction data to avoid troubles with the $\omega\rho$ interference terms, we have the prediction⁸⁴

$$\langle \Sigma \rangle = \frac{\Sigma^+ + R \Sigma^-}{1 + R} = \left(\frac{\rho_{1-1}}{\rho_{11}} \right)_{\pi^- p \rightarrow \rho^0 n}$$

where R is the π^-/π^+ ratio from deuterium. Again the few-percent correction from the ω 's has been neglected. The photoproduction asymmetry was found to be approximately 0.5 at 0.2 and 0.4 GeV². The ratio of ρ^0 density matrices, however, came

out -0.3 when evaluated in the usual helicity frame.^{64,86} This is a very bad discrepancy; it implies that natural-parity exchanges in the t channel dominate photo-production⁷⁴ but that unnatural-parity exchange dominates⁸⁷ $\pi \rightarrow \rho^0$.

Various experimental checks were made to verify the discrepancy. For example, the ratio of density matrix elements was examined not only at the ρ peak but also for events in the ρ tails. One might expect that if the culprit were a background interference of some sort, the ratio would depend strongly on the relative amount of ρ events and background events. No significant change in the ratio was seen.⁸⁶ Further checks were made to insure that neither the S-wave background nor possible contributions from the ω terms could be causing the discrepancy.⁸⁸

So, many theorists went back and re-examined the assumptions which were made in the model (illustrating the theorem that there is nothing like a good discrepancy to stir up a great deal of theoretical interest). Two different suggestions were made as to why the σ_{\parallel} prediction was particularly unreliable. First, it had been pointed out that the frame in which one should evaluate the ρ^0 density matrix is ambiguous.⁸⁹ As the vector-meson mass approaches zero, a change of reference frame corresponds to a gauge transformation which does not affect the physical amplitude for photoproduction. It was suggested by Bialas and Zalewski⁹⁰ that the reference frame be rotated about the production normal in an effort to find a frame for which the prediction would work. They found that the Donahue-Högaasen frame⁹¹ (for which the real part of $\rho_{10} = 0$) gives extremal values for the ratio ρ_{1-1}/ρ_{11} . Further, the ratio when evaluated in this frame of reference did give agreement with the photoproduction asymmetry. Such a rotation about the production normal will of course leave the component of polarization along this direction invariant and thus σ_{\perp} is independent of these rotations.⁸⁴ Several groups of theorists, however, have pointed out that under certain assumptions the helicity frame is, indeed,

the natural frame to take when comparing the two processes. In particular, specific dynamic models seem to give better predictions in this frame than in others.^{89, 92, 93}

A second uncertainty in σ_{\parallel} was pointed out by Meiere.⁹⁴ He suggested that the amplitude A_5 (which must be 0 for photoproduction) is important when the vector-meson mass is unequal to 0. A_5 contributes only to σ_{\parallel} and the prediction for this component thus becomes uncertain.

Since σ_{\perp} appeared to survive the arguments above, it seemed natural to test the prediction

$$\frac{\sigma_1^+ + \sigma_1^-}{2} = g_{\gamma\rho}^2 \left[(\rho_{11} + \rho_{1-1}) \frac{d\sigma}{dt} \right]_{\pi^- p \rightarrow \rho^0 n}$$

Figure 18 shows that at 0.2 and 0.4 GeV² a factor-of-three discrepancy still remains if the value

$$\gamma_{\rho}^2/4\pi = 0.52$$

is used.⁹⁵ Although some authors^{90, 96} have quoted general agreement for this prediction, a close examination of their figures shows a discrepancy similar to that shown in Fig. 18. To obtain agreement a value $\gamma_{\rho}^2/4\pi$ of about 0.2 or 0.3 is necessary.^{63, 95, 97}

Given this σ_{\perp} discrepancy, the theorists have worked even harder. (a) Harari et al.,⁹⁸ have suggested that at small momentum transfers one should, in fact, expect a discrepancy in the simple vector dominance model; for example, they do not expect a peak in the quantity $(\rho_{11} \frac{d\sigma}{dt})_{\pi \rightarrow \rho}$ at small momentum transfers. Other theorists^{92, 93, 99, 100} however, have found dynamical models which contradict this suggestion. (b) Good numerical results have been obtained¹⁰¹ using the unconventional choice of quantization (z) axis along the production normal. (c) Schmidt¹⁰⁰ has found that in an extended electric Born model both σ_{\perp} and σ_{\parallel} have strong dependences on the vector-meson mass.

The original simple and complacent theory has thus become quite complicated while trying to explain this discrepancy. The various cures have left the patient badly crippled; even if it should turn out that the experimental numbers were wrong (see the next paragraph), the model will never be the same again. Not only for pion production but presumably for other processes described by the vector dominance model, the dynamics of the reactions seem to play an important role in the proper application of vector dominance ideas, especially as regards the mass extrapolation. Perhaps we should be amazed that the model has worked as well as it has.

A possible experimental explanation of the discrepancy has been put forward by the Notre Dame group.¹⁰² In the usual bubble chamber analysis of the ρ^0 density matrices, it is assumed that S and P waves and their interferences dominate the decay angular distributions. One of the terms of this decay angular distribution is then $\rho_{1-1} \sin^2\theta \cos 2\phi$ and it is the only term in $\cos 2\phi$. Thus, we expect that $\langle \cos 2\phi \rangle$ will be proportional to $\sin^2\theta$. Figure 19 shows that the ρ^- distribution for $\langle \cos 2\phi \rangle$ does have a $\sin^2\theta$ dependence at 4 GeV/c. The ρ^0 distribution, however, appears to have large statistical fluctuations or a rapidly varying dependence on $\cos\theta$. The χ^2 probability for the $\sin^2\theta$ fit shown is only 0.5%. The Notre Dame group takes this as evidence that a D-wave background is significantly affecting the decay angular distribution. D waves and their interferences with the S and P waves would contribute several additional $\cos 2\phi$ terms, making it impossible to obtain ρ_{1-1} .

It is not yet clear to me whether the distribution of Fig. 19 is simply a statistical fluctuation or whether D waves are actually causing the rapid variation with $\cos\theta$. It would be interesting to know how much D wave is necessary to reproduce the values shown and whether it is consistent with the $\pi\pi$ phase shift analyses. Other

groups with similar data should also make this analysis. The result affects not only vector dominance, of course, but also much published data on ρ^0 density matrices.

4. Neutral Pion Photoproduction

Differential cross sections^{49,103} for $\gamma p \rightarrow \pi^0 p$ are multiplied by $(s - M_p^2)^2$ and shown in Fig. 20. As for charged-pion photoproduction this parameterization causes the data to lie more or less along a common curve. The production mechanisms must be considerably different, however, since unlike π^\pm production, one-pion exchange is forbidden by C parity for π^0 photoproduction. In fact, the structure of the differential cross section is considerably different from that observed for charged pions. In the forward direction there seems to be a fall off rather than a peak. Further, there is a dip or shoulder near $-t = 0.5 \text{ GeV}^2$; this is the region where one would in fact expect a dip from the ω wrong-signature nonsense zero. Considerable theoretical interest has been shown in the mechanism filling the ω dip. Besides the ω , the requirement $C = -1$ leaves only the ρ , ϕ and B. Since the ρ also has a nonsense 0 in this region and the ϕ couplings should be small, B is left as the only candidate in a Regge pole picture.¹⁰⁴ With its lower-lying trajectory, one would expect the effects of the B to diminish with increasing energy. On the contrary, the dip appears to fill in rather than deepen. The insert to Fig. 20 shows that in the dip region the effective α is about + 0.15, considerably larger than that normally associated with the B trajectory.

The relative lack of energy dependence has given the Regge model difficulties. The curves shown in Fig. 20 are from the theory of Blackmon et al.¹⁰⁵ They use ω , ρ and B exchange with absorptive corrections, and end up with a rather high trajectory for the B, $\alpha_B(t) = 0.4 + 0.4 t$. Their fits appear to have a larger energy dependence than shown by the data, particularly in the forward direction, although

there is a scarcity of data at high energies and small t . Capella and Tran Thanh Van¹⁰⁶ proposed a model containing an ω pole plus ω -Pomeron cuts. At high energies the cuts dominate over the ω pole, filling in the dip region. Their formulation has the advantage of few free parameters and gives reasonably good fits. Contogouris et al.,¹⁰⁷ have made similar fits, and Frøyland¹⁰⁸ has also fit the data with a cut model.

Figure 21 shows the fits²⁵ which were used to get the α values shown in the insert of Fig. 20. The straight-line fits work amazingly well over a wide range of energies, the typical range being from 3 to 14 GeV. If cuts were taking over from the ω pole as the energy increased, one might expect to see a change of slope. However, the data appear to be quite consistent with the straight-line fits.

The 5.8 GeV DESY data⁴⁹ are plotted on a log-log scale in Fig. 22; this choice of scales expands the very-forward t region. In this region there is an increase in the cross section which appears as a very sharp spike at very small t values when plotted on a linear scale. This forward spike is from the Primakoff effect¹⁰⁹ (one-gamma-ray exchange, related to π^0 decay). The data are consistent with evasive Regge poles interfering constructively with the Primakoff amplitude. Gilman¹¹⁰ has used this constructive interference to show that the sign of the $\pi^0\gamma\gamma$ amplitude is opposite to that for $g_{\pi NN}$. This relative sign is related to recent PCAC work.¹¹¹ This is one of the few cases in photoproduction where one is specifically using the fact that we are dealing with an electromagnetic particle, the γ ray.

The asymmetry parameter for photoproduction of π^0 's by linearly-polarized γ rays is shown in Fig. 23. It was measured at CEA, using 3 GeV coherent bremsstrahlung from a diamond crystal; the two gamma rays from the π^0 and the recoil proton were detected.¹¹² Over the entire range of momentum transfer measured, σ_1 dominates the cross section. From the t -channel point of view this means that the process proceeds mainly by natural-parity exchange. The B meson, which had been used to fill in the dip, has unnatural parity and gave the asymmetry curve

marked Ader et al.¹⁰⁴ Instead, whatever is filling in the dip must be predominantly natural-parity, i. e., the ω or ρ or some higher-mass meson having their quantum numbers. Further, the vector dominance model indicates that the dip-filling mechanism is not dominated by isoscalar-photon amplitudes.¹¹³ As with charged-pion photoproduction, the theorists have thus been forced to consider cuts with results shown in the figure.

Preliminary results on $\gamma n \rightarrow \pi^0 n$ are available from CEA;¹¹⁴ as shown by Fig. 24, π^0 production from neutrons is about 80% of that from protons. The isoscalar-isovector photon interference terms are thus not negligible but are much less important than for π^\pm production. This information is very useful in eliminating certain of the theoretical models (or at least forcing their reformulation). To get good agreement in the vector dominance model, a large constructive interference between the ω -like and ρ -like photons was assumed for $\gamma p \rightarrow \pi^0 p$ in the region of the dip. The disagreement of the data with the dashed curve shows that this assumption is wrong and that there may be troubles with the VDM prediction (the comparison requires the addition and subtraction of three $\pi \rightarrow \rho$ reactions, so the result is not very precise). Frøyland¹⁰⁸ also predicted that in this region the production from neutrons would be rather small. The ω plus ωP cut models^{106,107} include no isoscalar photon amplitudes and therefore give a ratio of unity.

5. Backward Photoproduction of Pions

The differential cross sections for π^0 and π^+ photoproduction are shown in Fig. 25 over the complete angular range. Judging from the rather sparse data, it appears that at 5 GeV both π^+ and π^0 cross sections continue down at the rate of e^{3t} for about four orders of magnitude from the small t values. In the backward direction recent π^+ data have been obtained using the SLAC 1.6 GeV spectrometer.¹¹⁶ The backward π^0 cross section has been studied with the SLAC 20 GeV spectrometer detecting the high energy forward proton.¹¹⁷

Figure 26 shows the differential cross sections in the backward direction, multiplied by k^3 . This factor appears to do a good job of eliminating the energy dependence for both reactions over the complete range of u studied. Both cross sections show a turnover near 180° . This is understood as a kinematic effect, since three of the four s -channel helicity amplitudes vanish at 180° by angular momentum conservation. Although the π^0 cross section may show some structure near $u = -0.6 \text{ GeV}^2$, neither the π^+ nor the π^0 cross sections show a dip at $u = -0.15 \text{ GeV}^2$. It thus appears that the N_α (nucleon) trajectory with its wrong-signature nonsense zero is not dominant in this region.

Two theoretical groups^{118, 119} have fit both the π^+ and π^0 backward data assuming N_α and N_γ to have degenerate trajectories. They managed to avoid the problem of nonshrinkage by having the nucleon trajectories dominant at small u and the Δ trajectory dominant at large u . Both groups obtained reasonably good fits. The relatively large amount of N_γ trajectory needed for these fits, however, may be incompatible with the observed backward η photoproduction cross sections.¹¹⁷ The η appears to be produced in the backward direction roughly half as often as the π^0 in agreement with the $SU(6)_W$ prediction¹²⁰ of 27/49. The π^0 has been fitted to $s^{-3 \pm 0.2}$; the energy dependence for ρ^0 and η backward production are similar, $s^{-3.6 \pm 0.4}$ and $s^{-3.5 \pm 0.5}$, respectively.¹¹⁷

Backward photoproduction of Δ^{++} has also been observed.¹¹⁶ For this reaction only $I = 3/2$ exchange is possible in the u channel. The cross section appears to have a considerably steeper fall-off with momentum transfer than either the π^+ or π^0 cross sections.

Figure 27 shows the extrapolation of the Barger-Weiler fit¹¹⁸ together with the $180^\circ \pi^0$ data from DESY.¹²¹ The high energy extrapolation passes close to the mean of the cross section in the resonance region, as expected from duality principles.

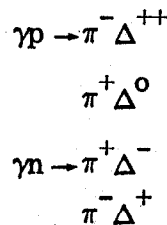
6. η Photoproduction

The process $\gamma p \rightarrow \eta p$ has been studied by two rather different experimental techniques. At SLAC the 1.6 GeV spectrometer was used to obtain missing-mass spectra.²⁵ The data shown in Fig. 28 were mainly taken near 6 GeV with a small amount from 9 GeV. Large contributions from the neighboring ρ step preclude η measurements at high energies. Also shown are 4-GeV data obtained at CEA by the detection of $\eta \rightarrow \gamma\gamma$ in lead-glass Cerenkov counters.¹²² The 4- and 6-GeV data show a considerable deviation from the $1/k^2$ dependence found for the other pseudoscalar mesons. However, very recent 4-GeV results¹²³ obtained at DESY by detecting the two-photon-decay mode are systematically higher than the CEA points, and together with the SLAC data indicate a $1/k^2$ dependence.

The angular distribution is considerably different from that for π^0 's. One would have expected ρ exchange to dominate the η cross section, giving a dip in about the same place as seen for π^0 photoproduction. Dar and Weisskopf¹²⁴ assumed only ρ exchange to be important and related the η cross section to that for ω production by pions. Gorczyca and Hayashi¹²⁵ included not only ρ exchange but also ω and B. Both predictions seem to give reasonable fits to the data in its present, somewhat uncertain state.

7. Δ Photoproduction

The reactions



have been studied with the missing-mass technique at SLAC.^{55, 126} It was found that the data did not show any phase-space background, and the yields were fitted

to single-pion production (where appropriate), the Δ , and a background of pions from ρ^0 decay. Uncertainties in the cross section of $\pm 15\%$ were assigned to account for the uncertainty in the background subtraction.

The Δ^{++} cross sections⁵⁵ are shown in Fig. 29. The effective α was calculated from the 8-to-16-GeV data and found to be consistent with 0. At large momentum transfers the Δ^{++} cross section follows the $\gamma p \rightarrow \pi^+ n$ cross section,⁵³ shown schematically by the dashed curves. At momentum transfers $< 0.2 \text{ GeV}^2$ the cross section rises as e^{12t} ; it reaches a maximum near $-t = m_\pi^2$, where it is a factor of 6 above the single- π^+ cross section. The forward peak region is shown in more detail in Fig. 30. The $t = 0$ cross section is down by a factor of 2 to 4 from the peak, an extrapolation to $t = 0$ giving $350 \pm 120 \mu\text{b GeV}^2$. To within errors this is the same forward cross section as found for single- π^+ production (see Fig. 14).

Although the shapes of the single- π^+ and Δ^{++} cross sections at small momentum transfers are remarkably different, both are reproduced to within 20 or 30% by gauge-invariant one-pion exchange models. As for single- π^+ production, there is an infinity of ways in which to make one-pion exchange for Δ production gauge invariant. Four years before the data became available, Stichel and Scholz¹²⁷ proposed a minimal way in which to make the theory gauge invariant. This involved keeping only terms to lowest order in the coupling constants and only those terms in which the γ ray interacts directly with the orbital current; also, some assumptions concerning isospin were made. As can be seen from Fig. 30, their prediction reproduces the data remarkably well at small momentum transfers.

As for single-pion production, the isoscalar-isovector photon interferences enter with opposite signs for charge-symmetric Δ production. The ratio of Δ^{++} to Δ^- production¹²⁶ at 16 GeV is shown in Fig. 31 where it is compared with the single π^-/π^+ ratio.⁵⁴ At momentum transfers $\gtrsim 0.2 \text{ GeV}^2$, the data show Δ^- being produced about twice as frequently as Δ^{++} . In this momentum-transfer region the

isoscalar photon amplitude must then be at least 17% of the isovector amplitude. At small momentum transfers the preliminary results indicate that Δ^{++} may have a slightly larger cross section than does Δ^- . This differs from single-pion photoproduction, which showed no evidence for interference at small momentum transfers.

Both isotopic spin-1 and -2 exchanges are allowed in the t channel. Making the usual assumption that I = 2 exchanges can be neglected,

$$\frac{\frac{d\sigma}{dt}(\gamma n \rightarrow \pi^+ \Delta^-)}{\frac{d\sigma}{dt}(\gamma p \rightarrow \pi^+ \Delta^0)} = 3 .$$

Since both processes involve positive pions, there is no ambiguity concerning isoscalar and isovector interference terms. Neglecting the few percent Glauber corrections (see Ref. 54 and Section IV.9), a deuterium-to-hydrogen ratio of 4 to 1 is thus expected. The ratio¹²⁶ is plotted in Fig. 32 as a function of $\sqrt{-t}$ for 16 GeV. Experimentally the ratio is about 3 instead of 4, and may show some t dependence. The data thus require amplitudes corresponding to I = 2 exchange in the t channel. If one parameterizes the Δ^0 cross section by

$$\frac{d\sigma}{dt}(\gamma p \rightarrow \pi^+ \Delta^0) = \sum_{i=1}^8 |A_1 + A_2|_i^2$$

(where the subscripts 1 and 2 refer to the isotopic spin exchanged in the t channel and the subscripts i refer to the various helicity amplitudes), then Δ^- production is given by

$$\frac{d\sigma}{dt}(\gamma n \rightarrow \pi^+ \Delta^-) = \sum_{i=1}^8 3 \left| A_1 - \frac{1}{3} A_2 \right|_i^2$$

In order to obtain a deuterium-to-hydrogen ratio of 3, A_2 must be at least 15% of A_1 . Although this result can be interpreted in terms of exotic meson exchange, it could also be explained by double Regge-pole exchange, giving Regge cuts. A third

interpretation would be to invoke s -channel effects. A similar test can be made for the π^- data; experimentally this test is not as sensitive as the π^+ test and is consistent both with the ratio 4/3 given by pure $I=1$ exchange and with $I=2$ exchange amplitudes similar to that required for the π^+ data.

As for single-pion photoproduction, any serious curve fitting of the Δ 's must consider all available data. To consistently fit the various charge states one must include not only isoscalar photon amplitudes, but also amplitudes looking like $I=2$ in the t channel.

8. Vector Dominance for Δ 's

For single-pion production isospin and time reversal arguments were necessary to obtain the vector dominance relation. For Δ production the two processes

$$\begin{aligned} \rho^0 p &\rightarrow \pi^- \Delta^{++} \\ \pi^+ p &\rightarrow \rho^0 \Delta^{++} \end{aligned}$$

are not so simply related, but rather involve a line reversal. This means that Regge pole amplitudes for trajectories with opposite signature will change relative sign going from one reaction to the other.¹²⁸

Neglecting the line reversal troubles, a vector dominance comparison¹²⁶ is shown in Fig. 33. An average of Δ^- and Δ^{++} photoproduction is taken to eliminate the $\rho\omega$ interference terms; the 10% ω contribution has been neglected. The storage ring coupling constant⁹ $\gamma_\rho^2/4\pi = 0.52$ was used and the ρ^0 density matrix was evaluated in the standard helicity frame. At all momentum transfers for which data exist there is a factor-of-four discrepancy. This contradicts the results of Dar¹³⁰ who assumed that Δ^- production would be considerably less than that for Δ^{++} . If one believes in the vector dominance model, the discrepancy can be used to gain insight into the dynamics of these processes, namely, large interferences are required between trajectories of opposite signature. Note that to leading order in s , the trajectories must belong to the same spin-parity sequence if they are to interfere.

A recent model by Gotsman¹³¹ does have trajectories of opposite signature and shows agreement with vector dominance. A word of caution should be interjected at this point. It is hard to estimate cross sections for double resonance production such as $\pi^+ p \rightarrow \rho^0 \Delta^{++}$. A re-analysis¹³² of the 8 GeV data used to make the comparison of Fig. 33 has shown that the cross section may be $\frac{1}{2}$ to 2 times larger than originally given;¹²⁹ this would reduce the discrepancy shown in Fig. 33.

9. K⁺ Photoproduction

Total cross sections for Λ and Σ^0 photoproduction are shown in Fig. 34. As for pion photoproduction, multiplying the cross sections by k^2 gives a very flat dependence at high energies. The DESY bubble chamber data¹³⁴ below 5 GeV do not tie on well with the high energy counter data;¹³⁵ this is especially true for Σ^0 . The high energy Λ and Σ^0 cross sections are the same to within 20% and are each roughly one-third of the single- π^+ cross section.

The SLAC 20 GeV/c spectrometer was used to measure the differential cross sections¹³⁵ for Λ production shown in Fig. 35. At large momentum transfers, the cross sections fall off as e^{3t} . Unlike the π^+ cross sections, however, they reach a maximum at M_K^2 and have a forward dip, a factor of about $\frac{1}{2}$ down from the maximum. The absence of a sharp forward peak as seen for π^+ production presumably means that one-K exchange is not important, which seems rather odd since the K and π are members of the same SU(3) nonet. The difference has been explained,^{73, 75, 136} however, as being the result of the large mass differences. In the cut model of Frøylund¹³⁷ the evasive K-exchange amplitude interferes constructively (rather than destructively as for the pion case) with the cut amplitude. The effective Regge α is also shown in the figure; as usual, it lies rather close to 0 in contradiction to a simple Regge picture.

The ratio of Σ^0/Λ photoproduction¹³⁵ from hydrogen is shown in Fig. 36. This ratio is typically 0.8 with a systematic decrease at small momentum transfers at the lower photon energies. The Σ production being comparable to Λ production is another indication of K exchange not playing an important role; since the $Kp\Sigma$ coupling is thought¹³⁸ to be much smaller than the $Kp\Lambda$ coupling, K exchange would give $\Sigma/\Lambda \ll 1$. K^* exchange has been used in various models^{75, 139} to explain the observed Σ/Λ ratio. The Σ^0/Λ ratio also disagrees with the quark model prediction^{140, 141} 1:27 at $\theta = 0$, and $< 1:3$ elsewhere. The results are consistent with an $SU(6)_W$ calculation,¹⁴² however, 405 amplitudes (not present in the quark model) being used in the calculation. The arrows at $t = 0$ in Fig. 36 show the results of these calculations.

Recent data on Y^* production at 11 GeV were obtained¹⁴³ with the SLAC 20 GeV/c spectrometer and are shown in Fig. 37. The missing-mass resolution is not good enough to separate $Y_1^*(1385)$ and $Y_0^*(1405)$, Fig. 37c showing the sum of the cross sections for these two Y^* 's. All of the cross sections shown are within a factor of $\frac{1}{2}$ or 2 of the Λ cross section and all appear to have the same general t dependence.

Deuterium-to-hydrogen ratios¹⁴³ are shown in Fig. 38. Since $K^+\Lambda$ can only be produced from protons, one expects a ratio of unity minus a few percent Glauber correction. The average of the Λ ratio, 1.02 ± 0.04 , is consistent with this expectation.

The Σ 's can be produced from both neutrons and protons. In terms of isospin exchange in the t channel,

$$\frac{\frac{d\sigma}{dt}(\gamma n \rightarrow K^+ \Sigma^-)}{\frac{d\sigma}{dt}(\gamma p \rightarrow K^+ \Sigma^0)} = 2 \frac{|A_{1/2} - 1/2 A_{3/2}|^2}{|A_{1/2} + A_{3/2}|^2}$$

where the sum over helicity amplitudes has been suppressed for simplicity. If one

neglects $I = 3/2$ in the t channel, the above ratio becomes 2:1. In terms of a deuterium-to-hydrogen ratio one then expects 3:1 in contradiction to the observed average value 2.37 ± 0.11 . To within errors this ratio is independent of momentum transfer. The data imply that $A_{3/2}$ must be $\geq 10\%$ of $A_{1/2}$. As for Δ production, this result can be interpreted in terms of exotic mesons or cuts or s -channel effects depending on one's tastes.

The D:H ratio for the step at 1400 is also shown in Fig. 38. Although the error bars are large, the average value 1.18 ± 0.30 is considerably closer to the ratio found for Λ 's than to that for Σ 's. If one assumes that the deuterium-to-hydrogen ratios for the 1385 and 1405 are the same as for the Σ and Λ , respectively, then the 1385 accounts for only $12 \pm 22\%$ of the hydrogen step.

Backward production of Λ and Σ^0 has been measured¹⁴⁴ at 4.3 GeV with the SLAC 1.6 GeV/c spectrometer. As shown in Fig. 39, the results have a smooth fall-off with u , similar to that observed previously for¹¹⁶ π^+ production. The average value of the $\Sigma^0:\Lambda$ ratio is 1.7 ± 0.15 with no noticeable variation over the u range measured. Note that this is about twice the value observed in the forward direction. Decuplet exchange (U -spin 1) predicts¹⁴⁵ $\Sigma^0/\Lambda = 1/3$ in disagreement with the data, suggesting that decuplet exchange is not dominant.

10. Comparison with SU(3) Predictions

The data presented above can be used to test various SU(3) predictions. The ones which we shall discuss here were derived in a straightforward manner assuming only that the photon is a U -spin singlet and that U spin is conserved.

The first of the SU(3) predictions is a triangle relation¹⁴⁵ shown schematically in Fig. 40. Although present experiments do not measure the relative phases of the three amplitudes shown, their lengths can be obtained by taking the square root of the appropriate cross section. One can then use the standard cosine formula

to calculate $\cos \phi$ and the SU(3) prediction is satisfied if

$$|\cos \phi| \leq 1 .$$

For momentum transfers $> 0.1 \text{ GeV}^2$ this is indeed the case. At smaller momentum transfers, however, the K^+ amplitudes shrink because of the dip in the cross sections while the π^+ amplitude grows; the two short K^+ vectors cannot add up to make the long π^+ vector and a breakdown of the SU(3) prediction occurs. As mentioned previously, this breakdown has been blamed^{73, 75, 136} on the mass differences. In the backward direction¹⁴⁴ it was found that $\cos \phi$ was less than 0, in contrast to the forward results.¹³⁵

The second set of SU(3) predictions are¹⁴⁵

$$\frac{d\sigma}{dt}(\gamma n \rightarrow K^+ Y_{1385}^{*-}) = \frac{1}{3} \frac{d\sigma}{dt}(\gamma n \rightarrow \pi^+ \Delta^-),$$

$$\frac{d\sigma}{dt}(\gamma p \rightarrow K^+ Y_{1385}^{*0}) = \frac{1}{2} \frac{d\sigma}{dt}(\gamma p \rightarrow \pi^+ \Delta^0) .$$

As shown in Fig. 41, there is a large discrepancy for both of these predictions over the full range of t measured. Although the Δ data were taken at 16 GeV and the Y^* at 11 GeV, the $(s-M^2)^2$ factor should correct for this difference quite well. Taking an effective $\alpha = \pm 0.2$ would change the relative normalizations by only $\pm 15\%$. The K^+ results from protons are the sum of the cross sections for $Y^*(1385)$ and $Y^*(1405)$; as discussed above, $Y^*(1385)$ probably contributes less than one third of the cross section represented by these points. Thus, the discrepancy may well be a factor of 3 or more worse than shown in Fig. 41a. Since the discrepancy occurs over a wide range of momentum transfers, it is not as easy to put the blame on the $K\pi$ mass difference. A similar discrepancy has been noted for reactions initiated by K mesons.¹⁴⁶

V. MULTIBODY FINAL STATES

Satz¹⁴⁷ has used vector dominance and the quark model to predict the cross sections for γ multibody final states from π p inelastic scattering cross sections. In general, these predictions agree rather well with experiment, an example being shown in Fig. 42.

Some bubble chamber data exist^{21,22,134} on reactions with three or more pions in the final state. No clear picture as yet exists for these reactions, but it has already become apparent that Δ^{++} and ρ^0 production play an important role. Other mesons, such as A_1 and A_2 , have also been seen.

VI. REACTIONS OFF COMPLEX NUCLEI

1. Total Photon Cross Sections From Complex Nuclei

The total cross section measured from hydrogen ($\sim 120 \mu\text{b}$) implies a mean free path for γ rays in nuclear matter of several hundred fermis. Thus, one might expect each of the nucleons in a complex nucleus to be equally efficient in absorbing the γ rays and the total cross section to be proportional to A . The vector dominance model, however, gives quite a different picture.¹⁴⁸ If the γ ray is really a ρ meson in disguise, one might expect the total cross section to go roughly as $A^{2/3}$. Recent theoretical work¹⁴⁹⁻¹⁵² has given these two A dependences as low- and high-energy limits of a more complete theory. The two diagrams of Fig. 43 are considered for forward Compton scattering (related by the optical theorem to the total cross section). In the first diagram the γ ray interacts directly at some point \vec{x} in the nucleus. In the second, the γ interacts at \vec{x}_0 to produce a real ρ meson which then converts back to a γ ray at \vec{x} . The finite mass of the ρ meson leads to a phase slippage of the two-step amplitude

$$\Delta\phi = q_{||} (x-x_0) = \frac{M_\rho^2}{2k} (x-x_0) \quad .$$

At low energies the phase slippage becomes large and the integration over \vec{x}_0 involves large cancellations; the two-step amplitude then becomes negligible, leaving only the first diagram with a cross section proportional to A. At high energies the two amplitudes remain in phase and interfere destructively, analogous to Glauber shadowing in deuterium. If one assumes the relative magnitudes of the amplitudes are given by the vector dominance model, the original vector dominance prediction is obtained, namely, that the cross section at high energies should have the same A dependence as for ρ^0 's incident on nuclei.

The dimensionless parameter giving the transition energy for the two A dependences is the phase difference over two mean free paths,

$$\Delta\phi = \frac{M_\rho^2}{2k} \times 2\lambda \quad .$$

For a cross section of 30 mb, $\phi = 1$ for $k = 6$ GeV. The detailed calculations show that the transition energy is somewhat less than this on the light elements and somewhat more for the heavy ones. Note that although we have talked in terms of only ρ dominance here, one should of course include the ω and ϕ and possibly higher-mass vector mesons as well.

The Santa Barbara-SLAC collaboration¹⁶ has used its tagged-photon beam set-up to measure the A dependence of the total cross section. Their preliminary results are shown in Fig. 44 and indicate that the total cross section goes roughly as $A^{0.9}$, for the energy range between 7 and 18 GeV. Shadowing effects are thus appreciable (a factor of 1.6 for lead), but are not as strong as had been expected from VDM arguments for these high energies. Assuming ρ dominance and imaginary forward $\gamma A \rightarrow \rho A$ amplitude, the data are compared directly with the ρ photoproduction A dependence^{153,154} in Fig. 44. This comparison avoids nuclear physics problems and shows a large discrepancy with ρ dominance.

The data can be fit by assuming the cross sections to have two parts, the first going as A and the second as given by ρ dominance. The best fit gives roughly equal contributions from the two terms, and $\gamma_\rho^2/4\pi = 1.3 \pm 0.2$ in agreement with the Cornell¹⁵³ and SLAC¹⁵⁴ experiments on ρ^0 production from complex nuclei, but in disagreement with the storage ring value.⁹ One interpretation which saves vector dominance is that the part going as A corresponds to a heavy ($M \gtrsim 1500$ MeV) vector meson, in which case the shadowing will increase with energy.

Similar results have been recently obtained by a DESY counter group;¹⁵⁵ using data with $A \leq 64$ they find a dependence $A^{0.95 \pm 0.02}$ at 5.5 GeV.

2. Coherent Photoproduction of ρ^0 's From Complex Nuclei

Groups at DESY,¹⁵⁶ Cornell,¹⁵³ and SLAC¹⁵⁴ have studied the photoproduction of ρ^0 's from complex nuclei. Considerable amounts of data have already been published in the literature, and more is yet to come in the next few months. Unfortunately, the data as interpreted by the various groups lead to inconsistent results. Everyone does agree, however, that at small t values the process is dominated by coherent diffractive production with diffraction-peak widths characteristic of the radii of the various nuclei used. At larger t the data fall off more slowly, corresponding to incoherent production from individual nucleons.

One of the principle reasons for studying ρ production from complex nuclei is to obtain the total ρ -nucleon cross section $\sigma_{\rho N}$ from the A dependence of the forward cross sections. Changing nuclei effectively changes the target thickness, and the ρ meson produced inside the nucleus may or may not escape depending upon the size of the nucleus and the ρ^0 attenuation length in nuclear matter. The latter is directly related to the total ρN cross section. To give an idea of the sensitivity of the A dependence to $\sigma_{\rho N}$, we note that the lead-to-beryllium ratio changes by about 25% for $\sigma_{\rho N}$ going from 30 to 40 mb.

The A dependence for ρ^0 photoproduction was first studied theoretically by Drell and Trefil¹⁵⁷ using an eikonal approximation; there have since been some refinements of the original theory.^{158, 159} Unfortunately, there are several theoretical problems which must be faced before obtaining $\sigma_{\rho N}$. The first is a model for the nuclear density. The three different groups have used three different models as outlined in Table 2. The hard sphere model used by the DESY group is probably somewhat unrealistic. Both the SLAC and Cornell groups used the Wood-Saxon model, but the Cornell group obtained its value for the effective radius from the Glauber-Matthiae¹⁶⁰ analysis of proton-complex nucleus scattering while the SLAC group assumed the radius to go simply as $A^{1/3}$. For carbon the Cornell group used a harmonic oscillator model and indeed for both beryllium and carbon the simple Wood-Saxon model may not be sufficient to describe these light nuclei. One can presumably avoid some of these nuclear physics problems by comparing the A dependence found for ρ^0 photoproduction directly with that obtained by the elastic scattering of π 's or protons from complex nuclei; such comparisons have been made by the Cornell group.

Another difficulty arises from the finite mass of the ρ meson. Unlike true elastic scattering, the $\gamma\rho$ mass difference leads to a parallel momentum transfer $q_{\parallel} \approx \frac{M_{\rho}^2}{2k}$. For the heavier elements with their very steep diffraction peaks the phase change implied by q_{\parallel} results in a considerable reduction of the forward cross section. This is especially critical at the lower momenta and is roughly a factor of 10 for lead at the DESY energies.¹⁶¹ An additional minor difficulty is that this q_{\parallel} effect will tend to suppress the higher-mass ρ 's more than the lower-mass ρ 's, thus giving a shift to the mass peak. If there is a real part to the forward scattering amplitude, it will result in a phase change much like that due to q_{\parallel} .¹⁶² This introduces an additional uncertainty in the theory, especially at the lower energies.

Another theoretical trouble has been recently pointed out.¹⁶³ Two-nucleon correlations may increase the effective cross section for a particle in a nucleus by 10 or 15% over the free-nucleon cross section.

There are other uncertainties in comparing the results of the different laboratories. The Breit-Wigner shapes used to fit the data differ somewhat. For example, there is a 7% difference in normalization between the SLAC and Cornell Breit-Wigner shapes. Both the Cornell and DESY experiments have apparatus with rather limited apertures. They are thus dependent upon knowledge of the decay angular distribution from other experiments.

Table 2 shows $\sigma_{\rho N}$ as obtained by the various groups from the A dependence of the cross sections. The Cornell group includes deuterium data when making the fits but the other labs include neither hydrogen nor deuterium. Analysis of the DESY data by the theorists give 26 mb (Ref. 158) and 25 ± 3 mb (Ref. 159). The SLAC group has re-analyzed the Cornell data in terms of their own particular nuclear model and find the value of 30 mb, indicating the uncertainties involved in the details of the models.

The absolute normalizations of the data give values for $\gamma_\rho^2/4\pi$, also listed in the table. The DESY group gets a value consistent with that of the Orsay storage ring,⁹ while both the SLAC and the Cornell groups get a value of 1.1. Vector dominance can be used to predict the forward cross section from hydrogen,

$$\begin{aligned} \left(\frac{d\sigma}{dt}\right)_{t=0} (\gamma p \rightarrow \rho p) &= \frac{\alpha/\hbar^2}{64\pi} \frac{\sigma_{\rho N}^2}{\gamma_\rho^2/4\pi} \\ &= 0.0935 \frac{\sigma_{\rho N}^2}{\gamma_\rho^2/4\pi} \mu\text{b}/\text{GeV}^2 \end{aligned}$$

for $\sigma_{\rho N}$ in mb. The implied values are shown in Table 2. The Cornell results

come out close to that actually measured, as one might expect, since the deuterium results were used in the analysis. The DESY results seem rather high, however, and the SLAC results low. Correlations between γ_ρ^2 and $\sigma_{\rho N}$ make it difficult to estimate the uncertainties of the calculated values; since this is in some sense a determination of the over-all normalizations of the experiments, the error should be small. Taken at face value, the discrepancy shown by the last two rows of Table 2 is correlated with energy and may be a symptom of some theoretical disease. A recent review¹⁶⁴ discusses the various troubles in some detail. All three groups are now analyzing data over broader energy ranges and this should help to decide whether the troubles are experimental or theoretical.

It might be mentioned that all three groups appear to be reasonably happy with their normalizations. The DESY group used essentially the same apparatus to test QED, getting the approved results.¹⁶⁵ Both the Cornell and SLAC experiments have directly measured the cross sections from hydrogen and also obtained the approved values. In particular, recent results from SLAC¹⁶⁶ give the forward ρ^0 cross section at 9 GeV as $122 \pm 17 \mu\text{b}$. Thus it is hard to believe that a factor-of-2 discrepancy in normalizations could cause the differences in γ_ρ^2 's.

Swartz and Talman¹⁶² have found that if the real-to-imaginary part of the forward ρ -nucleon amplitude at 6 GeV is $\alpha = -0.45$, the Cornell data yield more popular results: $\gamma_\rho^2/4\pi = 0.65 \pm 0.10$ and $\sigma_{\rho N} = 27 \text{ mb}$. This value for α is rather large, however, and the sign is such as to make the discrepancies between labs worse.

3. Photoproduction of ϕ 's From Complex Nuclei

The DESY group has studied the A dependence of ϕ photoproduction at 5.2 GeV. Their preliminary results reported at Vienna² gave $\sigma_{\phi N} = 12 \pm 4 \text{ mb}$, in agreement with quark model calculations, but a rather large value for $\gamma_\phi^2/4\pi$,¹⁶¹ 7.8 ± 1.7

compared with the storage ring value 2.8 ± 0.4 . Considerably more data and a final analysis should be available soon.

Recent data¹⁶⁷ from Cornell on ϕ production from deuterium and complex nuclei (mainly at 8 GeV) have been fitted to give $\sigma_{\phi N} = 20 \pm 3$ mb and $\gamma_{\phi}^2/4\pi = 8.5$, assuming the real part of the forward ϕN scattering amplitude to be negligible. If $\alpha_{\phi} = -0.35$, these numbers become 12 mb and 3.4, respectively.

4. Incoherent ρ^0 Photoproduction From Complex Nuclei

The Cornell group¹⁶⁸ has studied ρ^0 photoproduction at $-t = 0.1$ GeV². Since coherent production from carbon falls off roughly as e^{60t} , it should be negligible at this momentum transfer. They found no significant background under the ρ peak and the results shown in Fig. 45 were all taken at the ρ peak position. By working close to the bremsstrahlung end-point they were able to reduce the production of additional mesons along with the ρ^0 . However, there may be a 15% inelastic background in their data at 4 GeV and perhaps somewhat more at 8 GeV. The results are shown in Fig. 45 in terms of A_{eff} , the ratio of the cross section found from complex nuclei to that from free nucleons (as estimated from deuterium measurements).

The theory used to describe incoherent ρ^0 photoproduction from complex nuclei is essentially the same as that discussed for the total photon cross section from complex nuclei.¹⁴⁹⁻¹⁵² Again, one expects a large energy variation, the cross sections being suppressed at high energies due to more effective shadowing. As shown in Fig. 45, however, the results are independent of energy. Also shown in the figure are the low- and high-energy limits of the theory. Photoproduction of π^+ from complex nuclei (see Section VI.5) indicates that at this momentum transfer the exclusion principle suppresses the cross section by a factor of 1.5. If the points shown in Fig. 45 were increased by this factor, they would lie well above the theoretical curves.

5. π^\pm, K^+ Photoproduction From Complex Nuclei

The SLAC 20 GeV spectrometer group¹⁶⁹ has studied charged meson photoproduction from complex nuclei. Since these are charge-exchange reactions, the amplitudes are expected to be mainly incoherent. Fits were made to data near the bremsstrahlung end-point energy to obtain cross sections for single-meson production. Nuclear excitations of up to about 100 MeV were accepted by these fits. Fermi motion of the nucleons broadens the resolution somewhat, the effect being worse at large t . It was found that the simple Fermi gas model with a cutoff momentum of 260 ± 40 MeV/c was consistent with the data, but that larger excursions could not be tolerated. This uncertainty resulted in a $\pm 16\%$ systematic error for the data at 0.45 GeV^2 (the worst case).

Figure 46 shows Z_{eff} , the ratio of the differential cross sections from complex nuclei to that from hydrogen. Note that here we use Z_{eff} instead of A_{eff} since the π^+ mesons can only be produced from protons. No energy dependence was seen, the χ^2 for no energy dependence being 12 for 13 degrees of freedom. The theory, however, predicts a factor-of- $1\frac{1}{2}$ difference for lead at the two energies, as shown by the curves in Fig. 46, calculated using the formalism of Gottfried and Yennie¹⁵¹ and normalized at each momentum transfer to the carbon data.

Figure 47 shows the effects of nucleon correlations (including exclusion-principle suppression). The values of Z_{eff} for each element have been normalized to that obtained at 0.16 GeV^2 . The trend with momentum transfer is quite apparent; at small momentum transfers the recoiling nucleon has trouble finding an unfilled state. The predictions of the simple Fermi gas model (with cutoff momentum 260 MeV/c) are also shown in the figure. They appear to be poor at both small and large momentum transfers. As t goes to zero, the model predicts that the cross sections also go to 0, while experimentally they appear to drop to roughly

1/3 the value seen at large momentum transfers. Further, there appears to be a $(30 \pm 12)\%$ increase in Z_{eff} in going from $-t = 0.16$ to 0.45 GeV^2 ; the theory predicted only a 7% increase. If the exclusion-principle suppression is assumed to be negligible at the widest momentum transfer, the theoretical curves shown in Fig. 46 should have a normalization of unity at $-t = 0.45 \text{ GeV}^2$. Instead the curves had to be increased by a factor of 1.5 in order to normalize to the carbon data.

To parameterize the breakdown of the vector dominance model, the vector dominance value for the amplitude of the two-step process was multiplied by w . The best fit for w was found to be 0.31 ± 0.12 , the error including estimates of the uncertainties in the nuclear physics and $\sigma_{\rho N}$. Taking $\alpha_{\rho} = \pm 0.3$ changes w by less than 0.02.

The production of π^- was measured at 16 GeV, $-t = 0.16 \text{ GeV}^2$. After correcting for N/Z (since π^- 's are only produced from neutrons and π^+ 's only from protons), the π^-/π^+ ratio is consistent with that seen directly from deuterium.⁵⁴ This implies that the elements studied have equal neutron and proton spatial distributions in the nuclei.

The photoproduction of K^+ 's was studied at 16 GeV, $-t = 0.04 \text{ GeV}^2$. In this case, not only N/Z corrections are needed, but also corrections for the fact that the K cross sections on nucleons are significantly less than those for pions. After these corrections the A dependence for K^+ photoproduction was found to be the same as that for π^+ . Comparing the K^+/π^+ ratio from hydrogen to that from complex nuclei gives an independent estimate of the exclusion-principle suppression for π^+ 's at 0.04 GeV^2 : 0.57 ± 0.09 . This compares well with the ratio obtained by simply looking at the change in Z_{eff} when going from 0.45 to 0.04 GeV^2 : 0.53 ± 0.06 .

6. Summary of Photoproduction From Complex Nuclei

Four reactions have been discussed: (a) coherent ρ (and ϕ) photoproduction, (b) incoherent ρ photoproduction, (c) π^{\pm} , K^+ photoproduction, and (d) the total

γA cross section. The last three reactions do not compare well with the vector dominance model. By implication, then, one should suspect also the first reaction, originally hailed as a great triumph for the vector dominance model. The more recent experiments on coherent ρ production at higher energies have shown discrepancies, and in fact there appears to be an energy trend for the over all normalization of this process (see last two lines of Table 2). By assuming the Cornell normalization for coherent ρ production to be correct, Schmidt and Yennie¹⁷⁰ have achieved a qualitative understanding of these four processes by allowing the vector-meson amplitudes to have mass dependences.

REFERENCES

1. B. Richter, Proc. 14th Int. Conf. on High Energy Physics, Vienna, Austria (1969); p. 3.
2. S.C.C. Ting, Proc. 14th Int. Conf. on High Energy Physics, Vienna, Austria (1969); p. 43.
3. E. Lohrmann, Summary Talk, Lund Int. Conf. on Elementary Particles, Lund, Sweden (1969).
4. H. Rollnick, Proc. of Heidelberg Int. Conf. on Elementary Particles, Heidelberg, Germany (1967); p. 400.
5. R. L. Walker, Phys. Rev. 182, 1729 (1969).
6. B. Gittelman and W. Schmidt, Phys. Rev. 175, 1998 (1968).
7. Y. Nambu and J. J. Sakurai, Phys. Rev. Letters 8, 79 (1962).
8. M. Gell-Mann, D. Sharp and W. G. Wagner, Phys. Rev. Letters 8, 261 (1962).
9. J. E. Augustin, Phys. Letters 28B, 503 (1969).
10. E. D. Bloom et al., "Determination of the total photon-proton cross section from high-energy inelastic electron scattering," Report No. SLAC-PUB-653, Stanford Linear Accelerator Center, Stanford University, Stanford, California, (1969).
11. J. T. Beale, S. D. Ecklund and R. L. Walker, "Pion photoproduction data below 1.5 GeV," Report No. CTSL-42, California Institute of Technology, Pasadena, California (1966).
12. H. Meyer et al., "Total cross section for photoproduction of hadrons on protons between 1.5 and 6.3 GeV," submitted to the Int. Symposium on Electron and Photon Interactions at High Energies, Daresbury, England (1969).
13. J. Ballam et al., Phys. Rev. Letters 23, 498 (1969).
14. H. G. Hilpert et al., Phys. Letters 27B, 474 (1968).

15. J. Ballam et al., Phys. Rev. Letters 21, 1544 (1968).
16. D. O. Caldwell et al., "Total photoabsorption cross sections up to 18 GeV and the nature of photon interactions," University of California, Santa Barbara, California, contribution to this Conference (1969); and private communication.
17. V. D. Mur, JETP 17, 1458 (1963); 18, 727 (1964).
18. H. Abarbanel et al., Phys. Rev. 160, 1329 (1967).
19. M. J. Creutz, S. D. Drell and E. A. Paschos, Phys. Rev. 178, 2300 (1969).
20. Aachen-Berlin-Bonn-Hamburg-Heidelberg-München Collaboration, Phys. Rev. 175, 1669 (1968).
21. Y. Eisenberg et al., Phys. Rev. Letters 22, 669 (1969).
22. J. Ballam et al., " γp interactions at 5.25 GeV," Report No. SLAC-PUB-625, Stanford Linear Accelerator Center, Stanford University, Stanford, California (1969). (Submitted to Phys. Rev. Letters.)
23. J. Ballam et al., Phys. Rev. Letters 21, 1541 (1968).
24. M. Davier et al., "Multibody photoproduction between 2 and 16 GeV," Report No. SLAC-PUB-613, Stanford Linear Accelerator Center, Stanford University, Stanford, California (1969).
25. R. Anderson et al., "Neutral boson photoproduction on hydrogen at high energies," Report No. SLAC-PUB-644, Stanford Linear Accelerator Center, Stanford University, Stanford, California (1969). (Submitted to Phys. Rev.)
26. K. Schilling and F. Storim, Nucl. Phys. B7, 559 (1968).
27. G. McClellan et al., Phys. Rev. Letters 22, 374 (1969).
28. H. J. Lipkin, Phys. Rev. Letters 16, 1015 (1966); the model was extended to finite values of t by B. Margolis, Nucl. Phys. B6, 687 (1968).
29. M. Ross and L. Stodolsky, Phys. Rev. 149, 1172 (1966).

30. G. Kramer and J. L. Uretsky, Phys. Rev. 181, 1918 (1969).
31. P. Söding, Phys. Letters 19, 702 (1966).
32. R. T. Deck, Phys. Rev. Letters 13, 169 (1964).
33. L. Criegee et al., Phys. Letters 28B, 282 (1968); and U. Timm, private communication. Figure 5 is taken from Ref. 3.
34. G. Diambri-Palazzi et al., "Photoproduction of rho mesons from hydrogen and carbon by linearly polarized photons," Report No. CLNS-83, Cornell University, Ithaca, New York (1969).
35. J. Ballam et al., "Production of ρ^0 mesons by linearly polarized photons at 2.8 and 4.7 GeV," contributed to this Conference (1969).
36. J. Ballam et al., "Study of the reactions $\gamma p \rightarrow p \pi^+ \pi^- \pi^0$ and $\gamma p \rightarrow p K^+ K^-$ with 2.8 and 4.7 GeV linearly polarized photons," contributed to this Conference (1969).
37. Aachen-Berlin-Bonn-Hamburg-Heidelberg-München Collaboration, Phys. Letters 27B, 54 (1968).
38. G. McClellan et al., "Photoproduction of ϕ mesons from hydrogen and deuterium," Report No. CLNS-69, Cornell University, Ithaca, New York (1969).
39. H. Joos, Proc. Int. Conf. on Elementary Particles, Heidelberg, Germany, (1967); p. 349.
40. L. Stodolsky, Phys. Rev. Letters 18, 135 (1967).
41. Z. G. T. Guiragossian and A. Levy, Nucl. Phys. B11, 449 (1969).
42. Joel A. Shapiro, Phys. Rev. 179, 1345 (1969).
43. G. McClellan et al., Phys. Rev. Letters 23, 718 (1969).
44. N. Hicks et al., Phys. Letters 29B, 602 (1969).
45. M. Davier et al., "Observation of a πA_1 enhancement in high-energy photoproduction," contributed to this Conference (1969).

46. D. Earles et al., "Photoproduction of muon pairs: search for meson resonances with invariant masses between 900 and 1800 MeV," contributed to this Conference (1969).
47. Presented to this Conference by P. Joseph.
48. Frank Wolverton, private communication.
49. M. Braunschweig et al., Phys. Letters 26B, 405 (1968).
50. H. G. Hilpert et al., Nucl. Phys. B8, 535 (1968).
51. G. Buschhorn et al., Phys. Rev. Letters 17, 1027 (1966) and 18, 571 (1967); Phys. Letters 25B, 622 (1967).
52. P. Heide et al., Phys. Rev. Letters 21, 248 (1968).
53. A. M. Boyarski et al., Phys. Rev. Letters 20, 300 (1968).
54. A. M. Boyarski et al., Phys. Rev. Letters 21, 1767 (1968).
55. A. M. Boyarski et al., Phys. Rev. Letters 22, 148 (1969).
56. R. Diebold, "Compilation of photoproduction cross sections," Internal Report No. RD-19, Stanford Linear Accelerator Center, Stanford University, Stanford, California (1968). (Unpublished.)
57. For example, V. Barger and D. Cline, Phys. Letters 27B, 312 (1968).
58. D.R.O. Morrison, Phys. Letters 22, 528 (1966).
59. The SLAC 1968 data are the work of A. M. Boyarski et al., and are the same as quoted by Ref. 1.
60. Z. Bar-Yam et al., Phys. Rev. Letters 19, 40 (1967).
61. J. Frøyland and D. Gordon, Phys. Rev. 177, 2500 (1969).
62. H. Burfeindt et al., "Small momentum transfer π^+ -production with polarized photons," submitted to the Int. Symposium on Electron and Photon Interactions at High Energies, Daresbury, England (1969).

63. H. Burfeindt et al., " π^- -production with linearly polarized photons," submitted to the Int. Symposium on Electron and Photon Interactions at High Energies, Daresbury, England (1969).
64. C. Geweniger et al., Phys. Letters 28B, 155(1969).
65. C. Geweniger et al., Phys. Letters 29B, 41 (1969).
66. Z. Bar-Yam et al., "Photoproduction of single charged pions from deuterium with polarized photons," submitted to the Int. Symposium on Electron and Photon Interactions at High Energies, Daresbury, England (1969).
67. Z. Bar-Yam et al., contribution to the Int. Symposium on Electron and Photon Interactions at High Energies, Daresbury, England (1969).
68. J. S. Ball, Phys. Rev. 124, 2014 (1961).
69. Frank S. Henyey, Phys. Rev. 170, 1619 (1968).
70. S. D. Drell and J. D. Sullivan, Phys. Rev. Letters 19, 268 (1967).
71. P. di Vecchia et al., Phys. Letters 27B, 296 (1968).
72. J. D. Jackson and C. Quigg, Phys. Letters 29B, 236 (1969).
73. Nina Byers and G. H. Thomas, Phys. Rev. Letters 20, 129 (1968).
74. P. Stichel, Zeitschrift f. Physik 180, 170 (1964).
75. See for example:
 J. S. Ball, W. R. Frazer and M. Jacob, Phys. Rev. Letters 20, 518 (1968);
 S. Frautschi and L. Jones, Phys. Rev. 163, 1820 (1967);
 P. K. Mitter, Phys. Rev. 162, 1624 (1967);
 Y. Tomozawa, Nuovo Cimento 57A, 165 (1968);
 R. C. Brower and J. W. Dash, Phys. Rev. 175, 2014 (1968).
76. A. P. Contogouris and J. P. Lebrun, "Moving branch points and two-body inelastic reactions," McGill University preprint, McGill University, Montreal, Quebec, Canada (1969).

- M. L. Blackmon, G. Kramer and K. Schilling, "Regge-pole model with absorptive correction cuts for photoproduction of charged pions," Argonne National Laboratory preprint, Argonne, Illinois (1969).
- A. B. Kaidalov and B. M. Karnakov, Phys. Letters 29B, 376 (1969).
- G. Benfatto, F. Nicolò and G. C. Rossi, Lettere al Nuovo Cimento 1, 537 (1969), and Nota Interna 227, University of Rome, Rome, Italy.
77. See for example:
- D. Amati et al., Phys. Letters 26B, 510 (1968).
- K. Dietz and W. Korth, Phys. Letters 26B, 394 (1968).
- I. Bender et al., "Fixed poles in photoproduction of charged pions," Heidelberg preprint, Heidelberg, Germany (1968).
78. M. LeBellac, Phys. Letters 25B, 524 (1967);
- M. Aderholz et al., Phys. Letters 27B, 174 (1968).
79. J. P. Ader and M. Capdeville, " π -conspiracy and factorization in vector mesons and Δ (1236) isobar photoproduction," Bordeaux preprint PTB-31, Bordeaux, France (1969).
80. R. Diebold, Phys. Rev. Letters 22, 204 (1969).
81. A. Borgese and M. Colocci, Nuovo Cimento 56A, 245 (1968).
82. For example see:
- G. L. Kane et al., "Strong Regge cut model for photoproduction of pions," contribution to the Int. Symposium on Electron and Photon Interactions at High Energies, Daresbury, England (1969).
83. A. Bialas et al., Nucl. Phys. B6, 483 (1968); Phys. Letters 26B, 513 (1968).
84. M. Krammer and D. Schildknecht, Nucl. Phys. B7, 583 (1968).
85. R. Diebold and J. A. Poirier, Phys. Rev. Letters 20, 1532 (1968).

Similar results were obtained by:

- Margarete Krammer, Phys. Letters 26B, 633 (1968); 27B, 260 (E) (1968).
- A. Dar et al., Phys. Rev. Letters 20, 1261 (1968).
- I. Derado and Z. G. T. Guiragossian, Phys. Rev. Letters 21, 1556 (1968).
- C. Iso and H. Yoshii, Ann. Phys. 47, 424 (1968).
86. R. Diebold and J. A. Poirier, Phys. Rev. Letters 22, 255, 692(E) (1969).
87. J. P. Ader et al., Nuovo Cimento 56A, 952 (1968).
88. L. J. Gutay et al., Phys. Rev. Letters 22, 424 (1969).
89. H. Fraas and D. Schildknecht, Nucl. Phys. B6, 395 (1968).
90. A. Bialas and K. Zalewski, Phys. Letters 28B, 436 (1969).
91. J. T. Donohue and H. Högaasen, Phys. Letters 25B, 554 (1967).
92. M. LeBellac and G. Plaut, "Vector meson dominance and high-energy behavior," Nice preprint N TH 69/2, Nice, France (1969).
93. C. F. Cho and J. J. Sakurai, Phys. Letters 30B, 119 (1969).
94. F. T. Meiere, Phys. Letters 30B, 44 (1969).
95. R. Diebold and J. A. Poirier, Phys. Rev. Letters 22, 906 (1969).
96. Z. G. T. Guiragossian and A. Levy, Phys. Letters 30B, 48 (1969); note that these authors (as did several others) used an incorrect flux-phase space factor $|\vec{p}_\pi/\vec{p}_\rho|^2 = 1.22$ instead of the correct $|\vec{p}_\pi/\vec{p}_\gamma|^2 = 0.99$, when comparing the ρ^- and γ -initiated reactions. The correct factor implies a smaller value of $\gamma_\rho^2/4$ if the VDM comparison is to work.
97. D. Schildknecht, "Vector meson dominance and photoproduction," Report No. DESY 69/10, DESY, Hamburg, Germany (1969).
98. H. Harari and B. Horowitz, Phys. Letters 29B, 314 (1969); Y. Avni and H. Harari, Phys. Rev. Letters 23, 262 (1969).
99. G. Kane, private communication.

100. W. Schmidt, "Vector meson dominance and pion production," Report No. CLNS-72, Cornell University, Ithaca, New York (1969).
101. P. D. Mannheim and U. Maor, "Vector dominance in the transversity frame," Tel-Aviv preprint No. TAUP-94-69, Tel-Aviv, Israel.
102. N. N. Biswas et al., "Has the vector dominance model failed?" Notre Dame University preprint, Notre Dame, Indiana (1969).
103. R. Anderson et al., Phys. Rev. Letters 21, 384 (1969).
104. J. P. Ader, M. Capdeville and P. Salin, Nucl. Phys. B3, 407 (1967).
105. Maurice L. Blackmon et al., Phys. Rev. 183, 1452 (1969).
106. A. Capella and Tran Thanh Van, Lettere al Nuovo Cimento 1, 321 (1969).
107. A. P. Contogouris et al., "Regge cuts and neutral pion photoproduction," McGill University preprint, Montreal, Quebec, Canada (1969).
108. Jan Frøyland, Nucl. Phys. B11, 204 (1969).
109. H. Primakoff, Phys. Rev. 81, 899 (1951).
110. F. J. Gilman, "The sign of the $\pi^0 \rightarrow \gamma\gamma$ decay amplitude," Report No. SLAC-PUB-594, Stanford Linear Accelerator Center, Stanford University, Stanford, California (1969).
111. S. L. Adler, Institute for Advanced Study preprint (1968).
112. D. Bellenger et al., Phys. Rev. Letters 23, 540 (1969).
113. H. Harari, Phys. Rev. Letters 21, 835 (1968).
114. G. C. Bolon et al., "Photoproduction of π^0 's from neutrons at 4 GeV," Massachusetts Institute of Technology preprint, Cambridge, Massachusetts, submitted to this Conference.
115. G. C. Bolon et al., Phys. Rev. Letters 18, 926 (1967). L. Osborne, Proc. of Int. Symposium on Electron and Photon Ints. at High Energies, 1, 91 (1965).

116. R. L. Anderson et al., Phys. Rev. Letters 23, 721 (1969); see also
R. L. Anderson et al., Phys. Rev. Letters 21, 479 (1968).
117. D. Tompkins et al., Phys. Rev. Letters 23, 725 (1969).
118. V. Barger and P. Weiler, Phys. Letters 30B, 105 (1969).
119. J. V. Beaupré and E. A. Paschos, "A phenomenological analysis of π^+
and π^0 photoproduction at backward angles," Report No. SLAC-PUB-632,
Stanford Linear Accelerator Center, Stanford University, Stanford,
California (1969).
120. S. Meshkov, private communication.
121. G. Buschhorn et al., Phys. Rev. Letters 20, 230 (1968).
122. D. Bellenger et al., Phys. Rev. Letters 21, 1205 (1968).
123. Bonn group, quoted by K. Lübelmeyer, International Symposium on
Electron and Photon Interactions at High Energies, Daresbury, England (1969).
124. A. Dar and V. F. Weisskopf, Phys. Rev. Letters 20, 762 (1968).
125. B. Gorczyca and M. Hayashi, "The vector-dominance model and the γ photo-
production," Jagellonian University preprint, Cracow, Poland (1968).
126. A. M. Boyarski et al., "Measurement of the $\pi^\pm \Delta(1238)$ photoproduction
cross section off hydrogen and deuterium as a function of t at 16 GeV,"
contributed to this Conference.
127. P. Stichel and M. Scholz, Nuovo Cimento 34, 1381 (1964).
128. W. G. Wagner and D. H. Sharp, Phys. Rev. 128, 2899 (1962).
129. M. Aderholz et al., Nucl. Phys. B8, 45 (1968) and D.R.O. Morrison,
private communication.
130. A. Dar, Nucl. Phys. B11, 634 (1969).
131. E. Gotsman, "The vector dominance model and the reaction $\gamma p \rightarrow \pi^- \Delta^{++}$,"
UCSD-10P10-56; "VDM predictions for $\Delta(1240)$ photoproduction," UCSD-
10P10-63 (1969).

132. M. Walter, "On the energy dependence of the $\pi^+p \rightarrow N^*\rho^0$ production cross section," Report No. PHE 69-1, Deutsche Akademie der Wissenschaften zu Berlin-Zeuthen (1969).
133. H. Thom, Phys. Rev. 151, 1322 (1966).
134. Aachen-Berlin-Bonn-Hamburg-Heidelberg-München Collaboration, "Multipion and strange particle photoproduction on protons at energies up to 5.8 GeV," Report No. DESY 69/19, DESY, Hamburg, Germany (1969).
135. A. M. Boyarski et al., Phys. Rev. Letters 22, 1131 (1969).
136. C. C. Shih and Wu-Ki Tung, Phys. Rev. 180, 1446 (1969).
137. Jan Frøyland, Nucl. Phys. B12, 410 (1969).
138. J. K. Kim, Phys. Rev. Letters 19, 1079 (1967).
139. A. Borgese and M. Colocci, "A Regge cut model for the photoproduction of $K^+\Lambda$ and $K^+\Sigma^0$ from hydrogen at high energies," Report No. TH-1024, CERN, Geneva, Switzerland (1969).
140. A. M. Baldin, JETP Letters 3, 171 (1966).
141. J. Kupsch, Phys. Letters 22, 690 (1966).
142. S. Meshkov and R. Ponzini, Phys. Rev. 175, 2030 (1968).
143. A. M. Boyarski et al., "Photoproduction of K^+ -hyperons from hydrogen and deuterium at 11 GeV," contributed to this Conference.
144. R. L. Anderson et al., Phys. Rev. Letters 23, 890 (1969).
145. C. A. Levinson, H. J. Lipkin and S. Meshkov, Phys. Letters 7, 81 (1963).
146. S. P. Ying et al., "Differential cross section of the reaction $\pi^+p \rightarrow K^+Y^*$ (1385) at 4.0 and 5.05 GeV/c," University of Michigan preprint, University of Michigan, Ann Arbor, Michigan (1969).

147. H. Satz, Phys. Rev. Letters 19, 1453 (1967); Phys. Letters 25B, 27 (1967).
148. L. Stodolsky, Phys. Rev. Letters 18, 135 (1967).
149. M. Nauenberg, Phys. Rev. Letters 22, 556 (1969).
150. B. Margolis and C. Tang, Nucl. Phys. B10, 329 (1969).
151. K. Gottfried and D. R. Yennie, Phys. Rev. 182, 1595 (1969).
152. S. Brodsky and J. Pumplin, Phys. Rev. 182, 1794 (1969).
153. G. McClellan et al., Phys. Rev. Letters 22, 377 (1969).
154. F. Bulos et al., Phys. Rev. Letters 22, 490 (1969).
155. H. Meyer et al., "Total cross section for photoproduction of hadrons on D_2 , Be, C, Al, Ti and Cu between 1.5 and 6.3 GeV," DESY contribution to the International Symposium on Electron and Photon Interactions at High Energies, Daresbury, England (1969).
156. J. G. Asbury et al., Phys. Rev. Letters 19, 865 (1967) and 20, 1134(E), 227 (1968).
157. S. D. Drell and J. S. Trefil, Phys. Rev. Letters 16, 552, 832(E), (1966).
158. K. S. Kölbig and B. Margolis, Nucl. Phys. B6, 85 (1968).
159. J. S. Trefil, Phys. Rev. 180, 1379 (1969).
160. R. J. Glauber and G. Matthiae, "Nuclear structure determination from 20-GeV proton scattering," Report No. ISS 67/16, Istituto Superiore di Sanità, Rome, Italy (1967).
-
161. Ulrich Becker, "Photoproduction of ρ^0 and ϕ mesons in the forward direction at various atomic nuclei," thesis (February 1968). Translation available: Report No. SLAC-TRANS-92, Stanford Linear Accelerator Center, Stanford University, Stanford, California.
162. J. Swartz and R. Talman, "Real parts of vector meson scattering amplitudes, Report No. CLNS-79, Cornell University, Ithaca, New York (1969).

163. E. J. Moniz and G. D. Nixon, "Effect of correlations on high energy processes using nuclear targets," Stanford University perprint, Stanford, California (1969).
164. R. Wilson, *Lettere al Nuovo Cimento* 1, 952 (1969).
165. J. G. Asbury et al., *Phys. Rev.* 161, 1344 (1967).
166. F. Bulos et al., contribution to this Conference.
167. G. McClellan et al., "Photoproduction of ϕ mesons from complex nuclei," Report No. CLNS-70, Cornell University, Ithaca, New York (1969).
168. G. McClellan et al., *Phys. Rev. Letters* 23, 554 (1969).
169. A. M. Boyarski et al., "Single π^\pm and K^+ meson photoproduction from complex nuclei at 8 and 16 GeV," Report No. SLAC-PUB-671, Stanford Linear Accelerator Center, Stanford University, Stanford, California (1969), and private communication.
170. W. Schmidt and D. R. Yennie, *Phys. Rev. Letters* 23, 623 (1969).

TABLE I
VECTOR DOMINANCE CALCULATIONS FOR VECTOR MESON PHOTO-
PRODUCTION FROM HYDROGEN AT 10 GeV

V^0	$\frac{g_{\gamma V}^2}{4\pi}$ (a)	$g_{\gamma V}^2$	$\frac{d\sigma}{dt}(\gamma p \rightarrow V^0 p)_{0^\circ}$ (b)	$\sigma_{\text{tot}}(V^0 p)$	Contribution to $\sigma_{\text{tot}}(\gamma p)$
			$\mu\text{b}/\text{GeV}^2$	mb	μb
ρ^0	0.52 ± 0.03	$\frac{1}{290}$	120 ± 15	26 ± 2	91 ± 7
ω	3.7 ± 0.7	$\frac{1}{2000}$	16 ± 6	25 ± 5	12 ± 3
ϕ	2.8 ± 0.4	$\frac{1}{1500}$	3 ± 1.5	9.4 ± 2.4	$\pm(6 \pm 2)$

(a) Ref. 9.

(b) Estimate of 10 GeV forward cross section (obtained by crude average over various experiments).

TABLE II

SUMMARY OF THE THREE EXPERIMENTS ON $\gamma A \rightarrow \rho^0 A$

	DESY	CORNELL	SLAC
k(GeV)	2.7 - 4.5	6.2	8.8
Nuclear density	Hard sphere fixed r_0	Wood-Saxon variable C_0	Wood-Saxon fixed C_0
$\sigma_{\rho N}$ (mb)	31.3 ± 2.3	38 ± 3	30^{+6}_{-4}
$\gamma_{\rho}^2/4\pi$	0.45 ± 0.10	1.1 ± 0.15	1.1 ± 0.2
$\frac{d\sigma}{dt}(\gamma p \rightarrow \rho^0 p)_{0^0}$ $\mu\text{b}/\text{GeV}^2$			
Implied	204	123	76
Measured	150	130	120

FIGURE CAPTIONS

1. Compilation of data on the total γp cross section for hadronic interactions. The data are from Refs. 10, 11, 13, 15, 16, 12 (in the order listed in the figure). Both the laboratory photon energy k and the total energy W in the center-of-mass are shown. Systematic errors of $\pm 8\%$ are estimated for the electron-scattering results.
2. Compilation of total cross sections for vector meson photoproduction. The solid points are from the DESY bubble chamber (Ref. 20), the open circles from the SLAC annihilation beam (Refs. 21-23), the x's from the SLAC streamer chamber (Ref. 24) and the crosses from the SLAC 1.6 GeV/c spectrometer (Ref. 25). The open squares are from the SLAC backscattered laser beam (Ref. 36) and the open triangle from the Cornell spectrometer (Ref. 38).
3. Comparison of the predictions of a broken-SU(3) quark model with high energy ρ^0 photoproduction measured with the SLAC 1.6 GeV/c spectrometer (Ref. 25).
4. Comparisons of the Söding interference model with experimental results (from Ref. 24). (a) $\pi^+ \pi^-$ mass spectrum. (b) Slope of the cross section as a function of $\pi^+ \pi^-$ effective mass.
5. Asymmetry of ρ^0 photoproduction measured at DESY with wire spark chambers and a linearly polarized photon beam (Ref. 33).
6. Comparison of the predictions of a broken-SU(3) quark model with ϕ photoproduction measured by the SLAC 1.6 GeV/c spectrometer group (Ref. 25) and by the DESY-MIT counter group (Ref. 2) and the DESY bubble chamber group (Ref. 37).
7. Dipion mass distribution measured from carbon by the Cornell spectrometer group (Ref. 43). The photon energy is proportional to the $\pi\pi$ mass and is 8 GeV at $M_{\pi\pi} = 1600$ MeV.

8. Mass distributions showing a broad enhancement near 1520 MeV (from Ref. 45).
9. Compilation of total cross sections for various pion channels. The curves at low energies are from the Caltech compilation of counter data (Ref. 11; the π^0 data at the third resonance is from Ref. 48). The high energy π^0 data come mainly from a DESY counter experiment (Ref. 49). The line segments represent data from the DESY bubble chamber (Refs. 20, 50). The x's and solid circles for single π^\pm production are data from spectrometer groups at DESY (Refs. 51, 52) and SLAC (Refs. 53, 54), respectively. For Δ^{++} production the open and solid circles are from the SLAC streamer chamber (Ref. 24) and bubble chambers (Refs. 21, 22, 35); the x's are from the SLAC 20 GeV/c spectrometer (Ref. 55). Further details are given in Ref. 56.
10. Schematic comparison of the momentum-transfer dependences for various processes involving pseudoscalar-meson production. The data used to draw these curves were taken at 8 GeV (6 GeV for the π^0 curve); the factor $(s-M_p^2)^2$ makes the curves independent of energy to first approximation.
11. Differential cross sections for single π^+ production (Refs. 52, 53, 59). The curves are merely drawn to guide the eye. The effective Regge parameter α shown in the inset was calculated using only the data with $k \geq 8$ GeV.
12. Ratio of single pion production, π^-/π^+ from deuterium. The CEA, DESY and SLAC data are from Refs. 60, 52 and 54, respectively. The curves show the results of the Frøylund-Gordon fit (Ref. 61).
13. Compilation of the asymmetry of single pions produced by linearly polarized photons, plotted as a function of $\sqrt{-t}$ to expand the forward region. The two most forward π^+ points are preliminary (Ref. 62), as are the DESY π^- points (Ref. 63) except those at $\sqrt{-t} = 0.45$ and 0.63 GeV/c (Ref. 64). The other π^+ points are from Ref. 65 while the CEA points are from Ref. 66. The DESY

- data were taken at an energy $k = 3.4$ GeV and the CEA data at 3.0 GeV. The curves are the Fróyland-Gordon (Ref. 61) predictions for 3.4 GeV.
14. Single π^+ differential cross section, multiplied by $(s-M_p^2)^2$, and plotted as a function of $\sqrt{-t}$. The data references are the same as for Fig. 11. The dashed curve (CMSR) is from Ref. 71 and the dotted curve shows the "pseudomodel" results of Jackson and Quigg (Ref. 72).
 15. Feynman diagrams for single π^+ photoproduction.
 16. Cross sections for single-pion production by 3.4 GeV linearly polarized photons, as obtained by combining the data of Figs. 11, 12, and 13. The particle symbols represent amplitudes for t-channel exchange of the particles.
 17. Vector dominance comparison for single pions produced by unpolarized photons, from Diebold and Poirier (Ref. 85).
 18. Vector dominance comparison for single pions produced by photons with linear polarization perpendicular to the production plane (Ref. 95).
 19. Average value of $\cos 2\phi$ as a function of $\cos \theta$ for $\pi \rightarrow \rho$; ϕ and θ are the ρ decay angles in the helicity frame. The χ^2 values indicate the goodness of the best fits to the form $\sin^2 \theta$ expected if only S and P waves are present (from Ref. 102).
 20. Cross sections for π^0 photoproduction (Refs. 49 and 103). The curves show the results of the Regge cut model of Blackmon et al. (Ref. 105). The values of the Regge spin parameter α shown in the inset were taken from the fits shown in Fig. 21 (Ref. 25).
 21. Differential π^0 cross sections (Refs. 25, 49) at fixed t . The straight lines are fits to the data of the form $(s-M_p^2)^{2\alpha-2}$ (Ref. 25).
 22. Differential π^0 cross section (Ref. 49) on an expanded scale to show interference between the one-photon exchange amplitudes (Primakoff effect) and the ω and B

exchange amplitudes (from the fit of Ref. 104). The triangles show the theoretical limits assuming complete constructive or destructive interference.

23. Asymmetry of π^0 production by polarized photons (Ref. 112), compared with several theoretical models (Refs. 104, 105, 108).
24. Preliminary results on the ratio of π^0 cross sections from neutrons and protons at 4 GeV (Ref. 114). The curves show the predictions of Frøyland (Ref. 108) and Dar et al. (Ref. 85).
25. Compilation of π^0 and π^+ cross sections from Refs. 49, 53, 103, 115-117.
26. Backward photoproduction cross sections (Refs. 116, 117).
27. Comparison of the 180° DESY π^0 cross sections (Ref. 121) with the extrapolation of the Barger-Weiler fit (Ref. 118) to the high-energy backward cross sections.
28. Differential η cross sections (Refs. 25, 122) compared with π^0 production and two theoretical predictions (Refs. 124, 125).
29. Differential cross sections for Δ^{++} production (from Ref. 55). For comparison, the single π^+ cross sections (Ref. 53) are shown schematically by the dashed curves. The effective Regge α was calculated from the 8 to 16 GeV data.
30. Data of Fig. 29 plotted versus $\sqrt{-t}$ to better show the forward region. The curve shows the prediction of Stichel and Scholz (Ref. 127).
31. Ratio of Δ^{++} to Δ^- production at 16 GeV, plotted as a function of $\sqrt{-t}$ (Ref. 126). The curve schematically shows the π^- to π^+ ratio for single-pion production (Ref. 54).
32. Deuterium-to-hydrogen ratios at 16 GeV for Δ photoproduction in association with π^+ or π^- (Ref. 126). The horizontal lines at 4 and $4/3$ show the values expected for π^+ and π^- , respectively, assuming no $I = 2$ exchange in the t channel.

33. Vector dominance comparison of Δ production neglecting line-reversal effects. The data for $\gamma p \rightarrow \pi^- \Delta^{++}$ (Ref. 55) and $\pi^+ p \rightarrow \rho^0 \Delta^{++}$ (Ref. 129) were taken at 8 GeV. The photoproduction ratio Δ^-/Δ^{++} was taken at 16 GeV (Ref. 126).
34. Compilation of the total cross sections for $\gamma p \rightarrow K^+ \Lambda$ and $\gamma p \rightarrow K^+ \Sigma^0$ (Refs. 133-135, triangles, squares and circles, respectively). The cross sections have been multiplied by k^2 (photon laboratory energy) to better show the asymptotic behavior.
35. Differential cross sections for $\gamma p \rightarrow K^+ \Lambda$ (Ref. 135); the lines are merely drawn to guide the eye. The effective Regge α was calculated from the 8 to 16 GeV data.
36. The ratio of cross sections $\gamma p \rightarrow K^+ \Sigma^0$ to $\gamma p \rightarrow K^+ \Lambda$ (Ref. 135). The arrows at $t = 0$ show the results of $SU(6)_W$ calculations (Ref. 142).
37. Differential cross sections for K^+ production from hydrogen at 11 GeV (Ref. 143).
38. Deuterium-to-hydrogen ratios as a function of t for Λ, Σ and 1400-step at 11 GeV (Ref. 143). The average values are also shown.
39. Backward K^+ photoproduction (Ref. 144). The backward π^+ cross section (Ref. 116) is also shown schematically.
40. Comparison of the $SU(3)$ triangle prediction with experiment (Ref. 135). $|\cos \phi| > 1$ indicates a violation of the prediction.
41. $SU(3)$ comparison of $\Delta(1236)$ and $Y^*(1385)$ photoproduction (Ref. 143).
42. Comparison of four-charged-pion photoproduction with inelastic πp reactions using vector dominance and the quark model (Satz model, Ref. 147), from Ref. 24.
43. Diagrams considered in recent theoretical work (Refs. 149-152) on vector dominance for reactions in complex nuclei.

44. Total γA cross sections (Ref. 16) compared with $\sigma(\gamma A) = A\sigma(\gamma p)$ and with the vector dominance prediction using ρ^0 photoproduction (Refs. 154, 153).
45. Incoherent ρ^0 photoproduction at $-t = 0.1 \text{ GeV}^2$ (Ref. 168), uncorrected for exclusion-principle suppression; the vector dominance predictions are also shown.
46. Single π^+ photoproduction from complex nuclei (Ref. 168); the vector dominance curves have been normalized at each momentum transfer to the carbon data. Z_{eff} is the effective number of protons contributing to π^+ production, given by the ratio of the differential cross section from complex nuclei to that from hydrogen.
47. Exclusion-principle suppression shown by the dependence of Z_{eff} on three-momentum transfer, normalized to the data near $\Delta p = 400 \text{ MeV}/c$ for each element (Ref. 169).

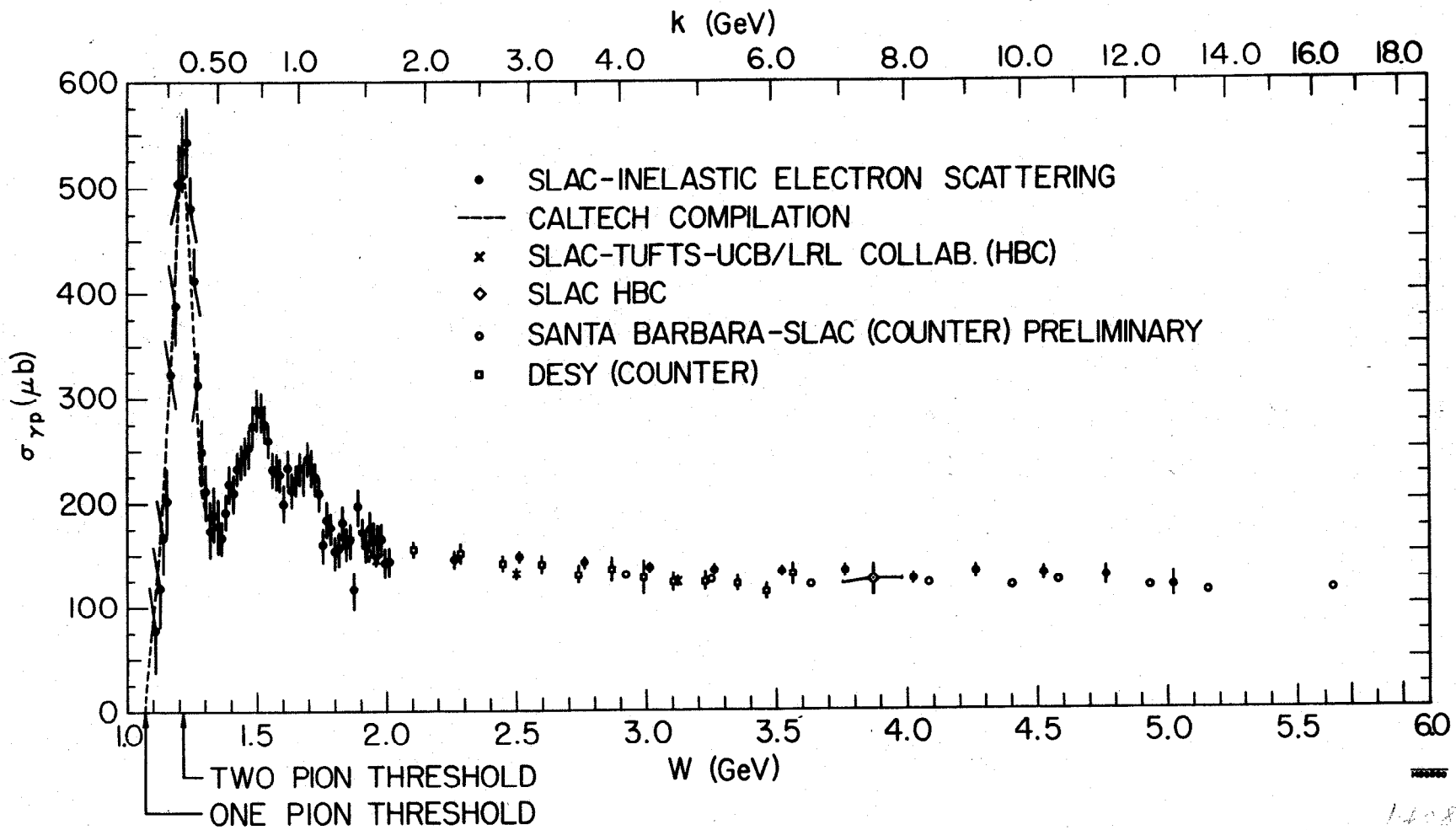
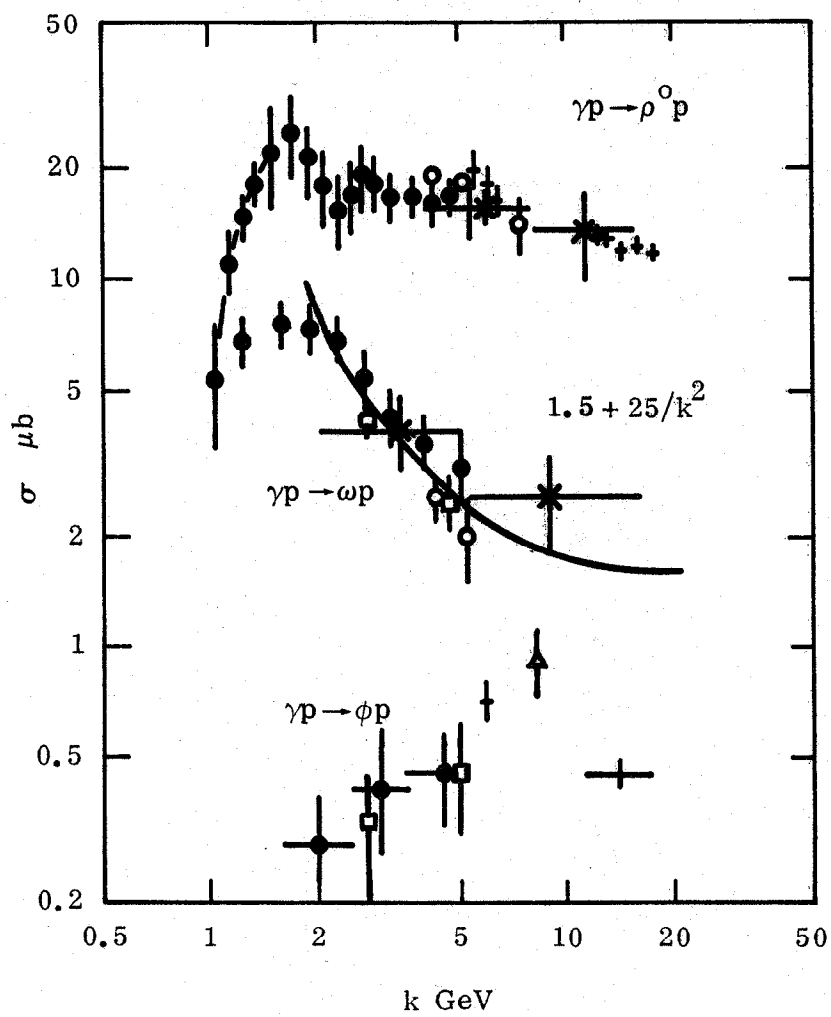


Fig. 1

140800



1408A41

Fig. 2

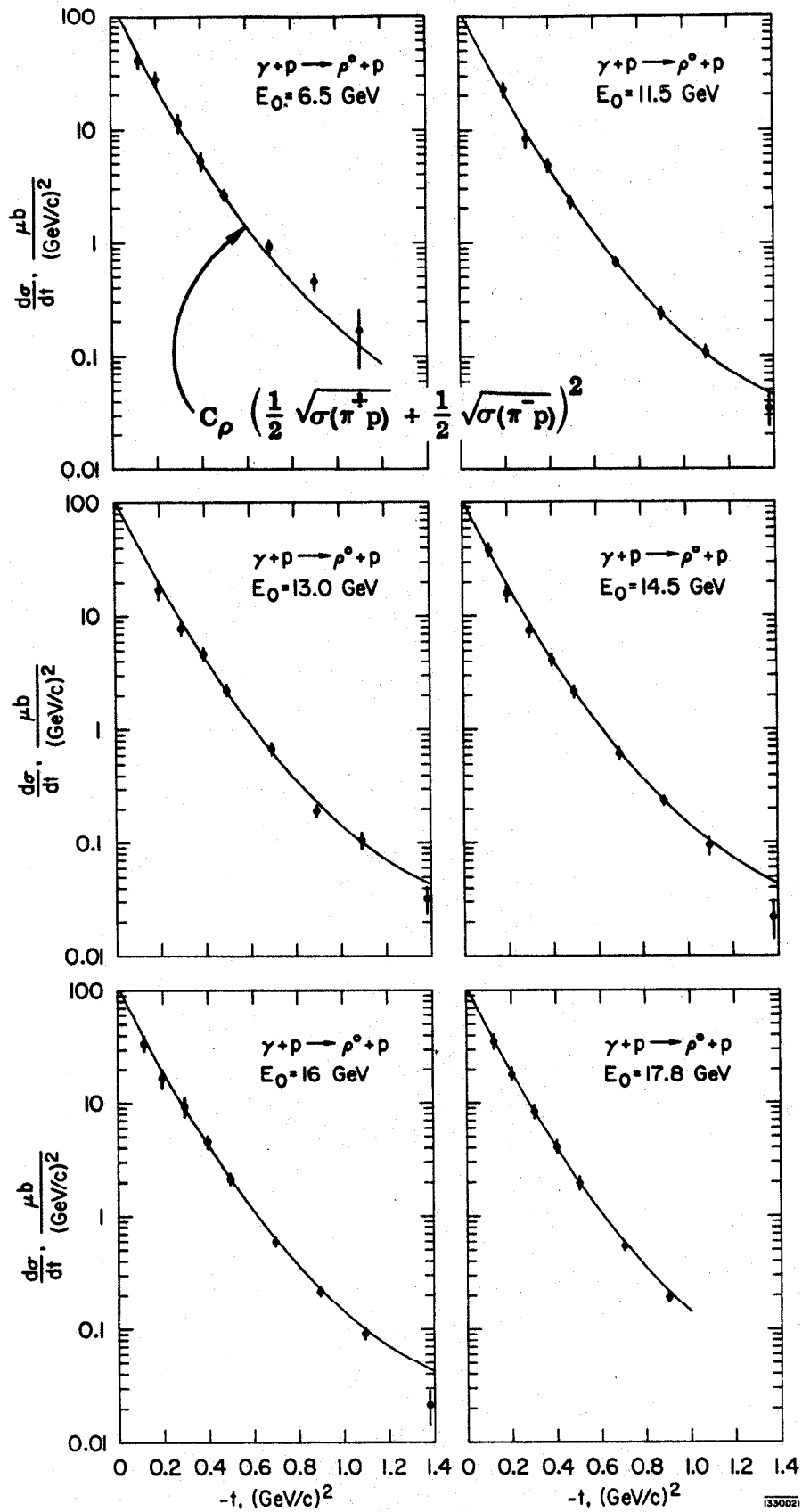


Fig. 3

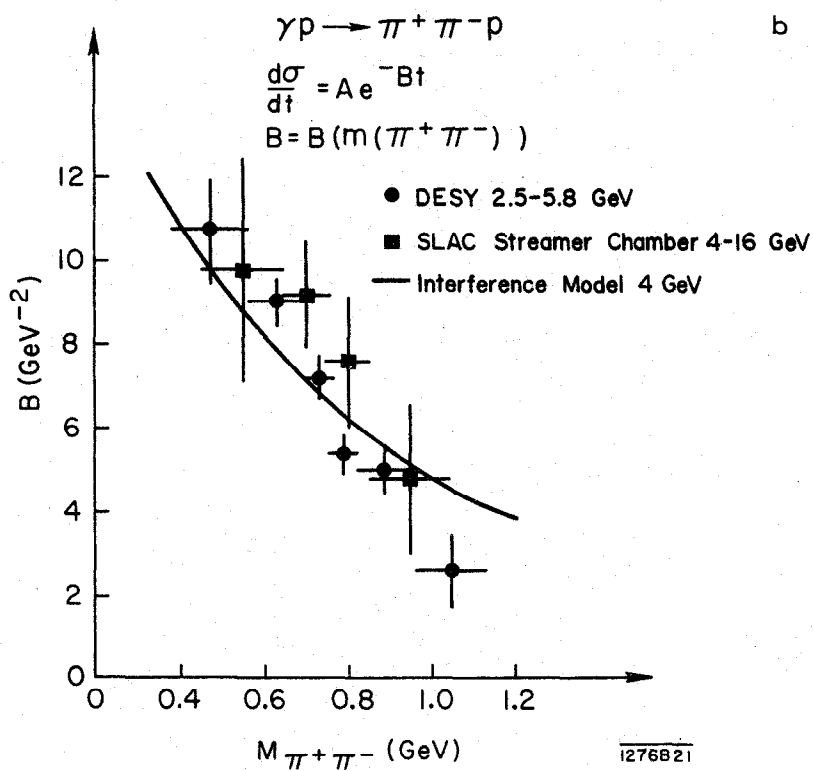
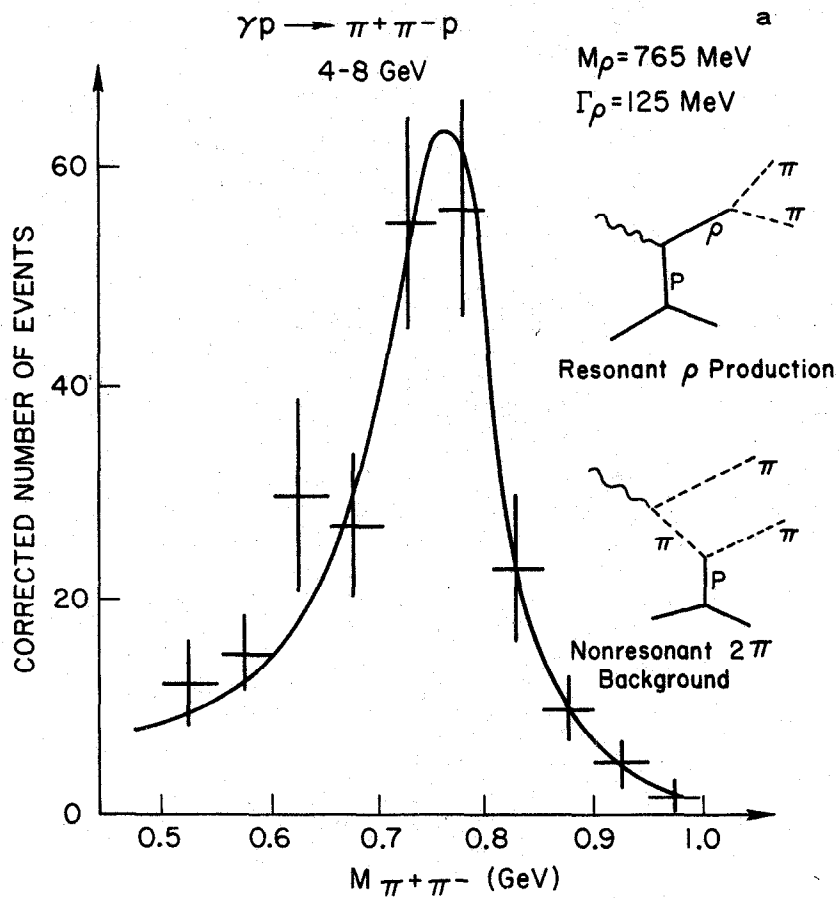


Fig. 4

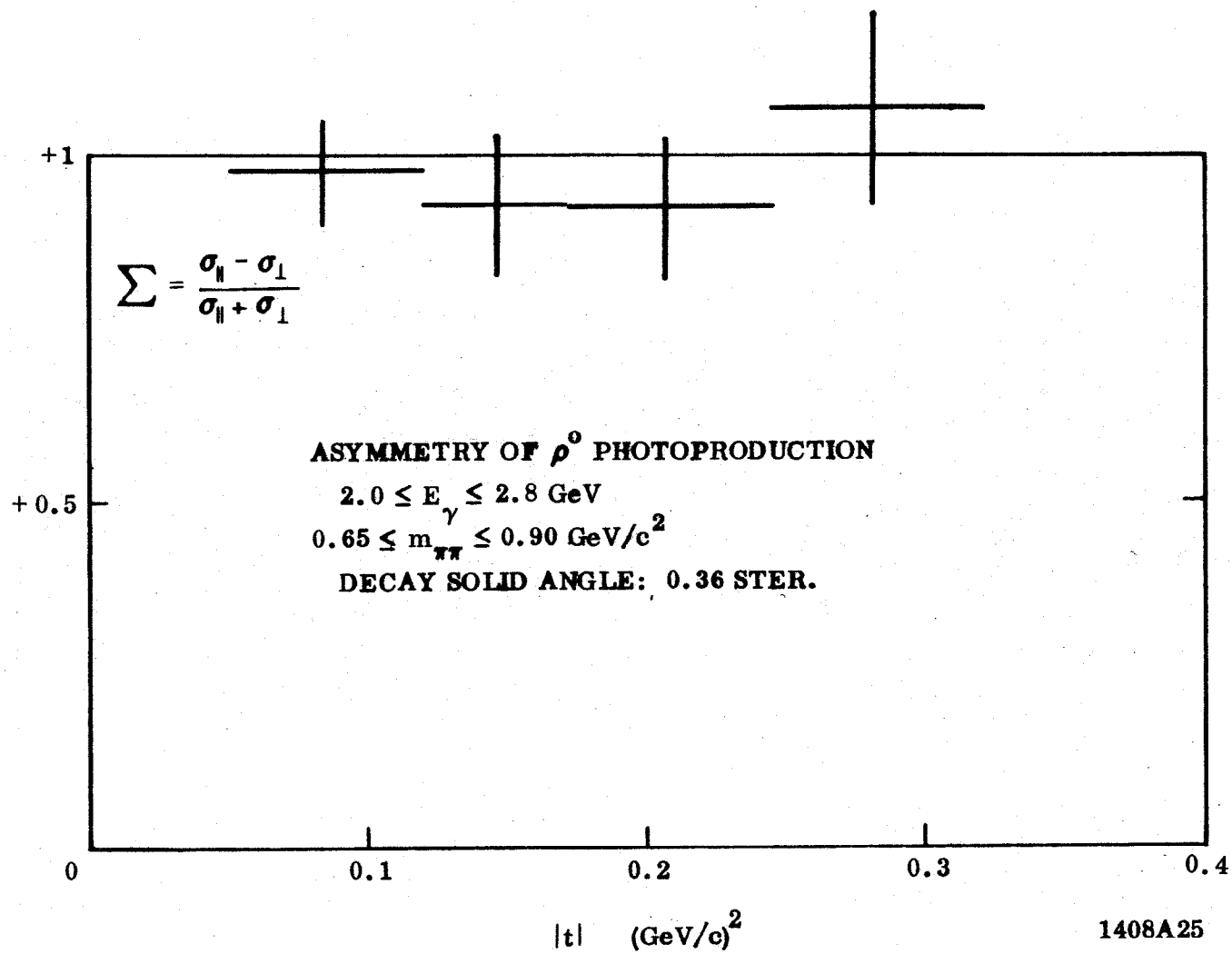


Fig. 5

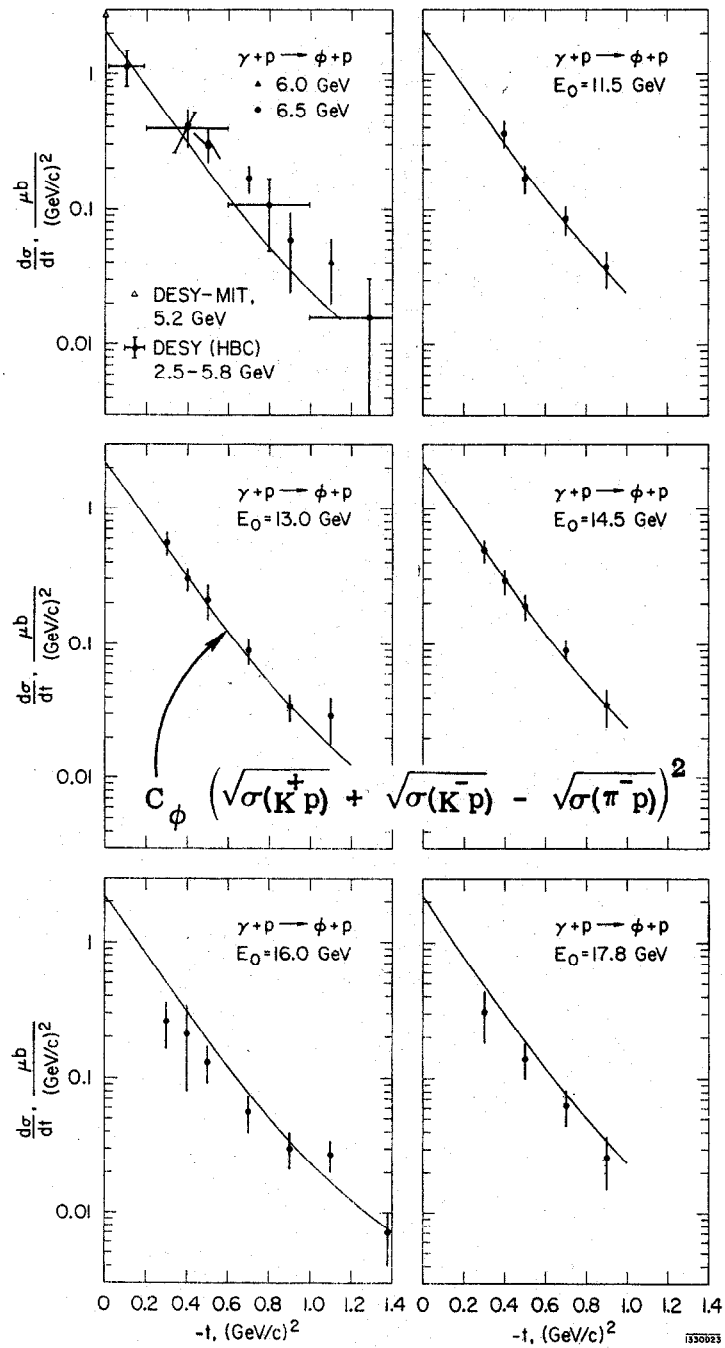


Fig. 6

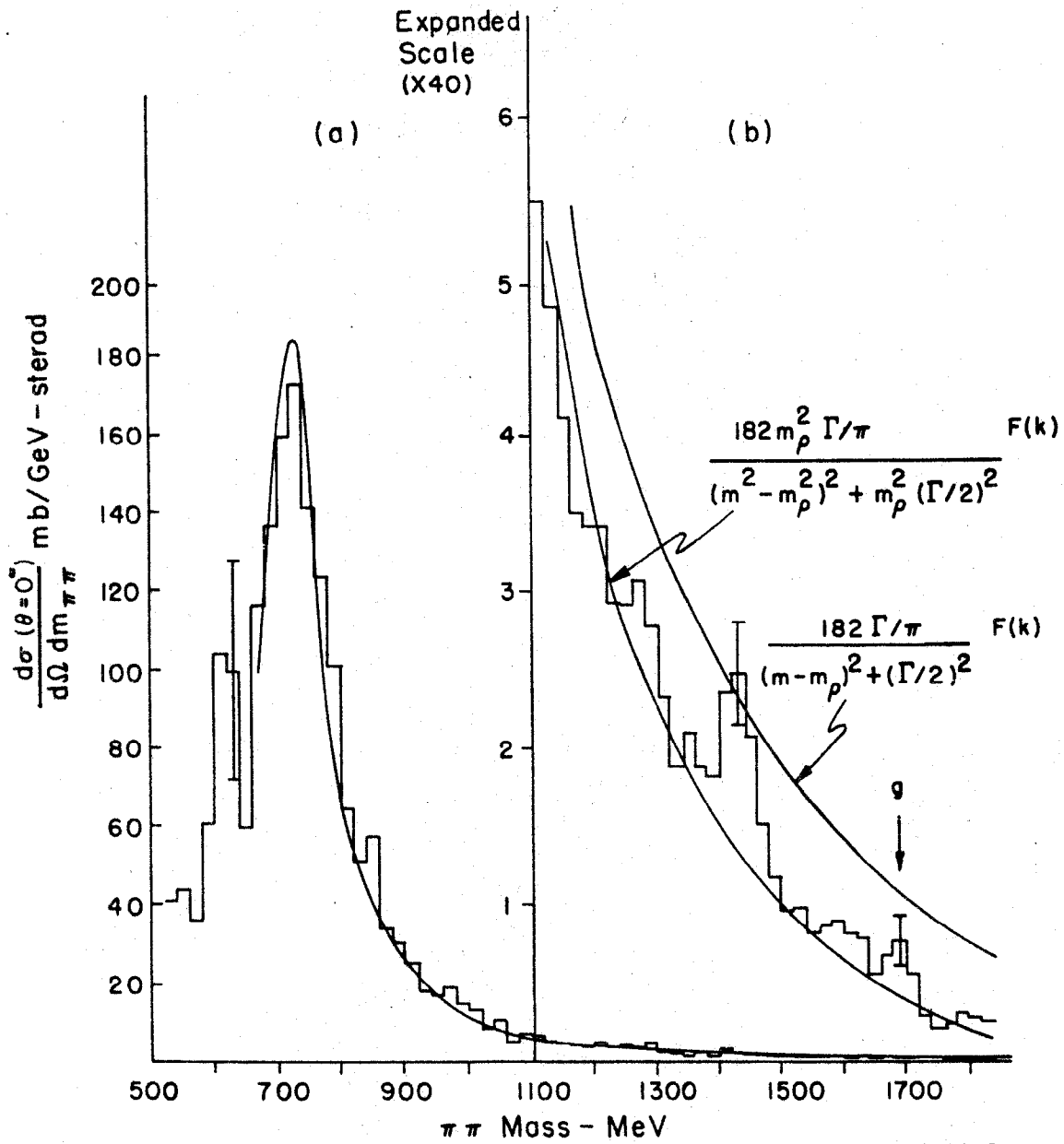


Fig. 7

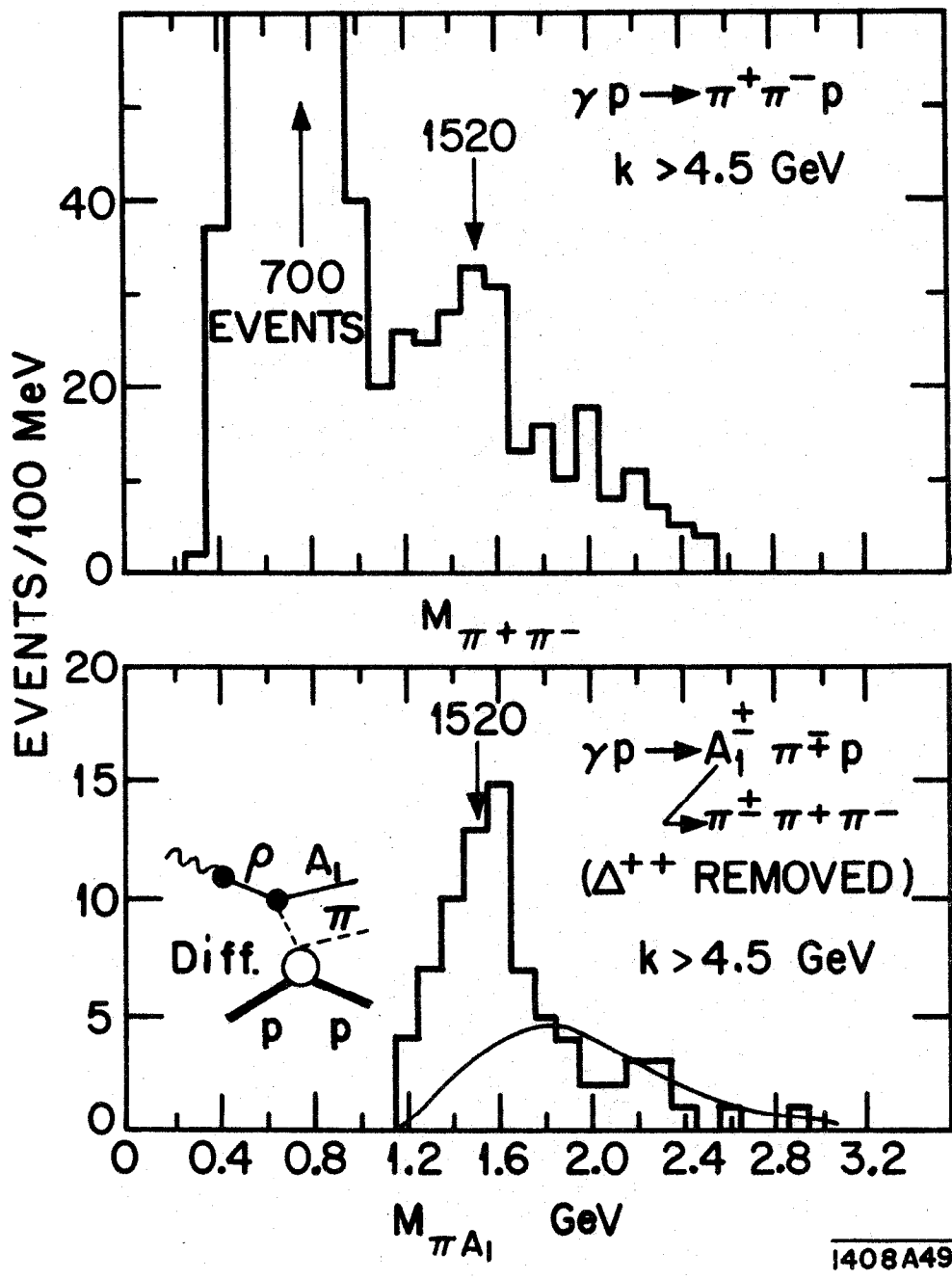


Fig. 8

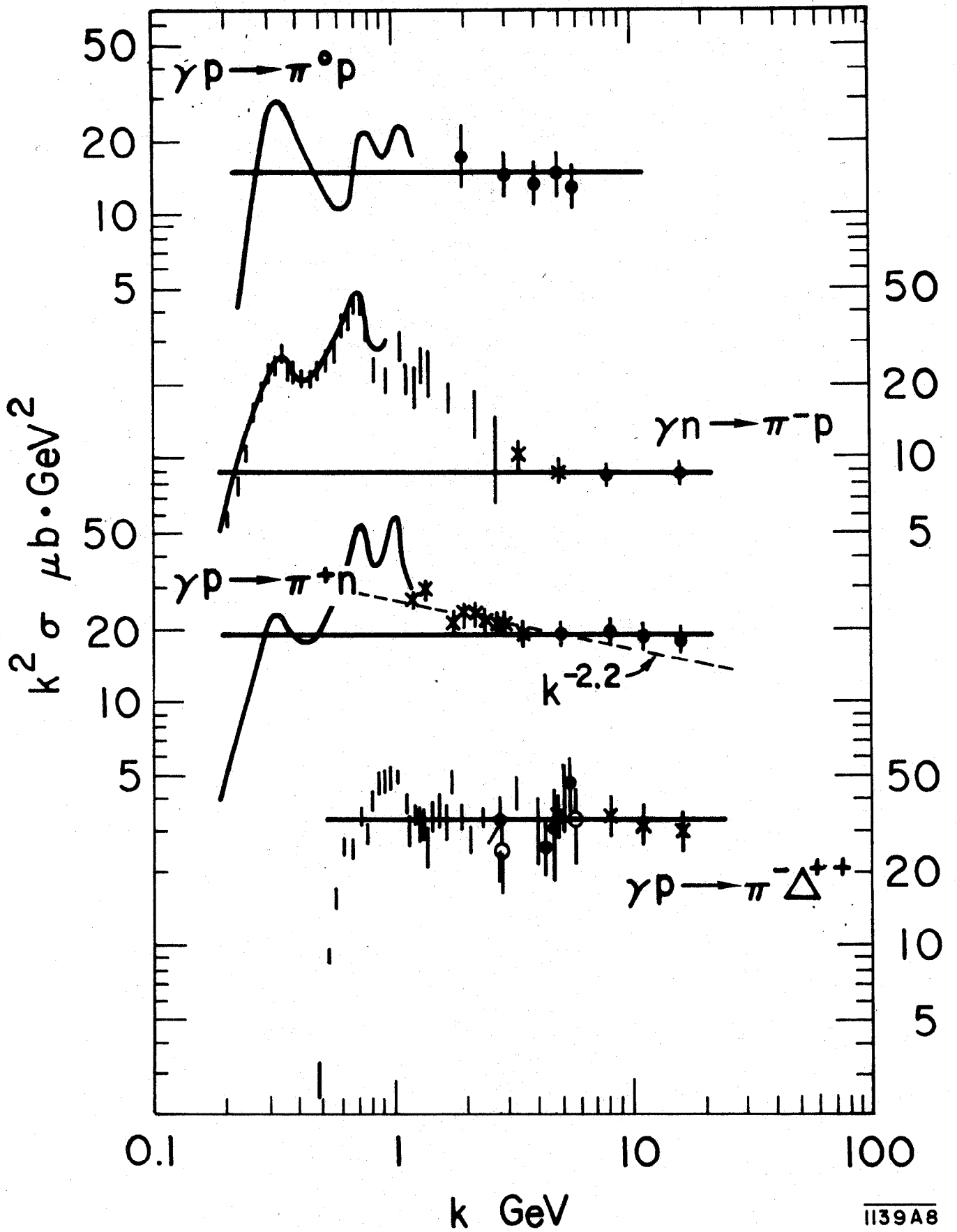


Fig 9

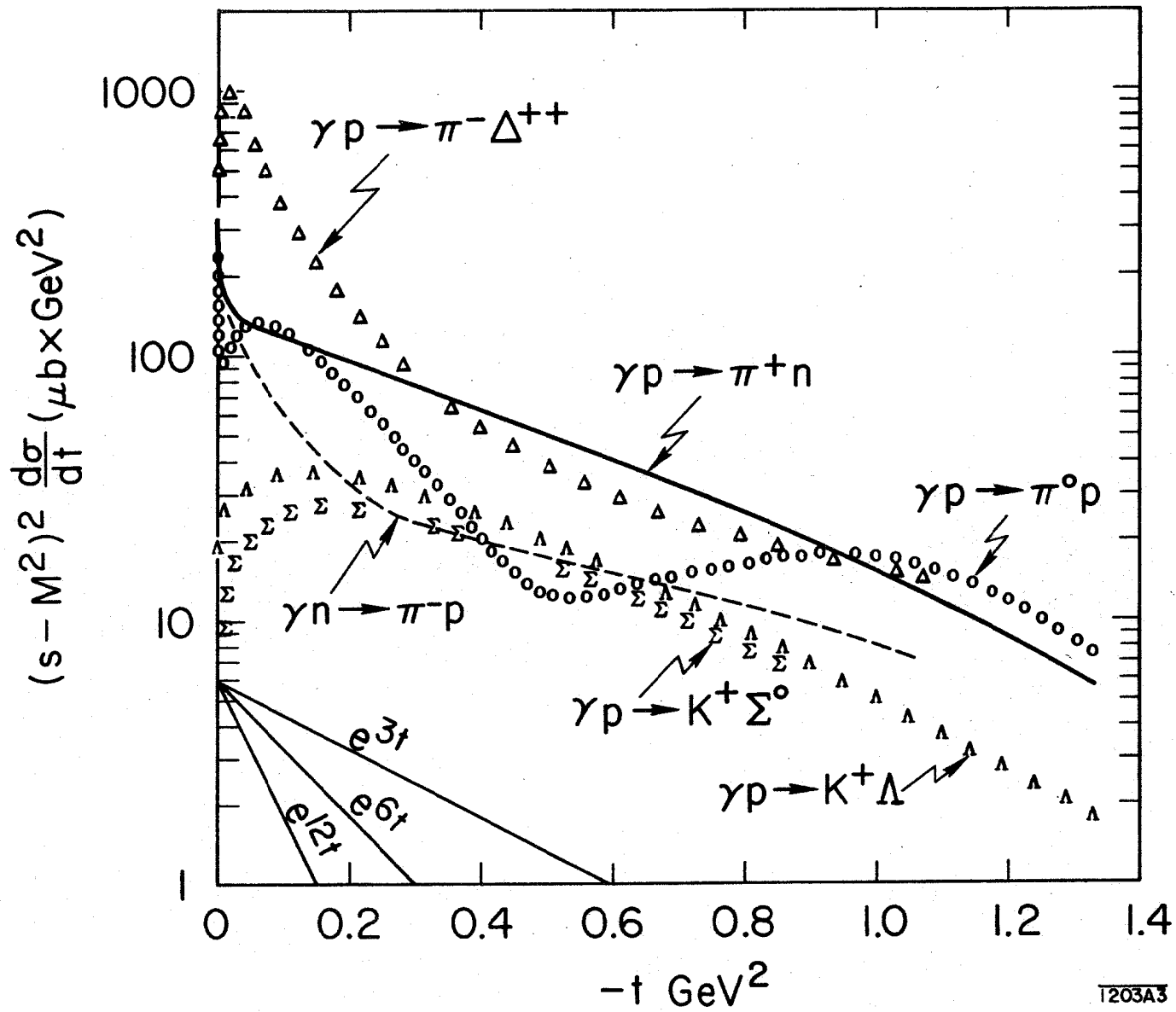


Fig. 10

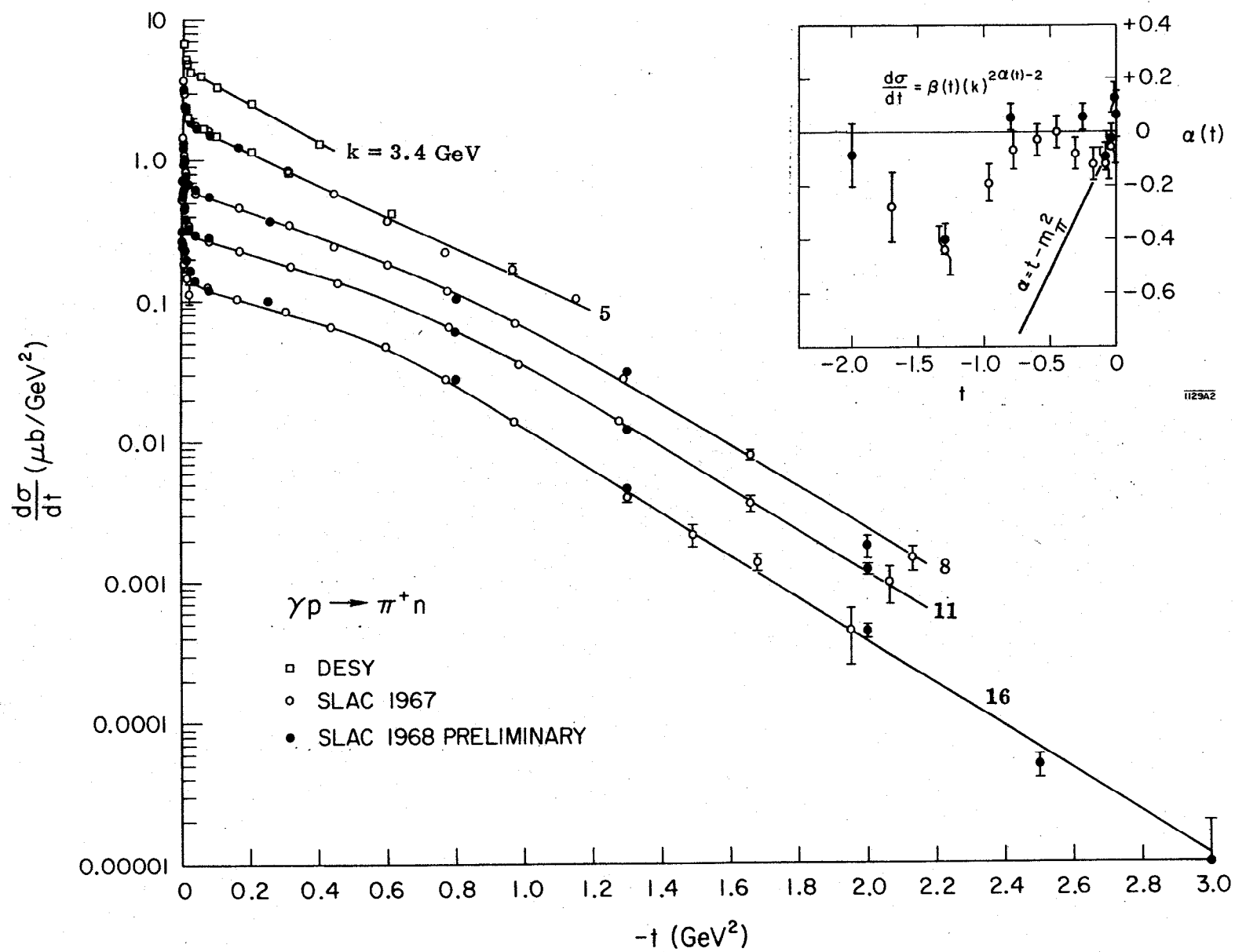


Fig. 11

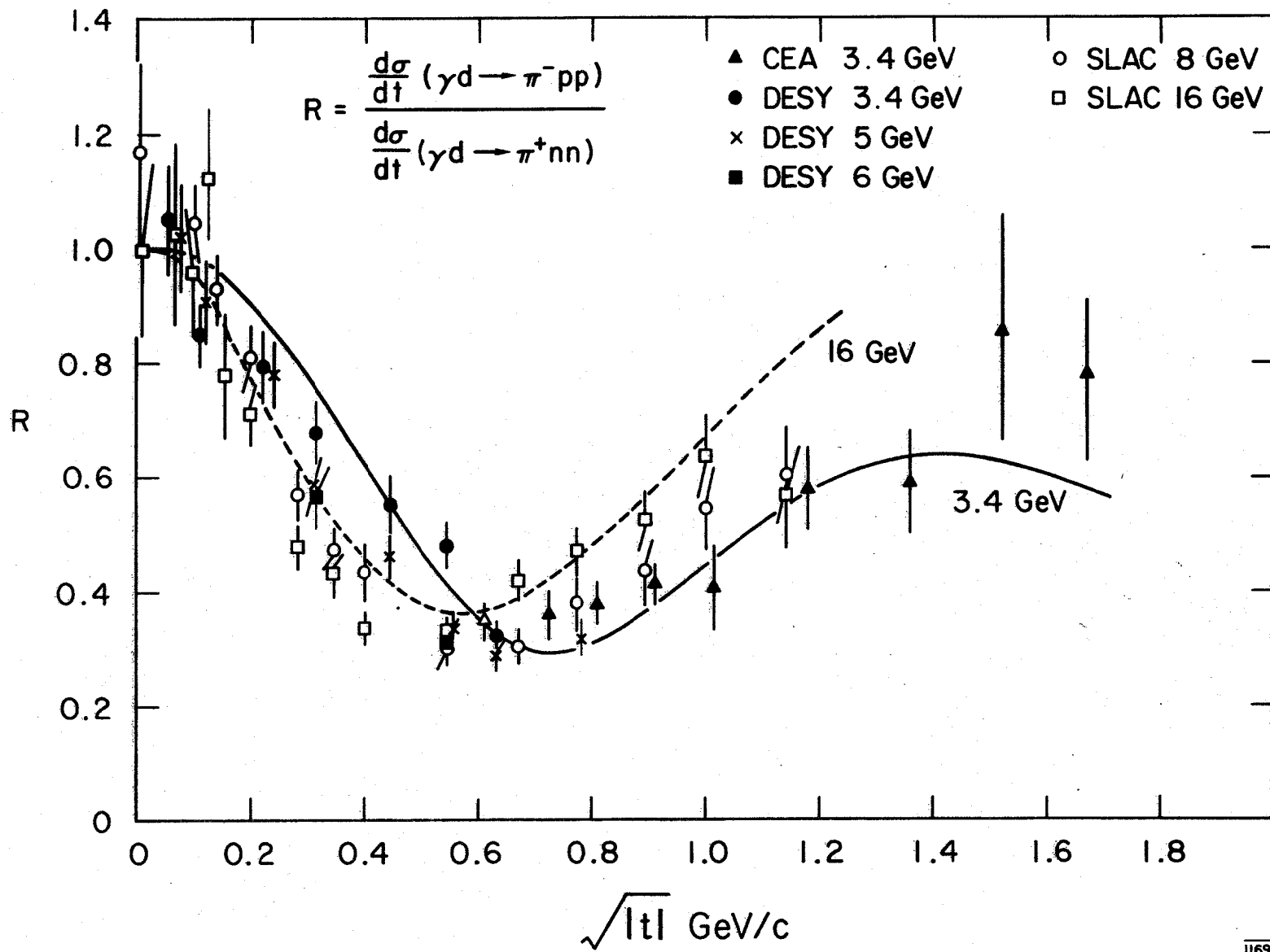
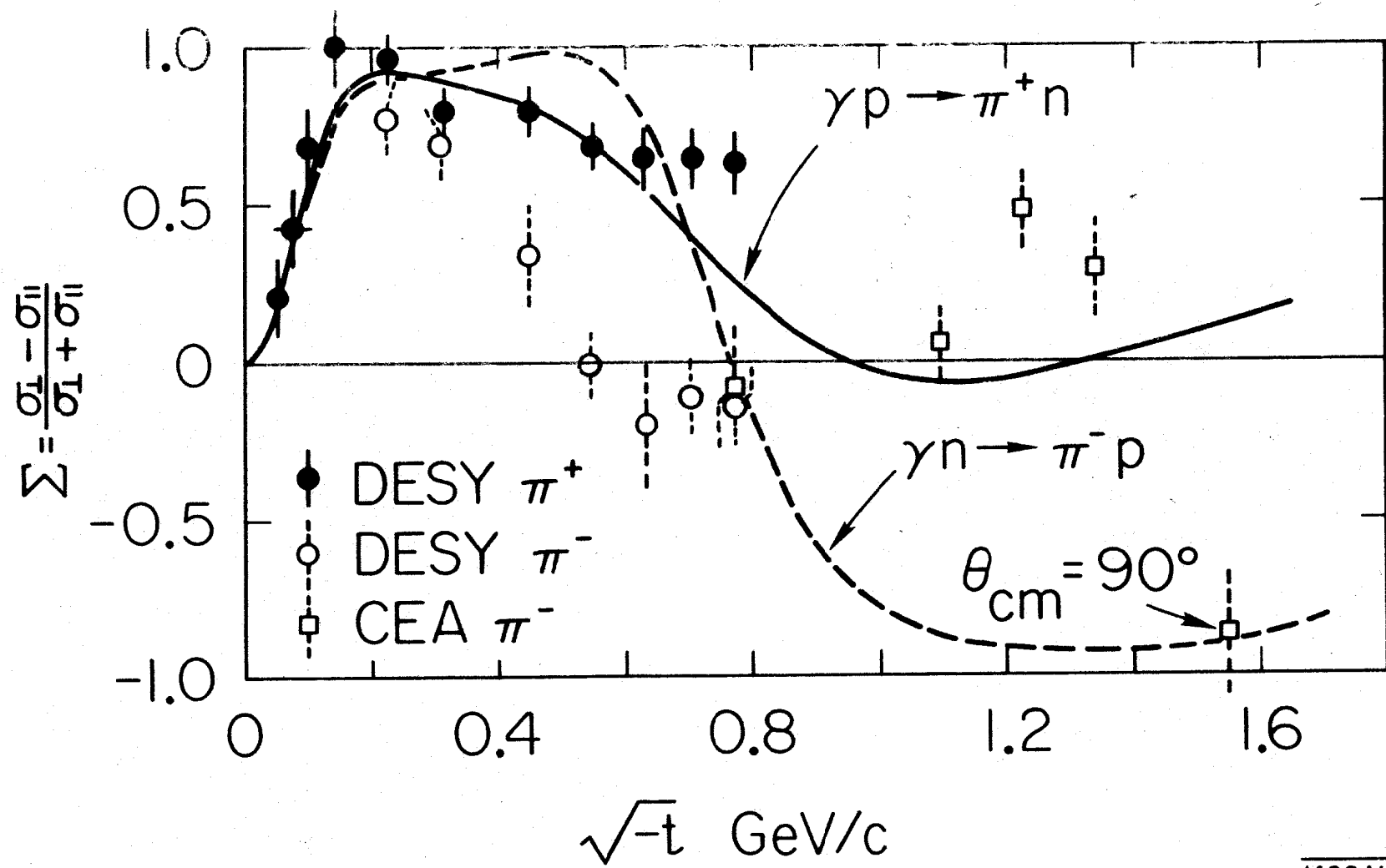


Fig. 12



1408A12

Fig. 13

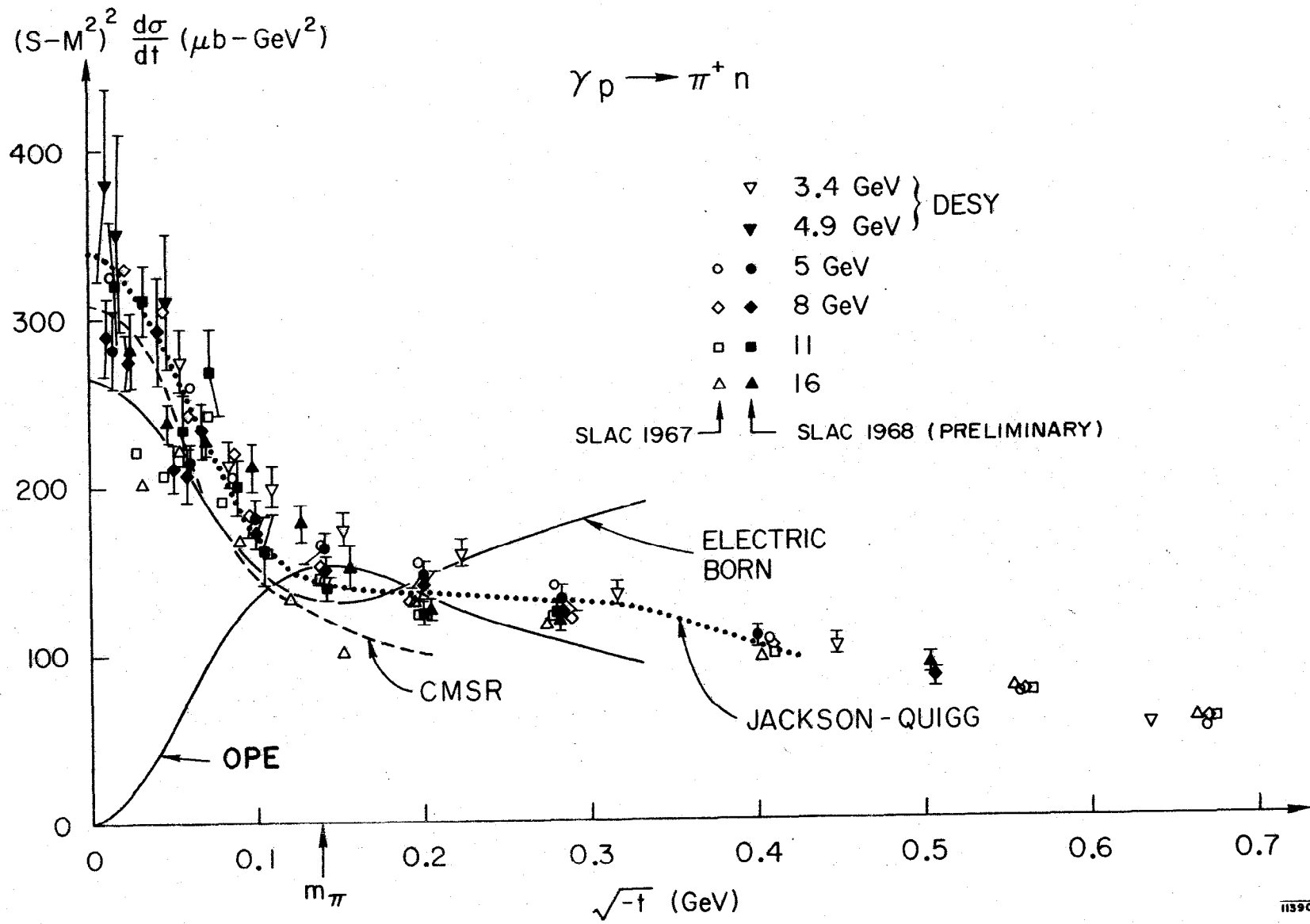
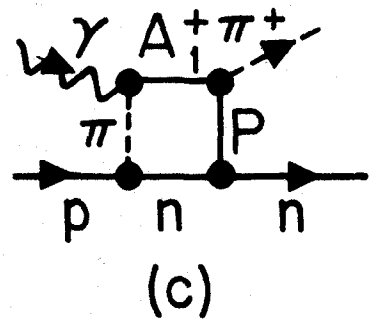
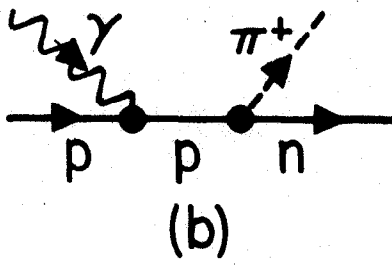
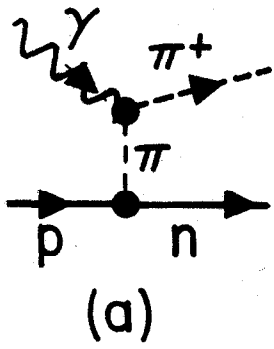


Fig. 14



1408A45

Fig. 15

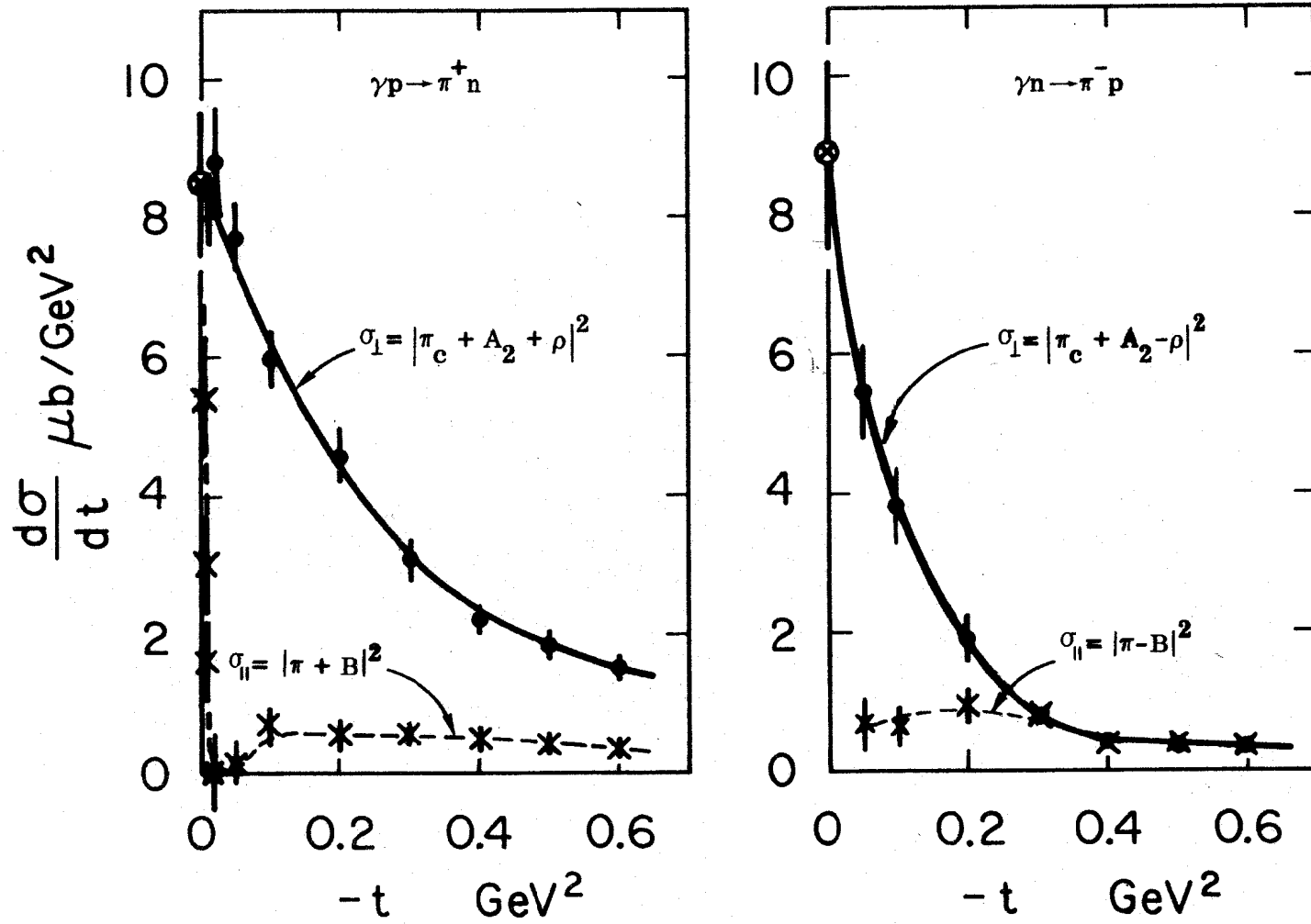
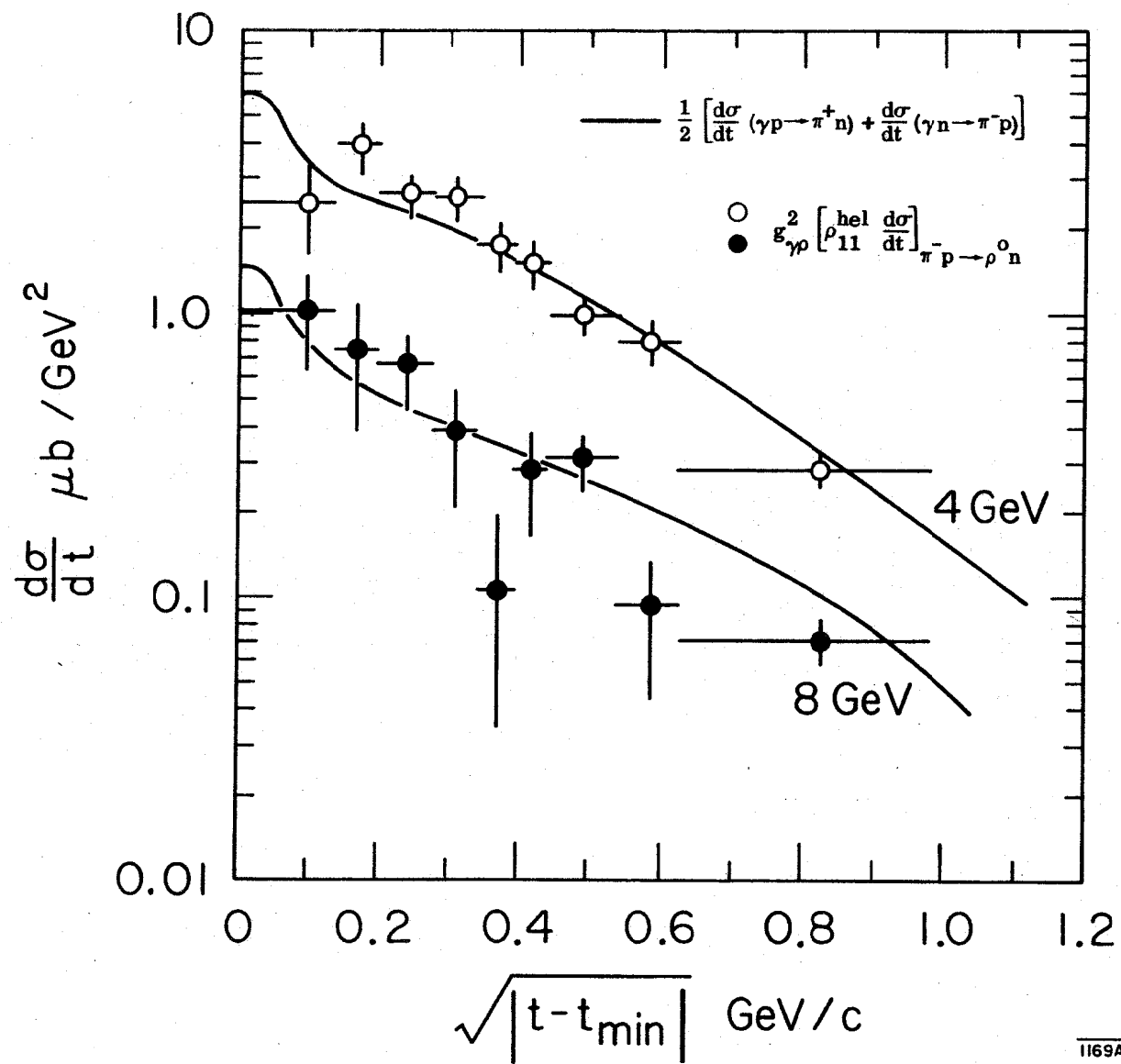


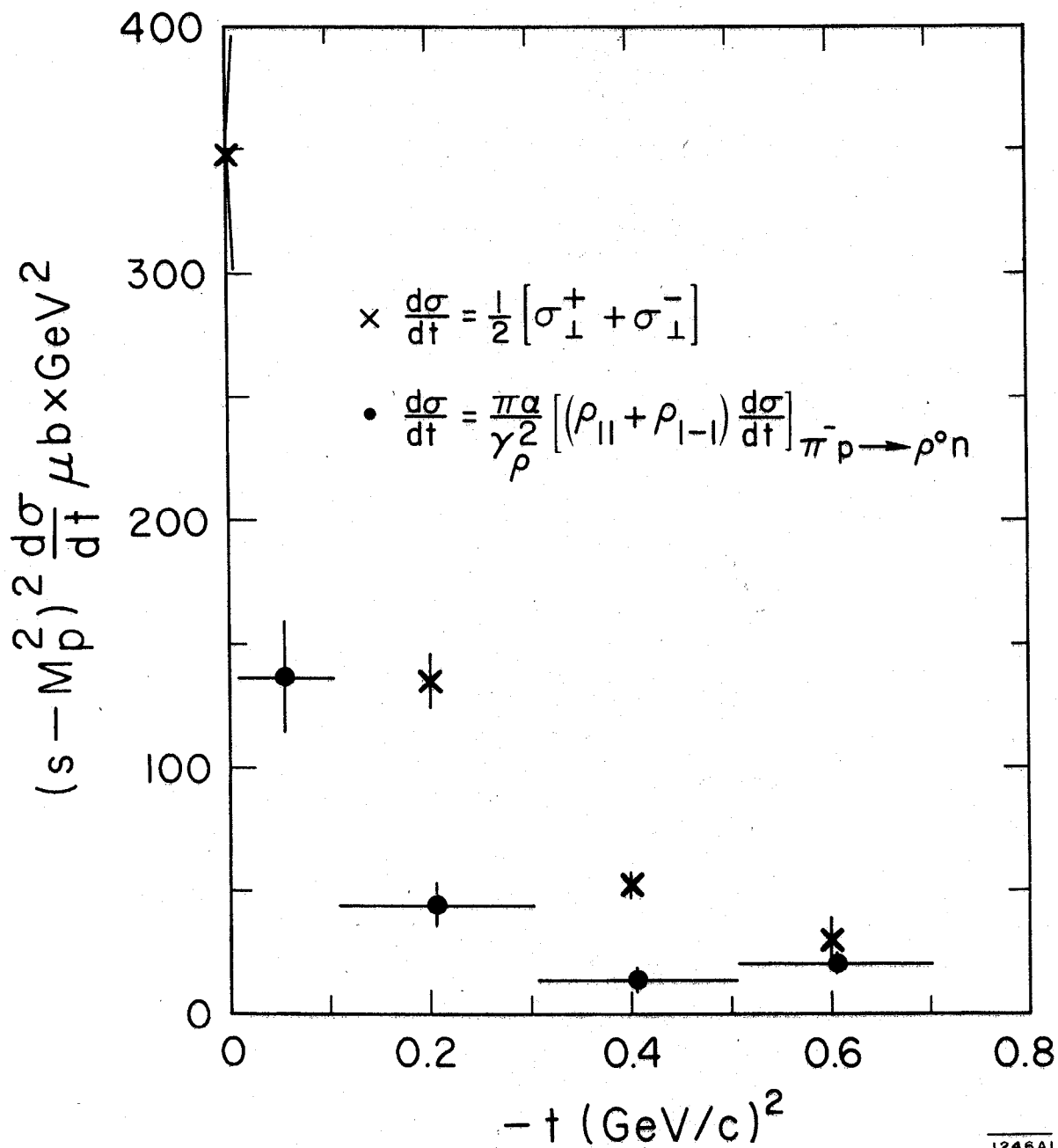
Fig. 16

1408A15



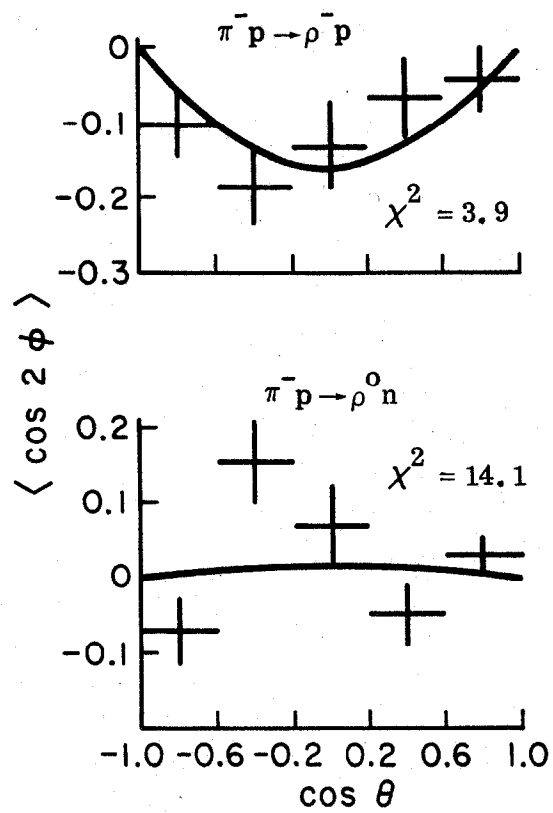
1169A1

Fig. 17



1246A1

Fig. 18



1408A14

Fig. 19

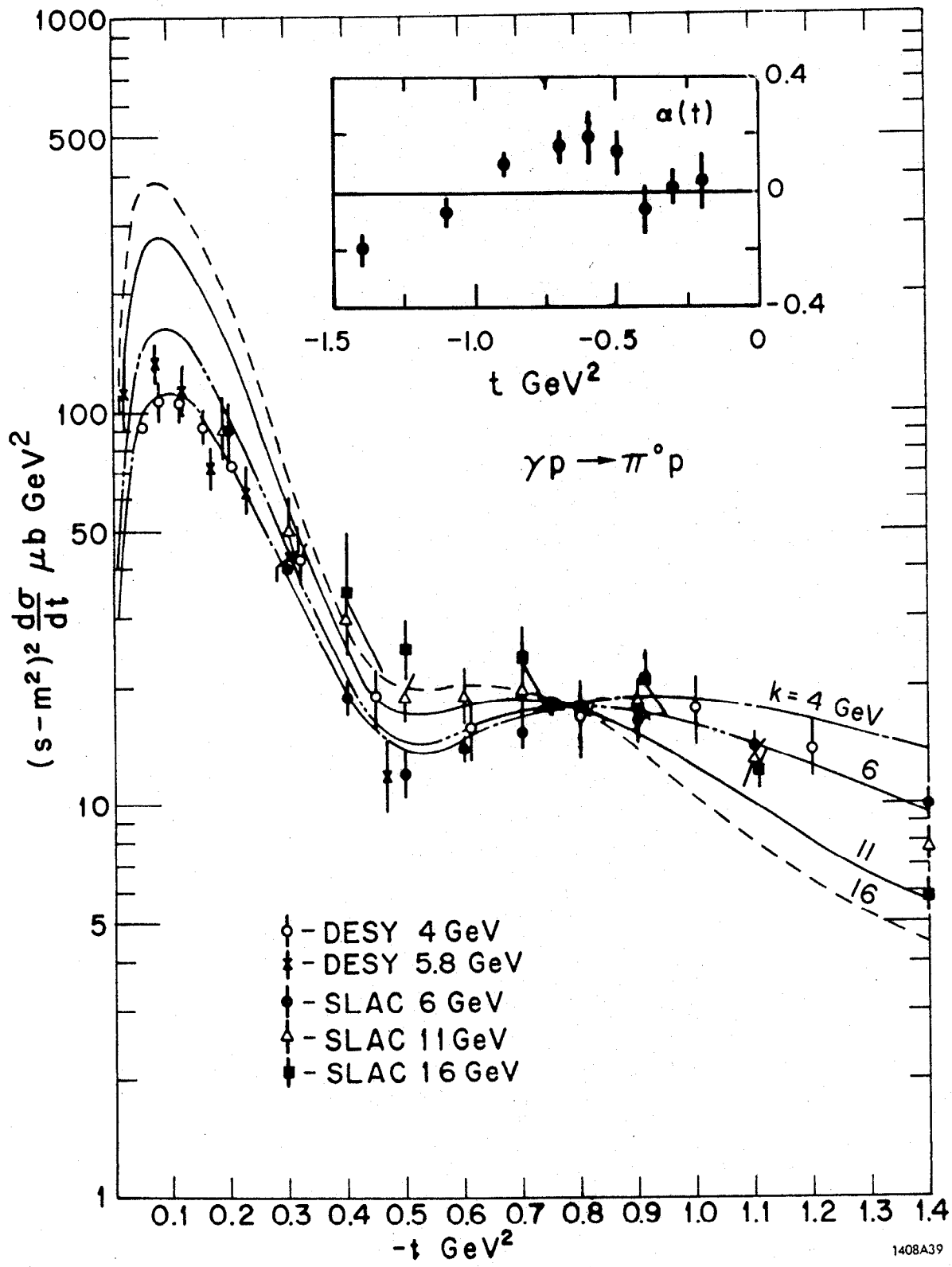


Fig. 20

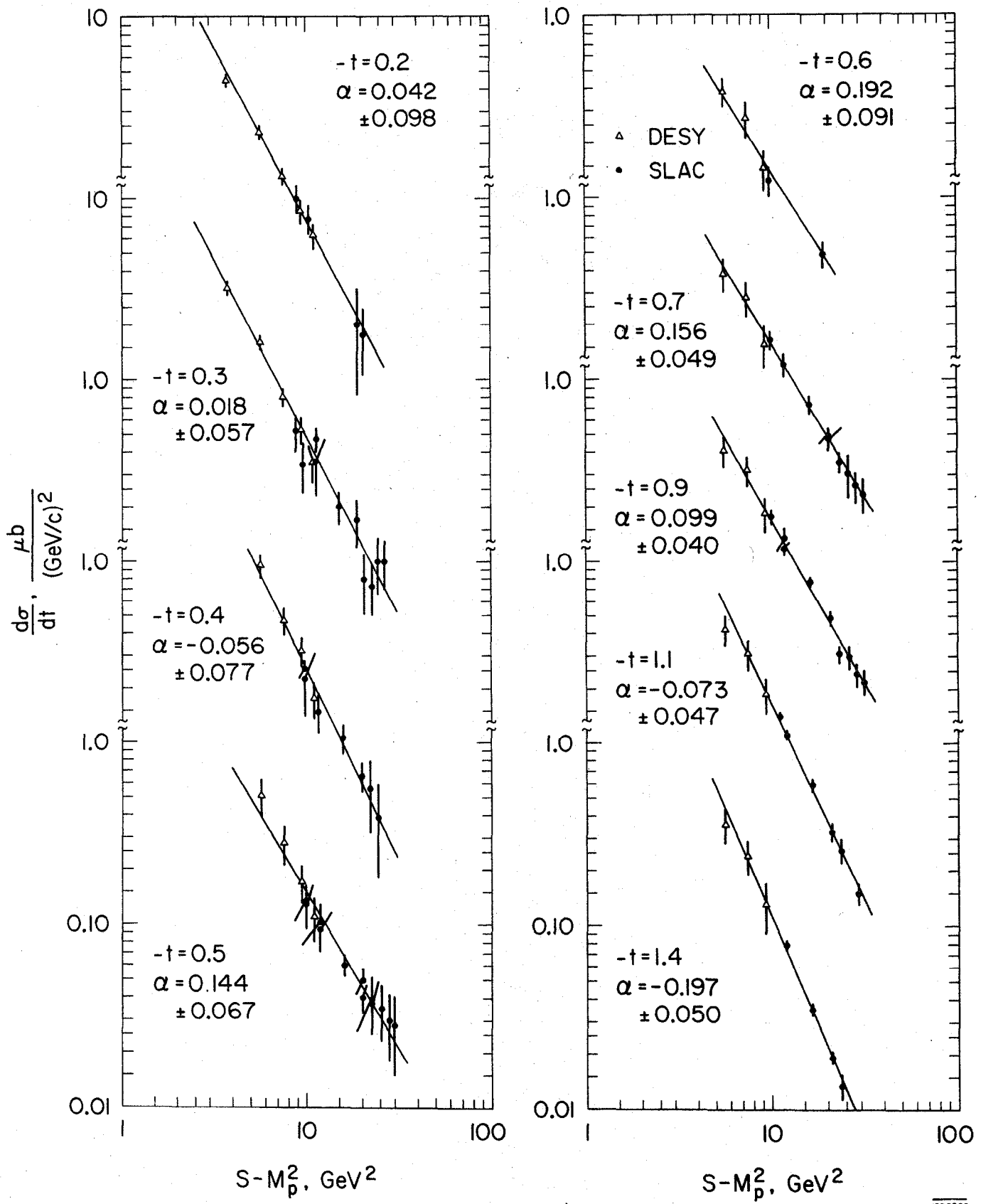
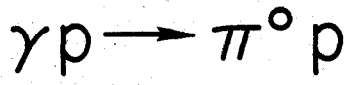


Fig. 21

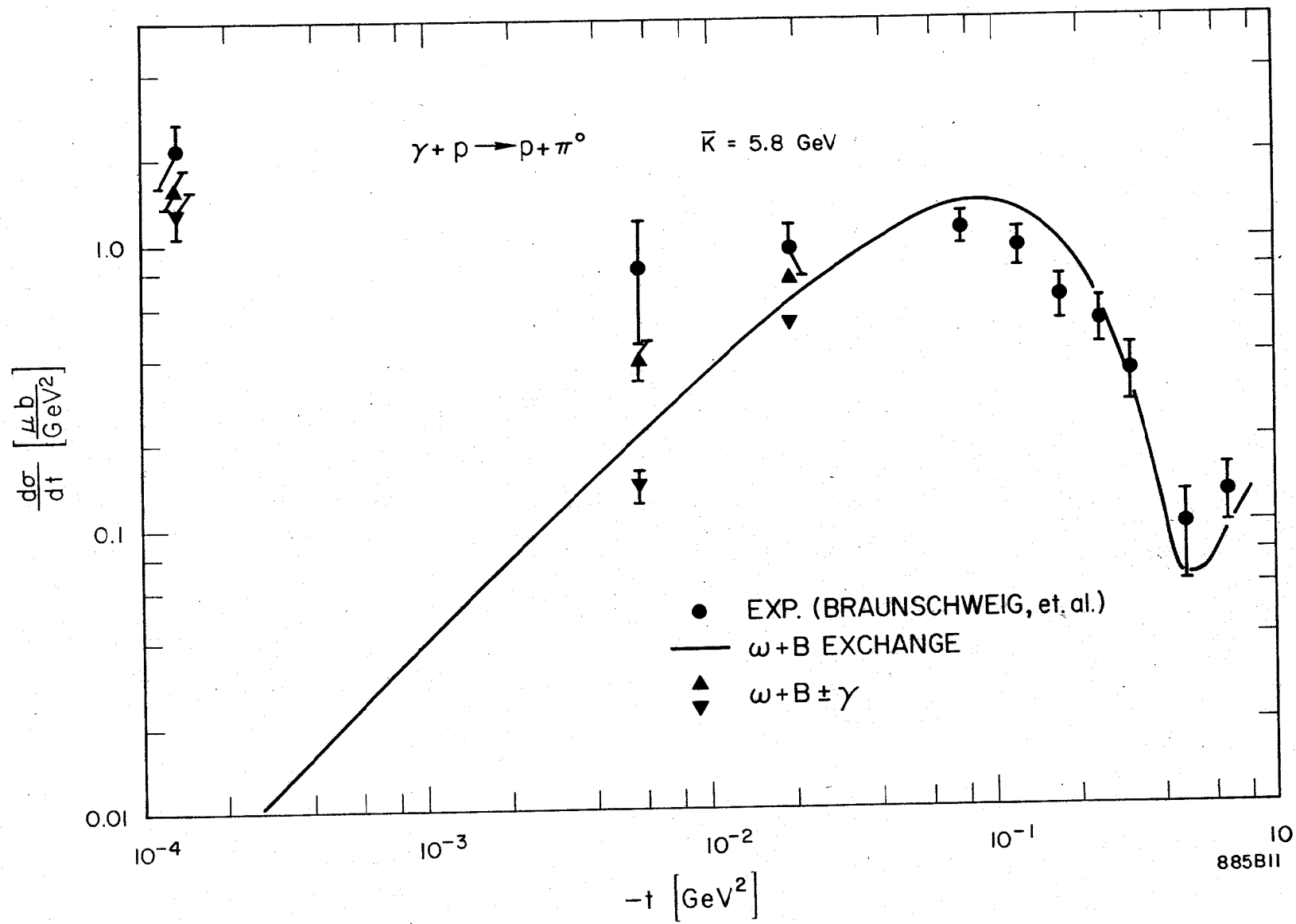
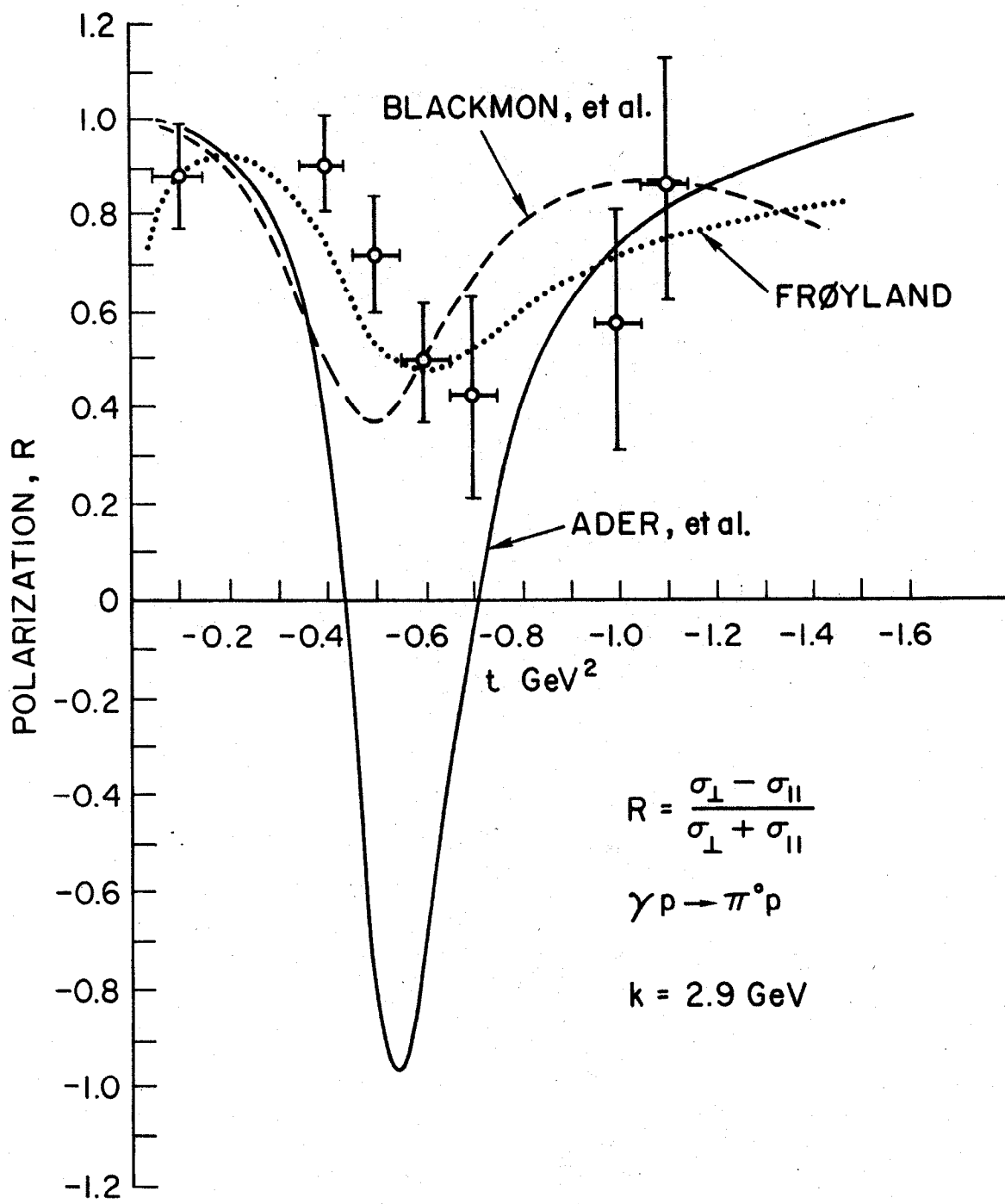


Fig. 22



1408A44

Fig. 23

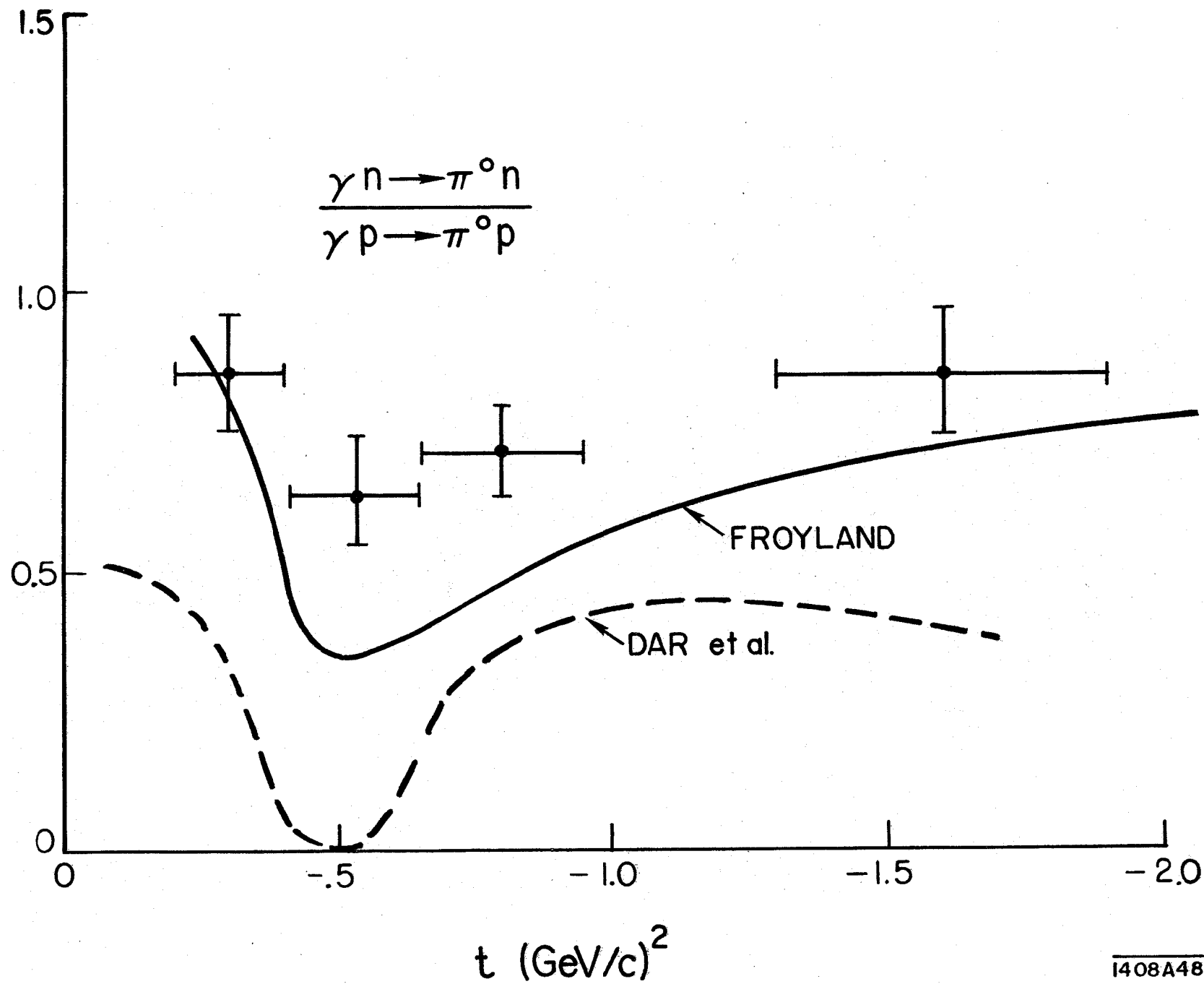


Fig. 24

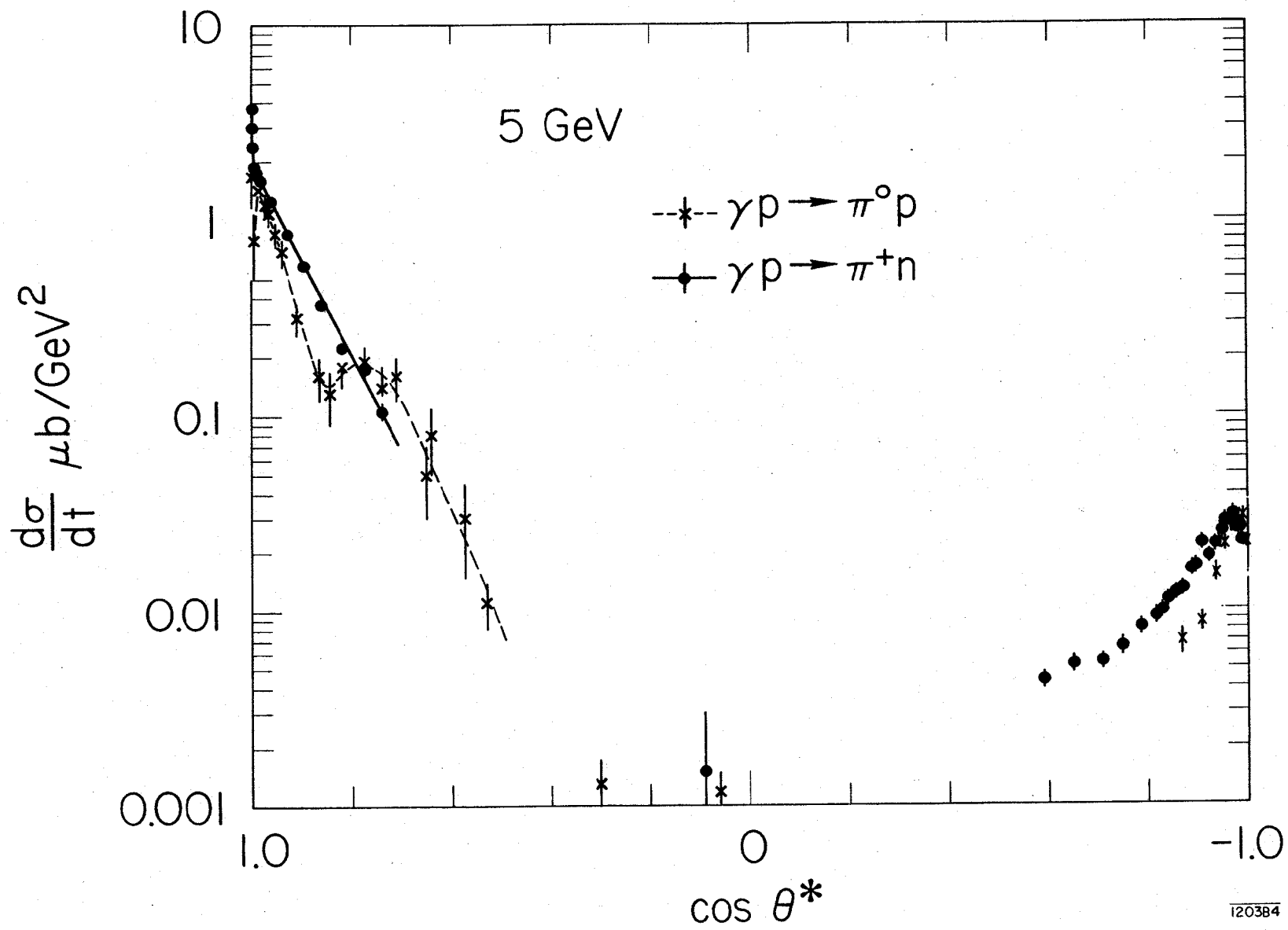


Fig. 25

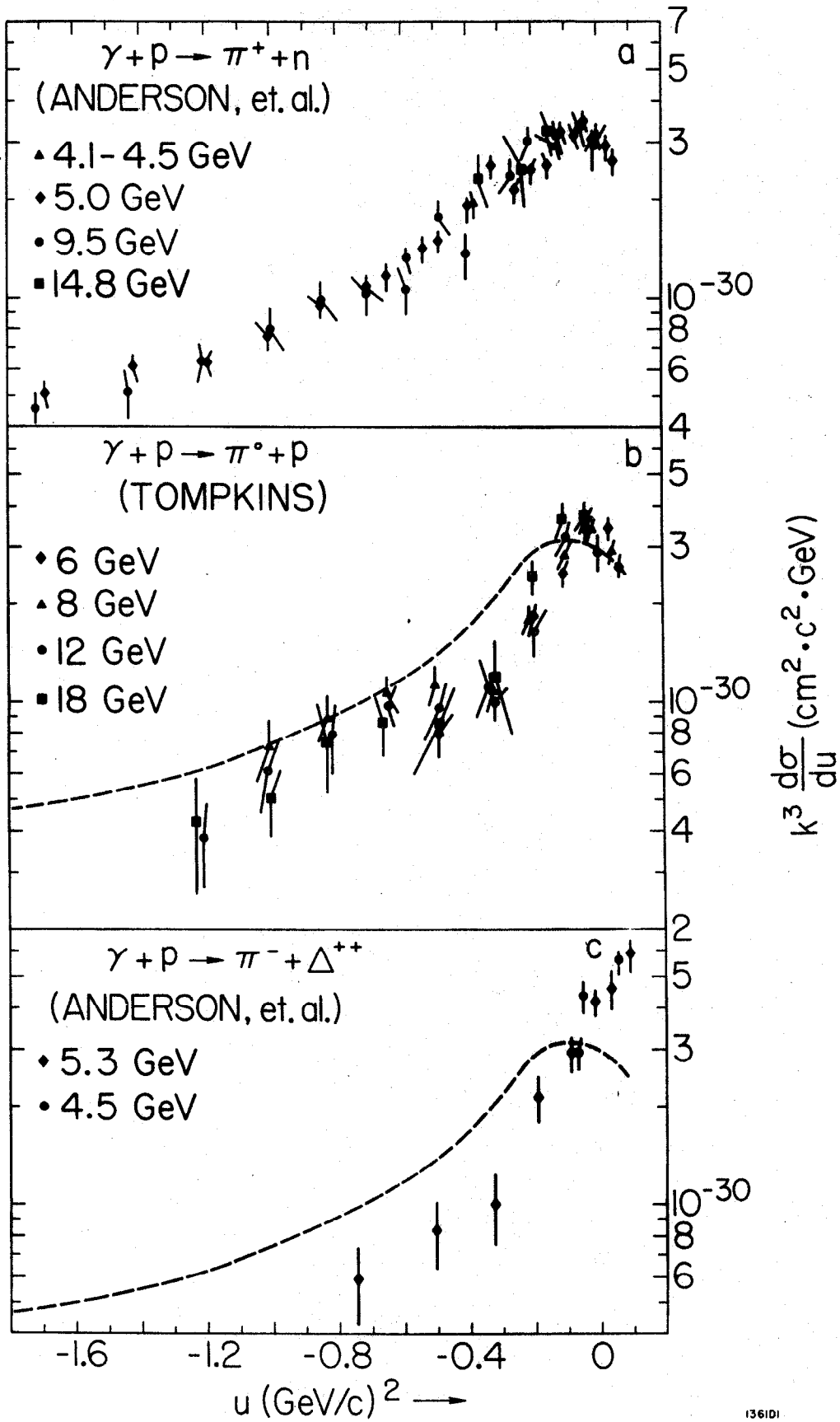
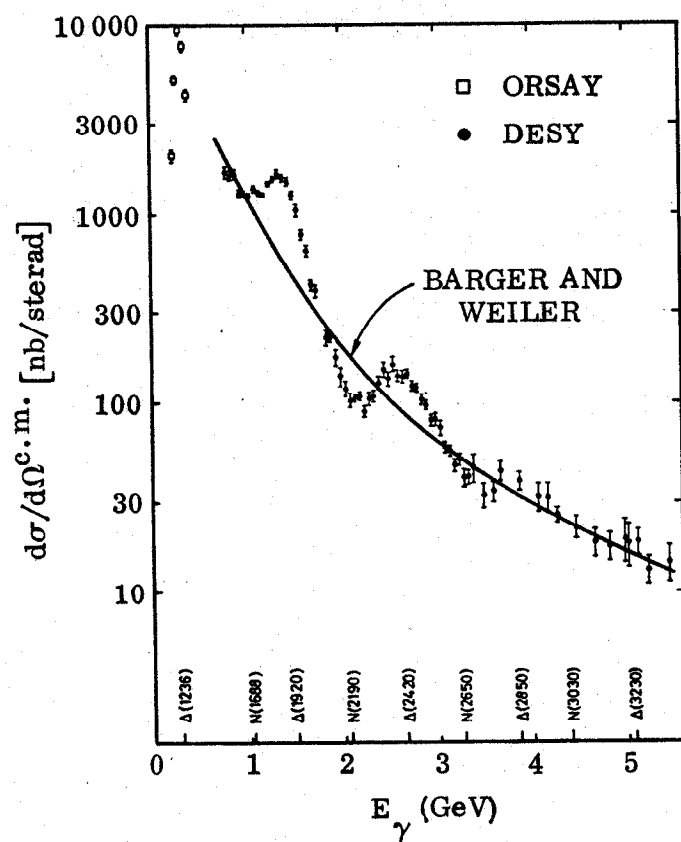


Fig. 26



1408A21

Fig. 27

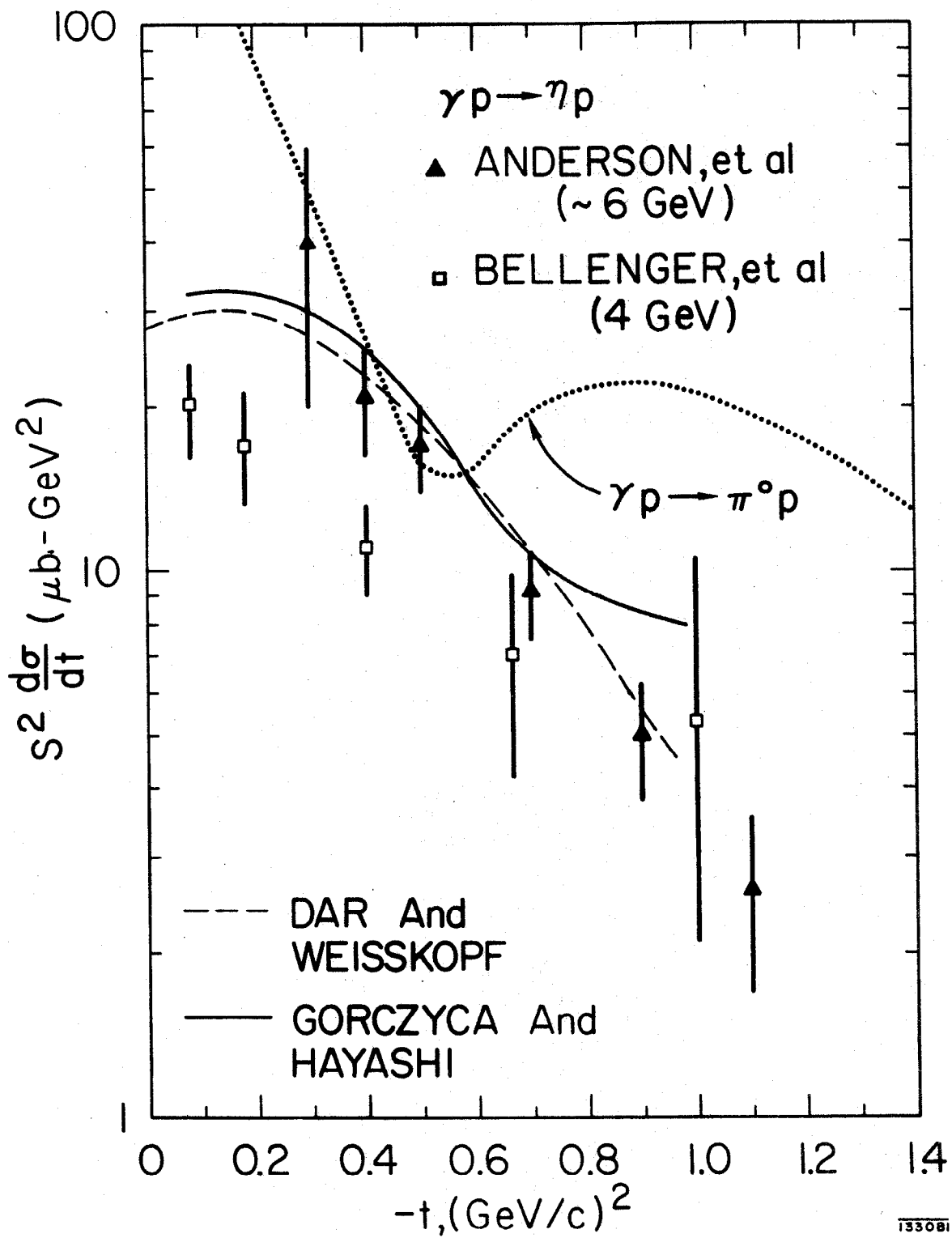


Fig. 28

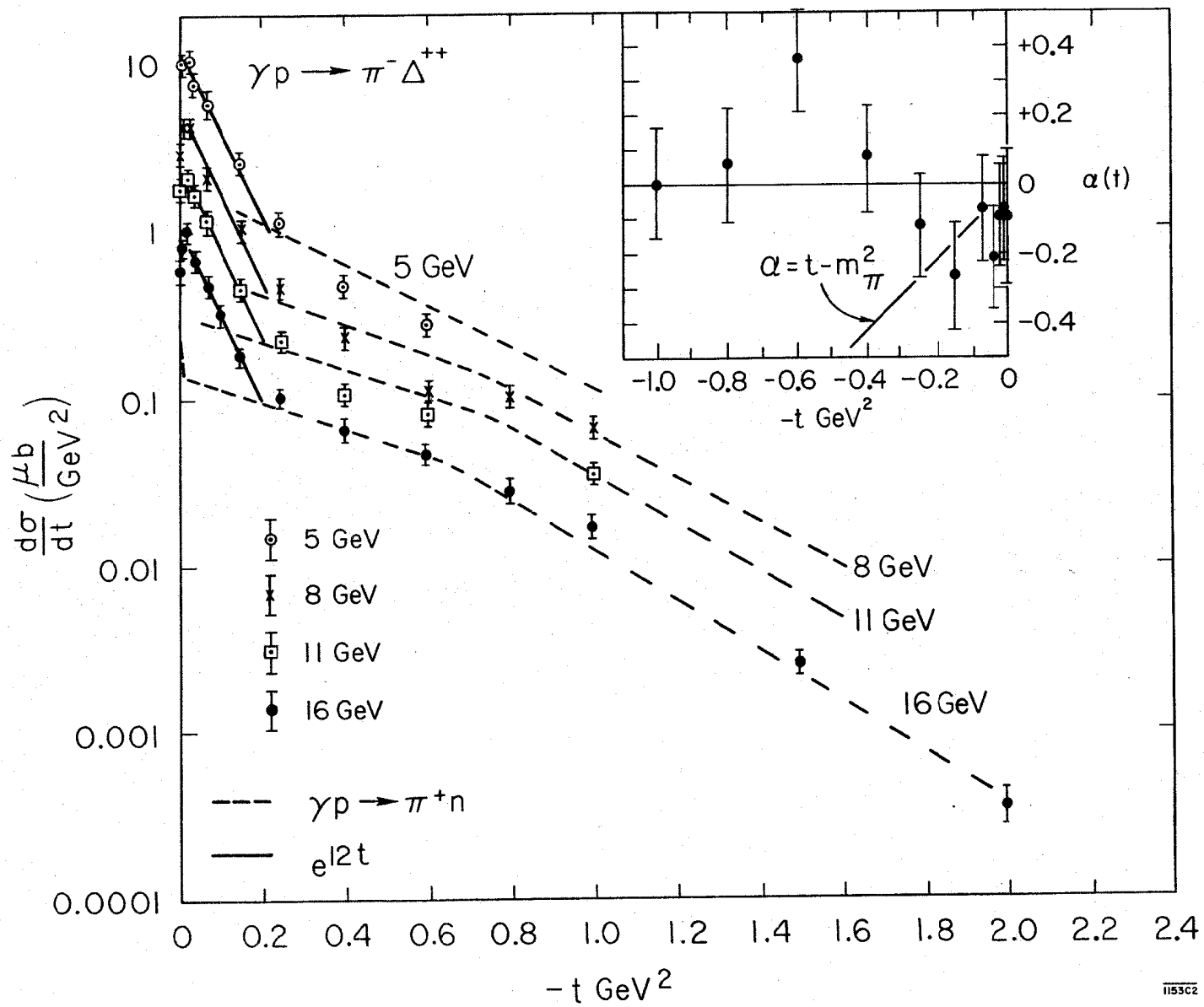


Fig. 29

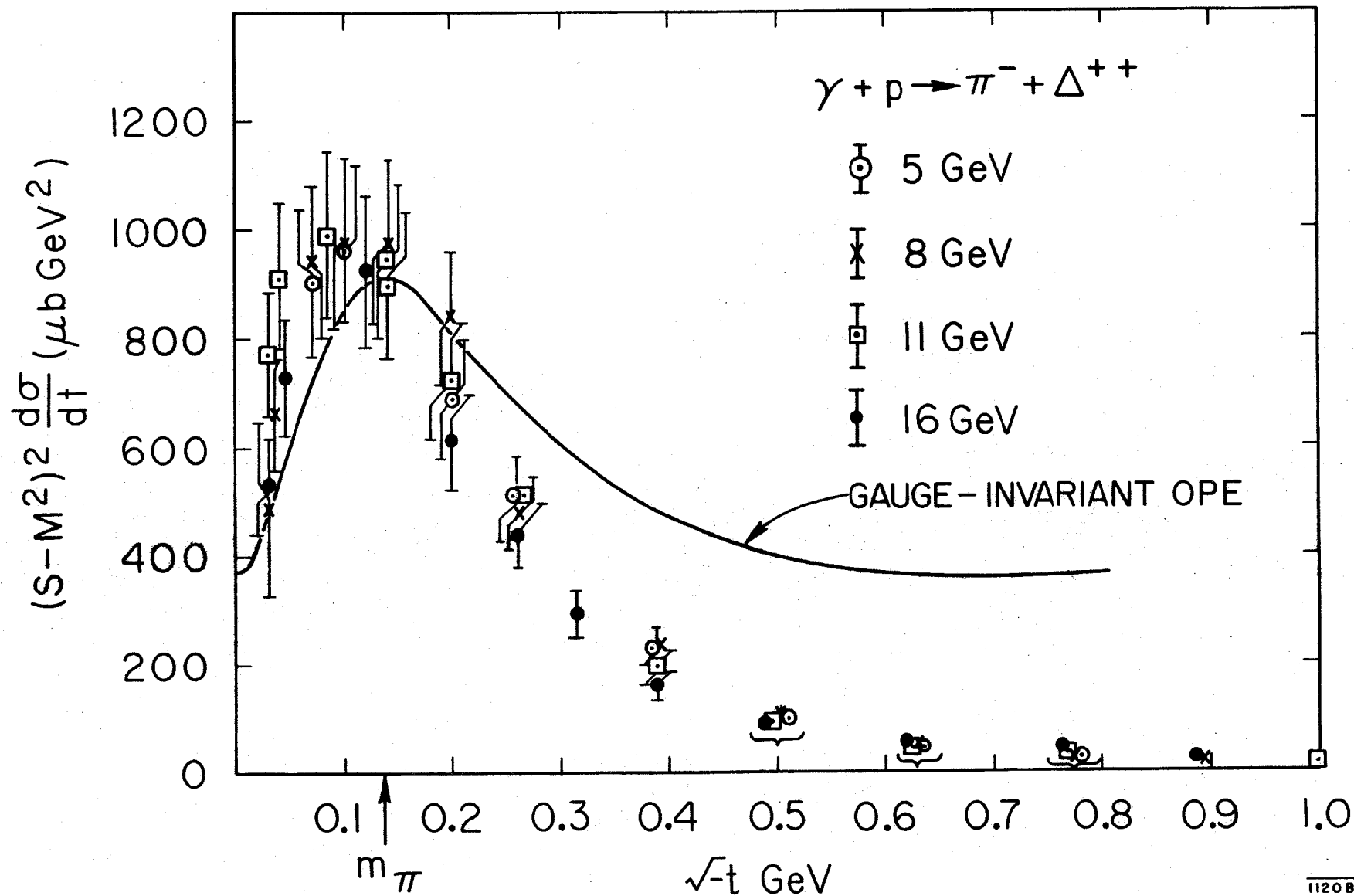


Fig. 30

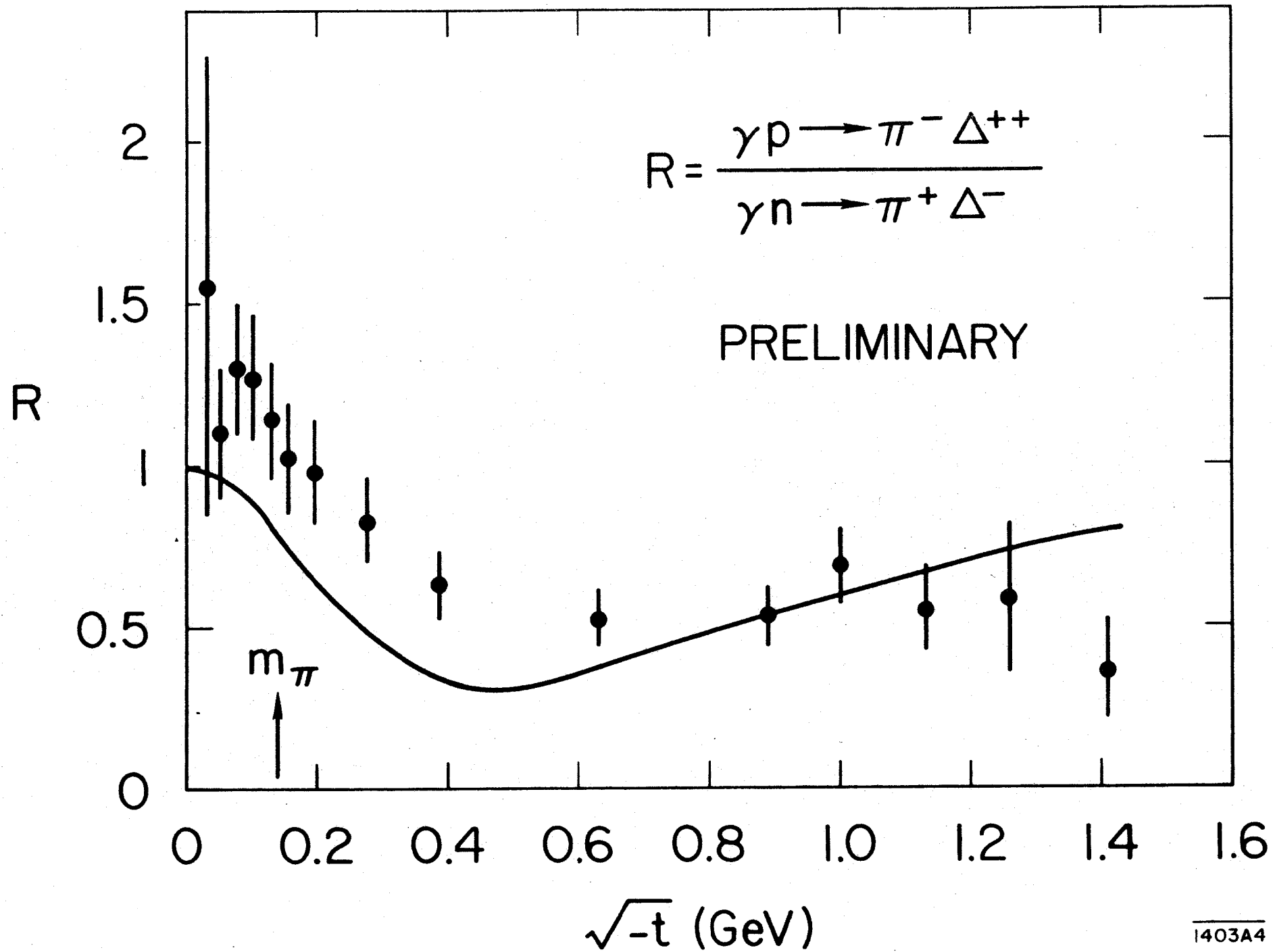


Fig. 31

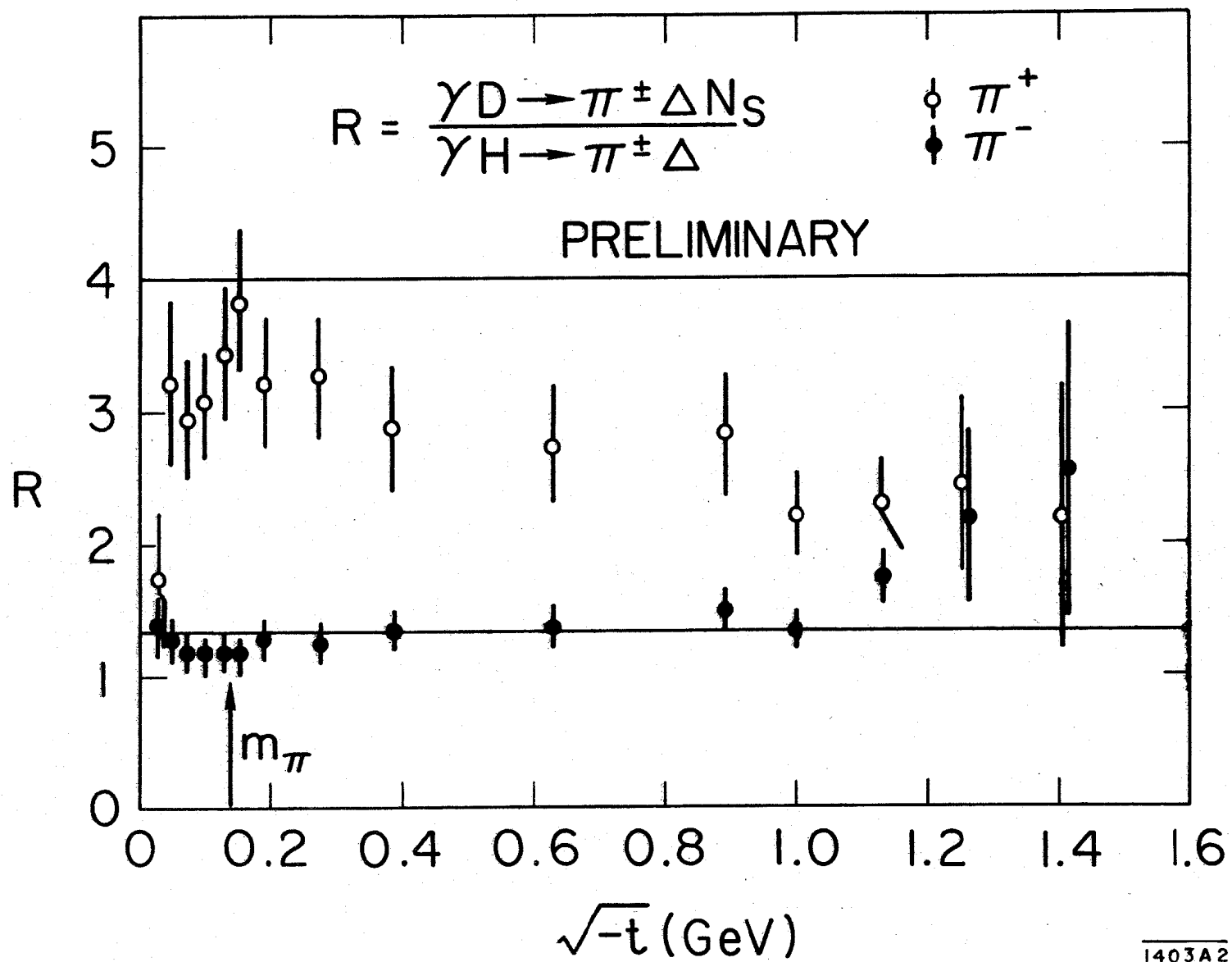


Fig. 32

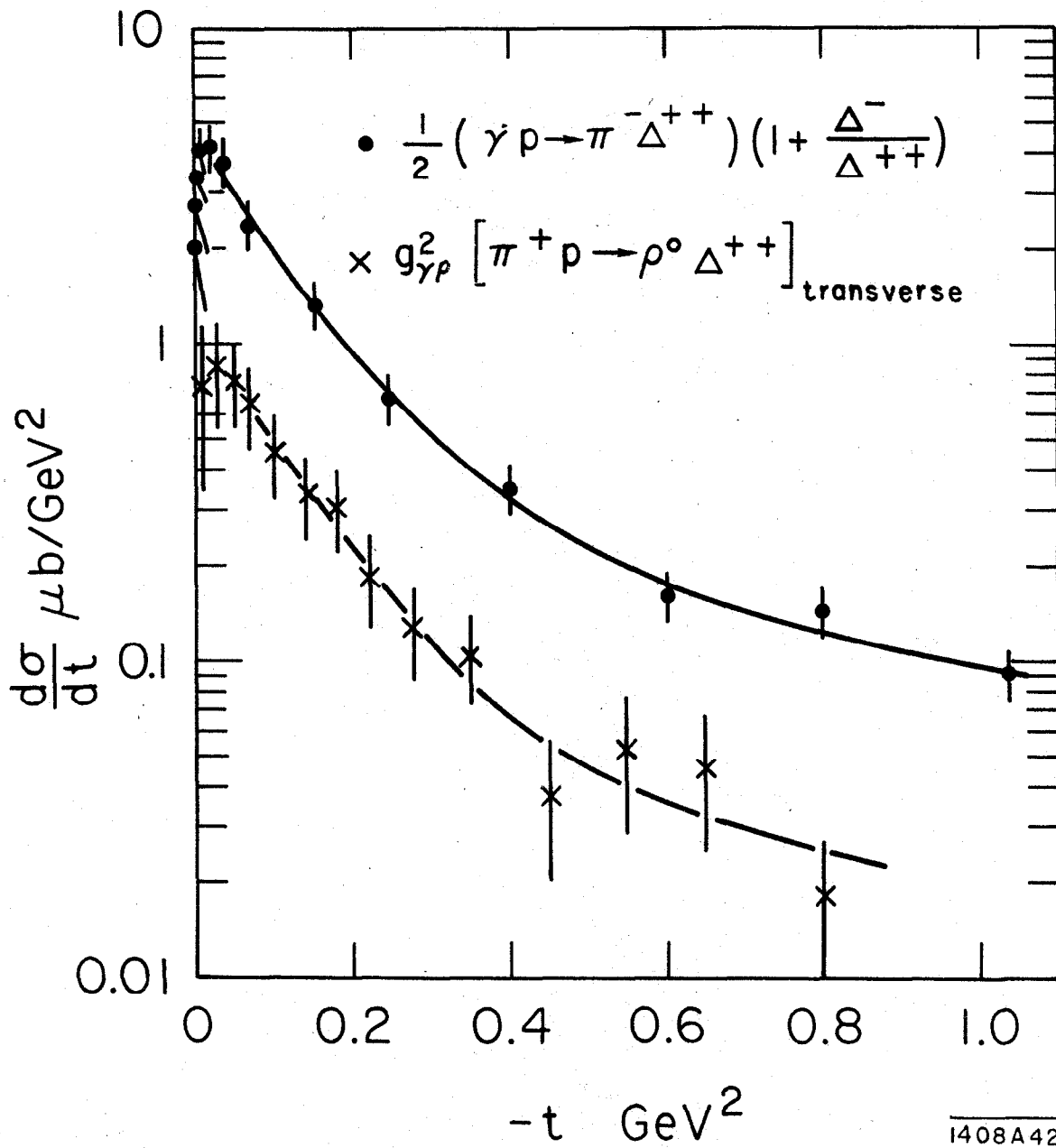
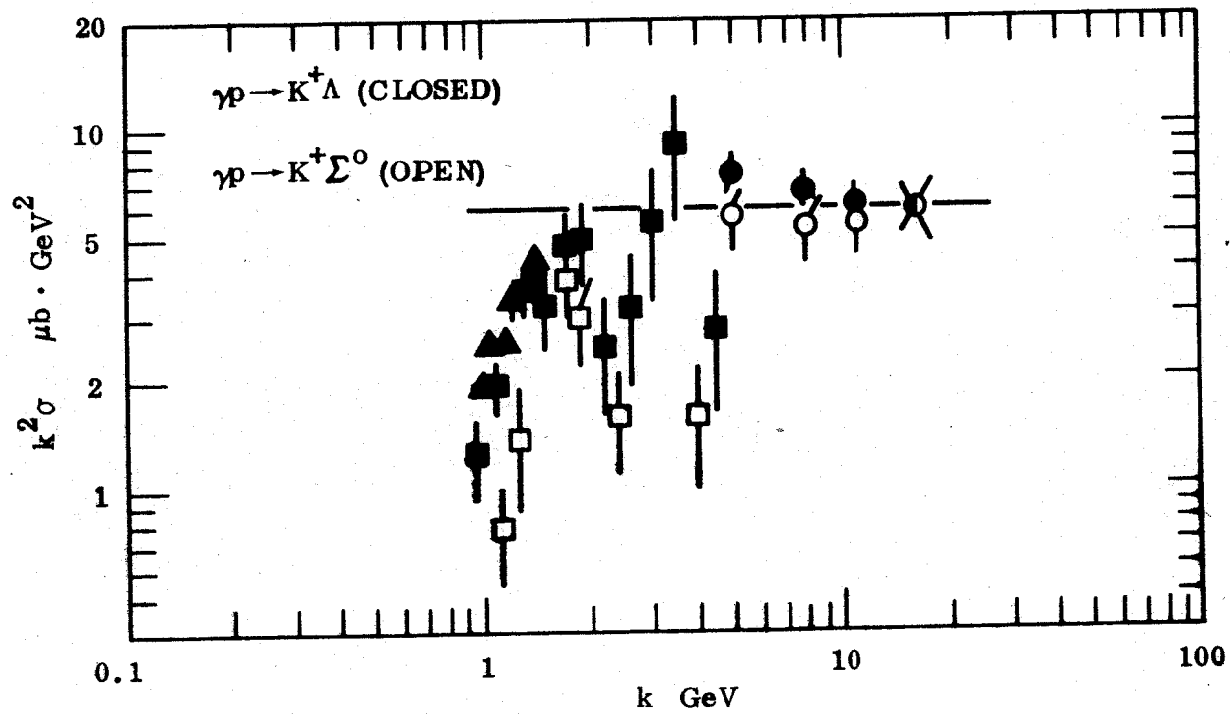
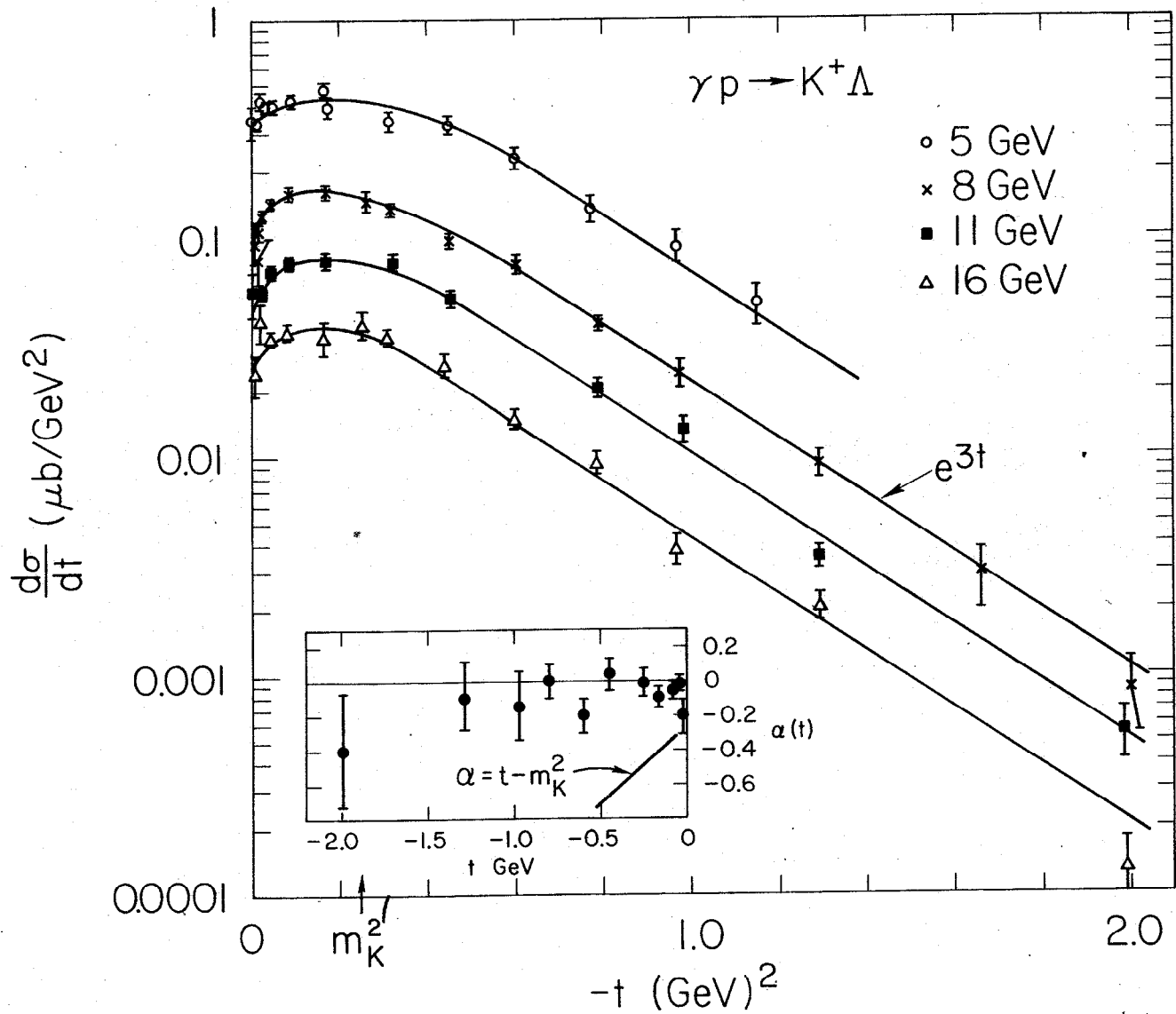


Fig. 33



1408A24

Fig. 34



1408 A52

Fig. 35

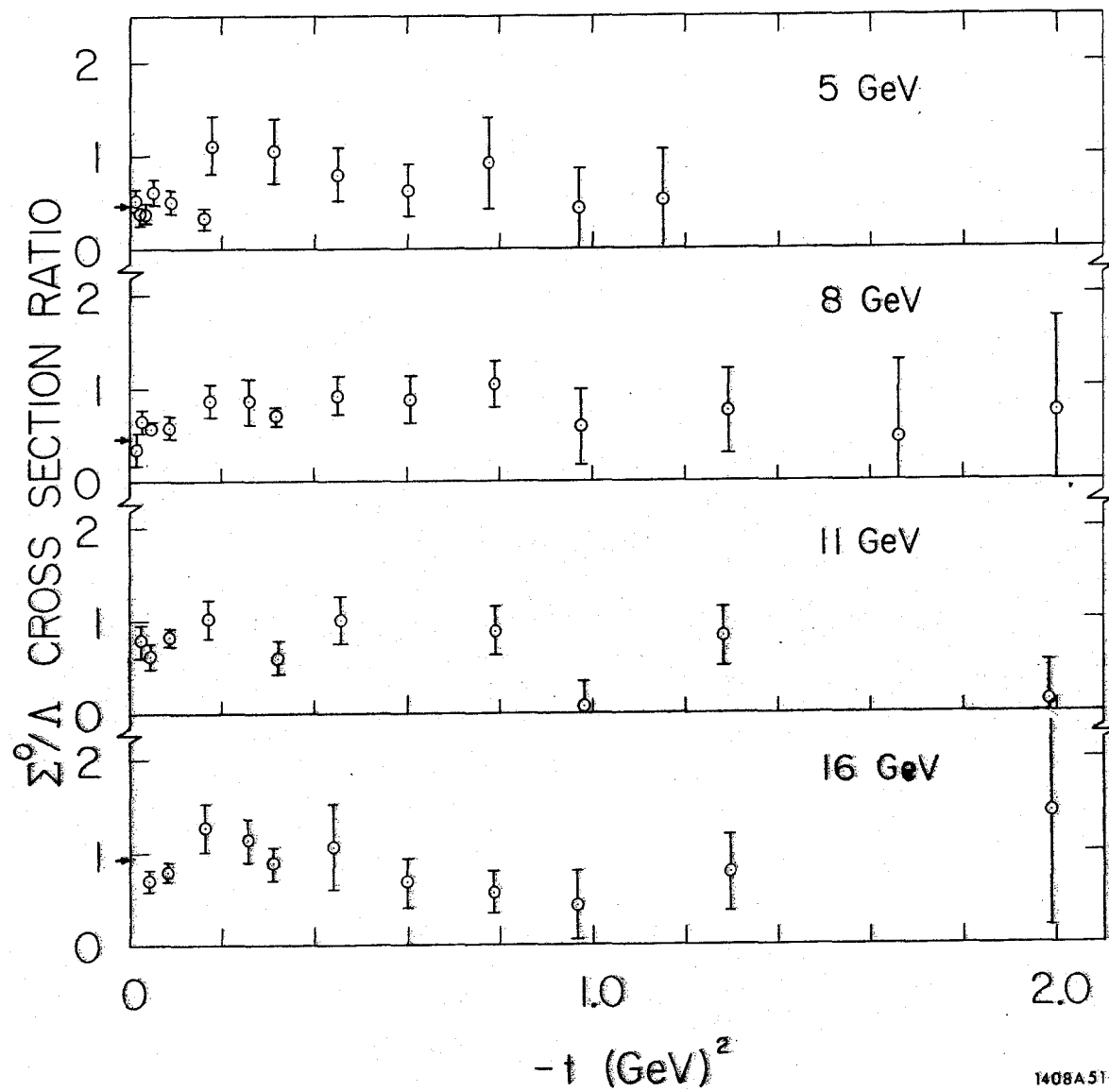


Fig. 36

1408A51

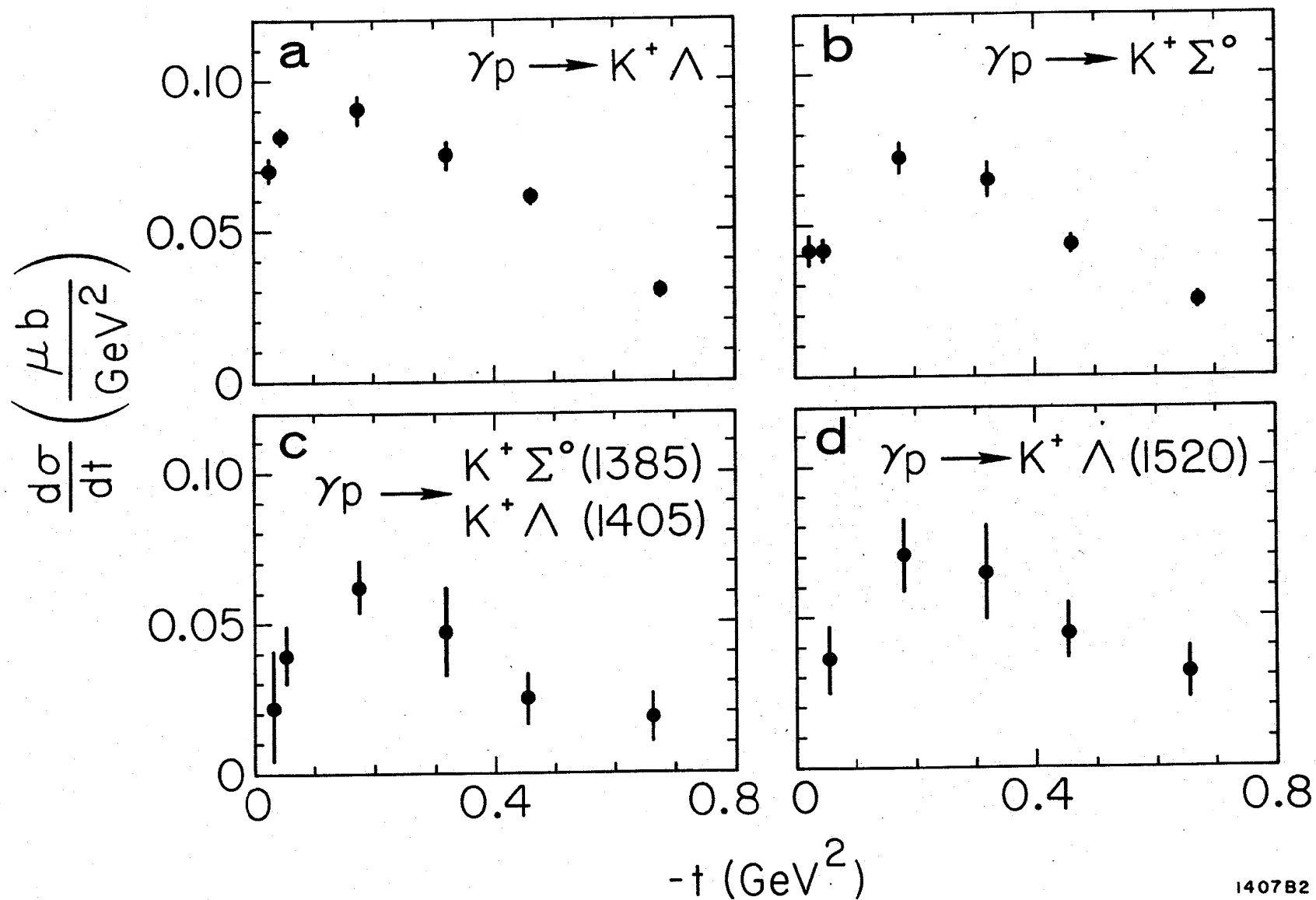
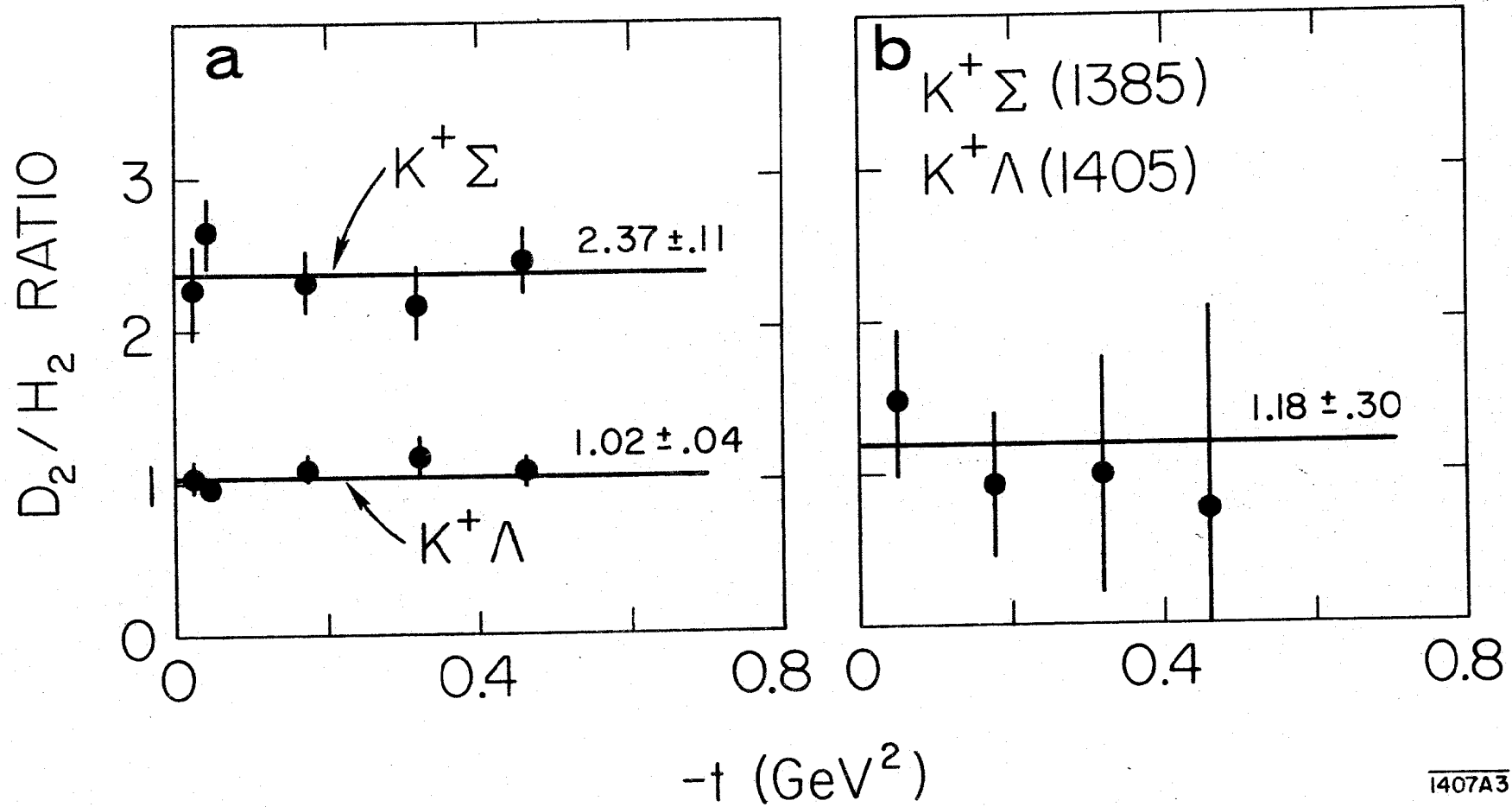


Fig. 37



1407A3

Fig. 38

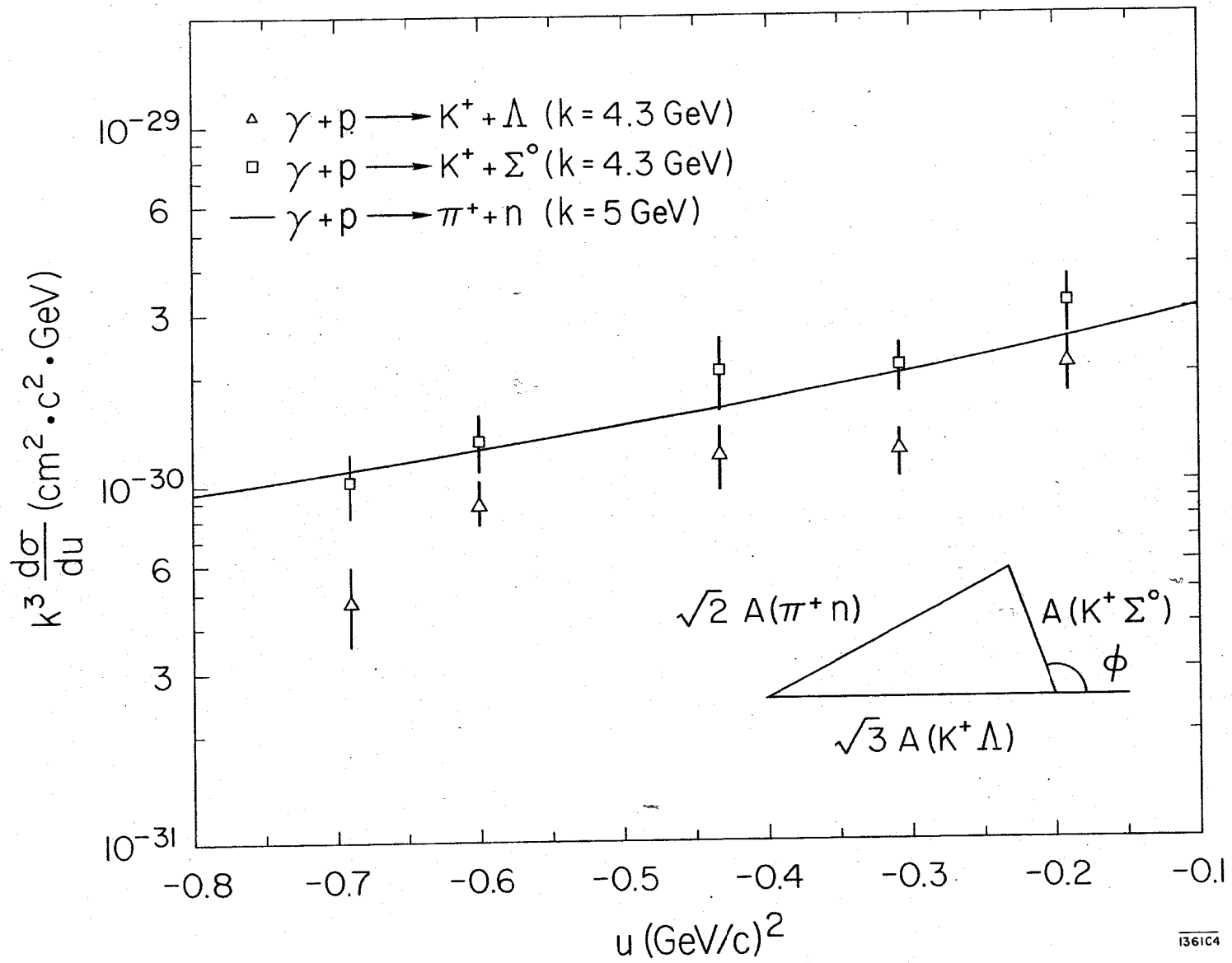


Fig. 39

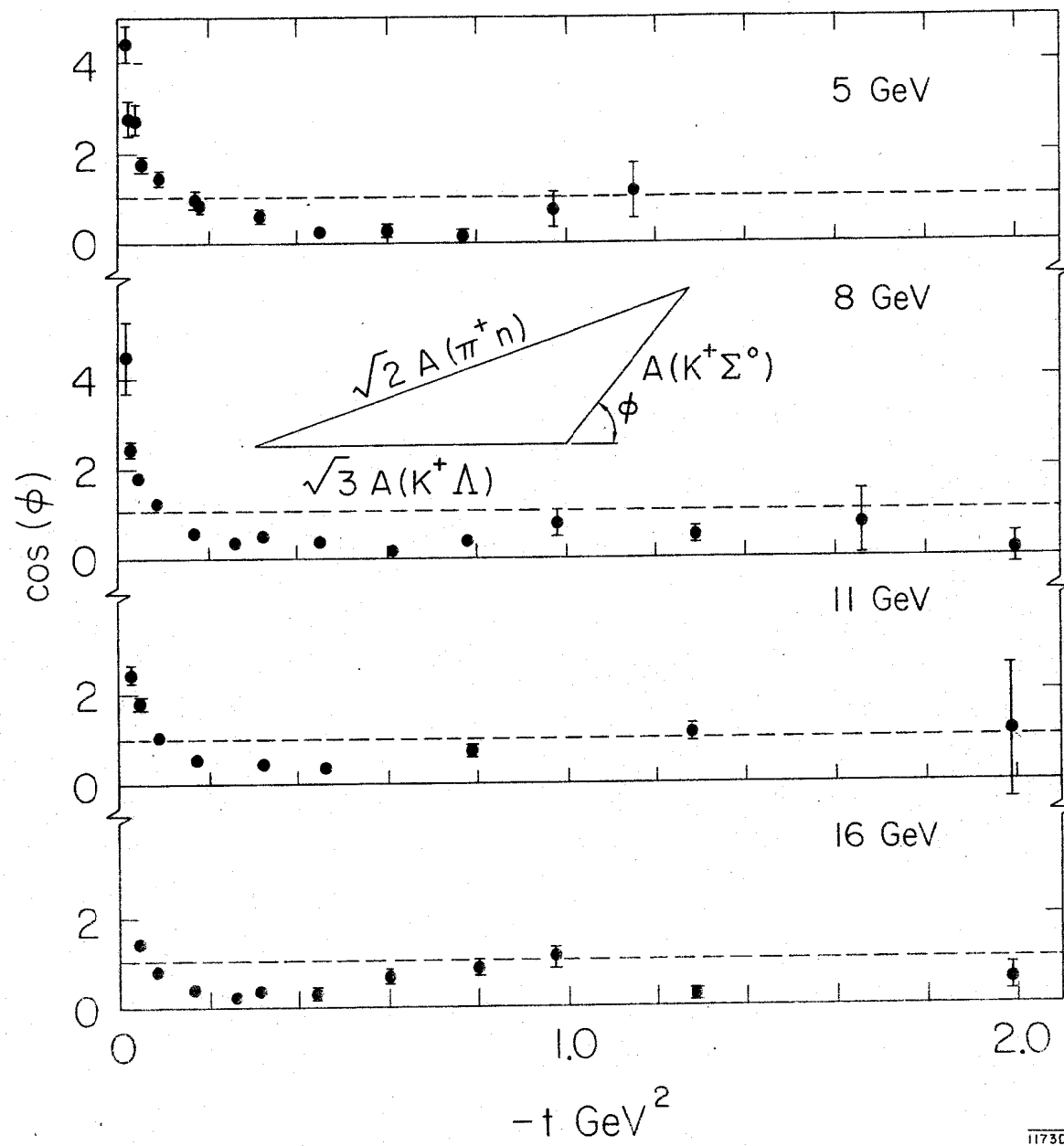
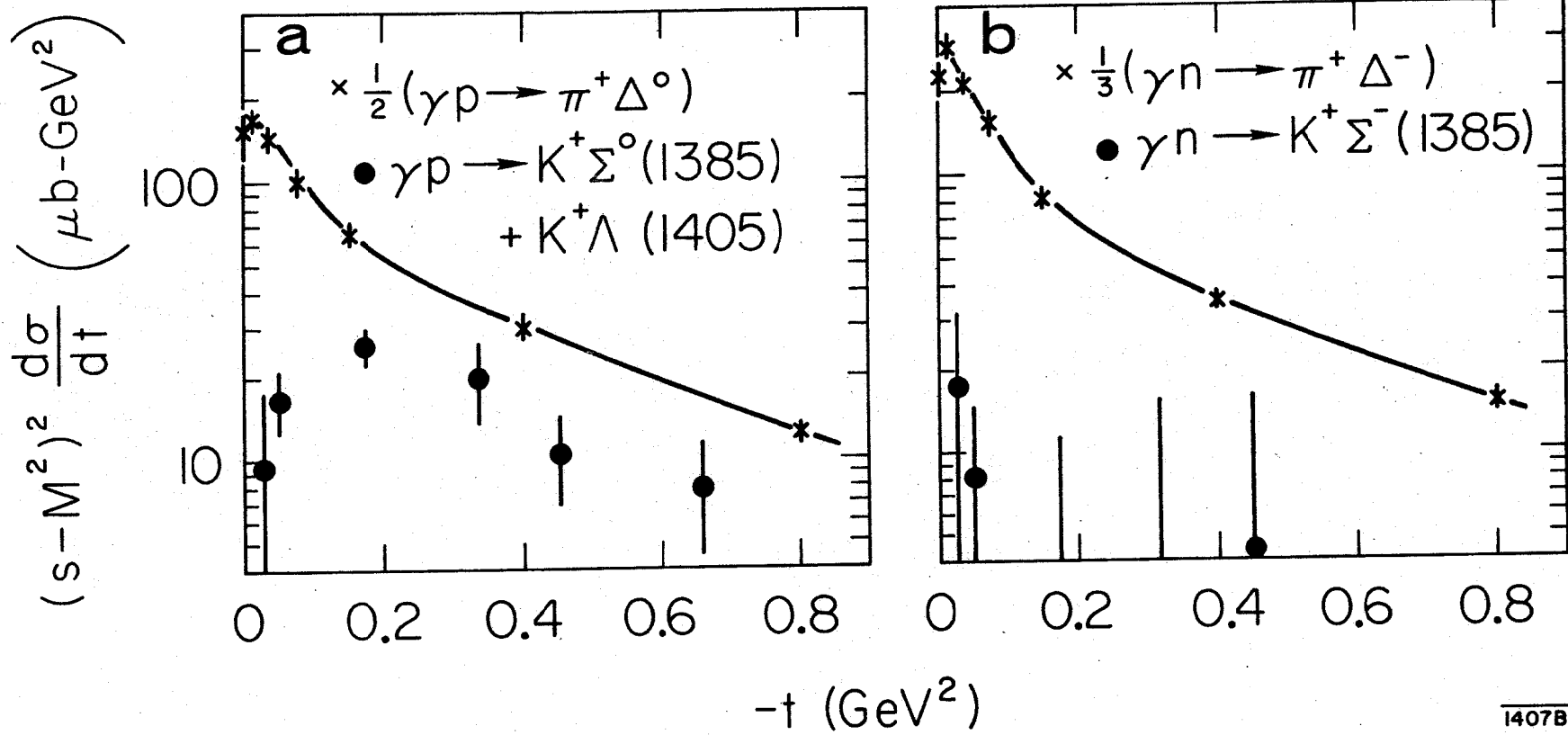


Fig. 40



1407B4

Fig. 41

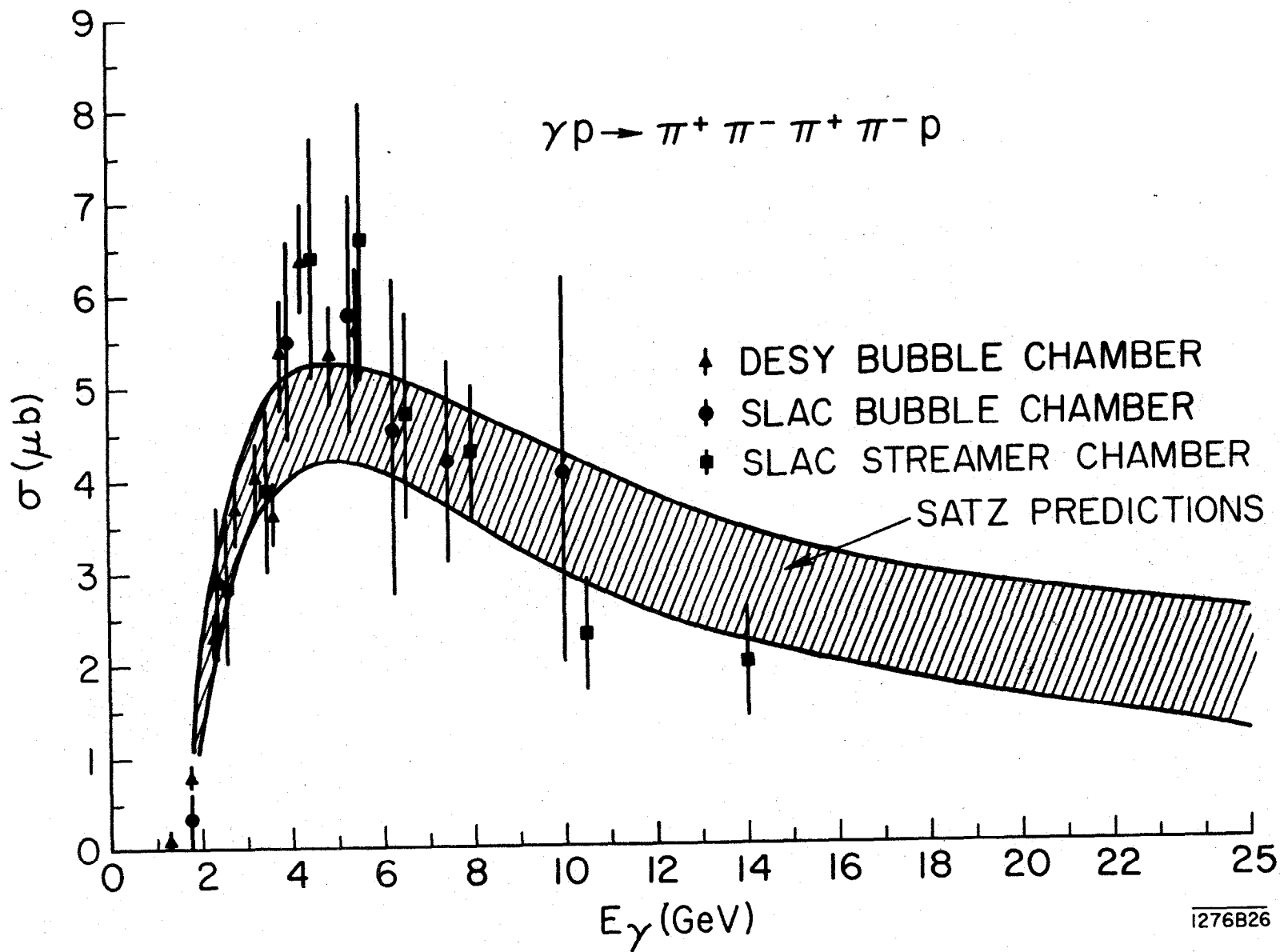
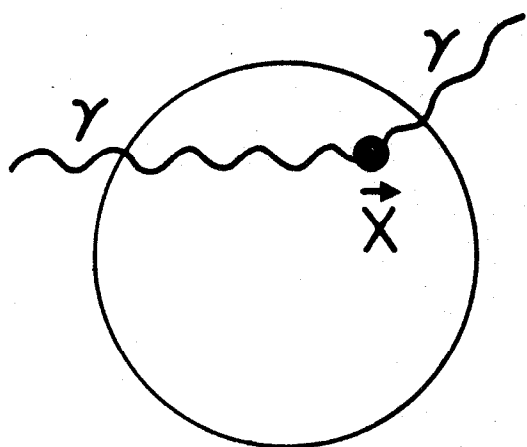
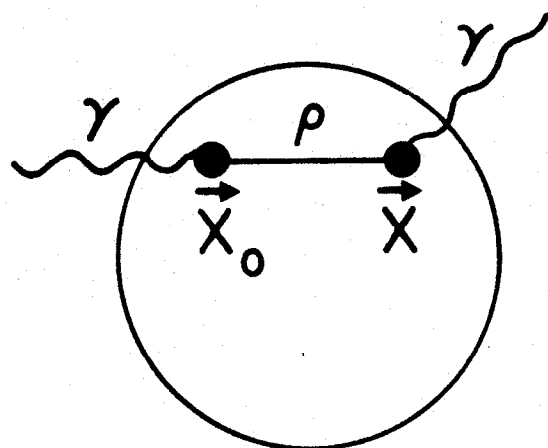


Fig. 42



ONE-STEP
(a)



TWO-STEP
(b)

1408A46

Fig. 43

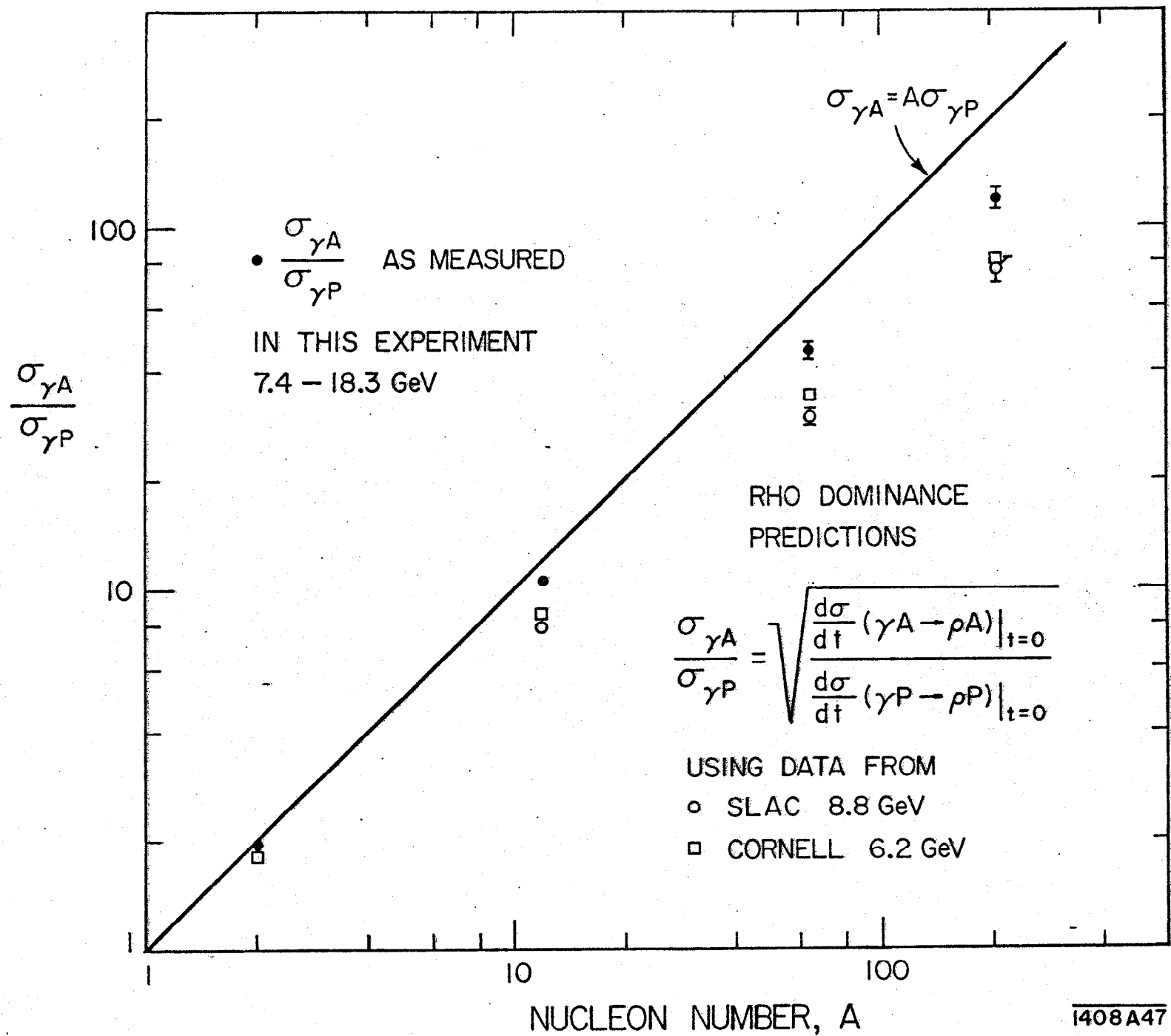
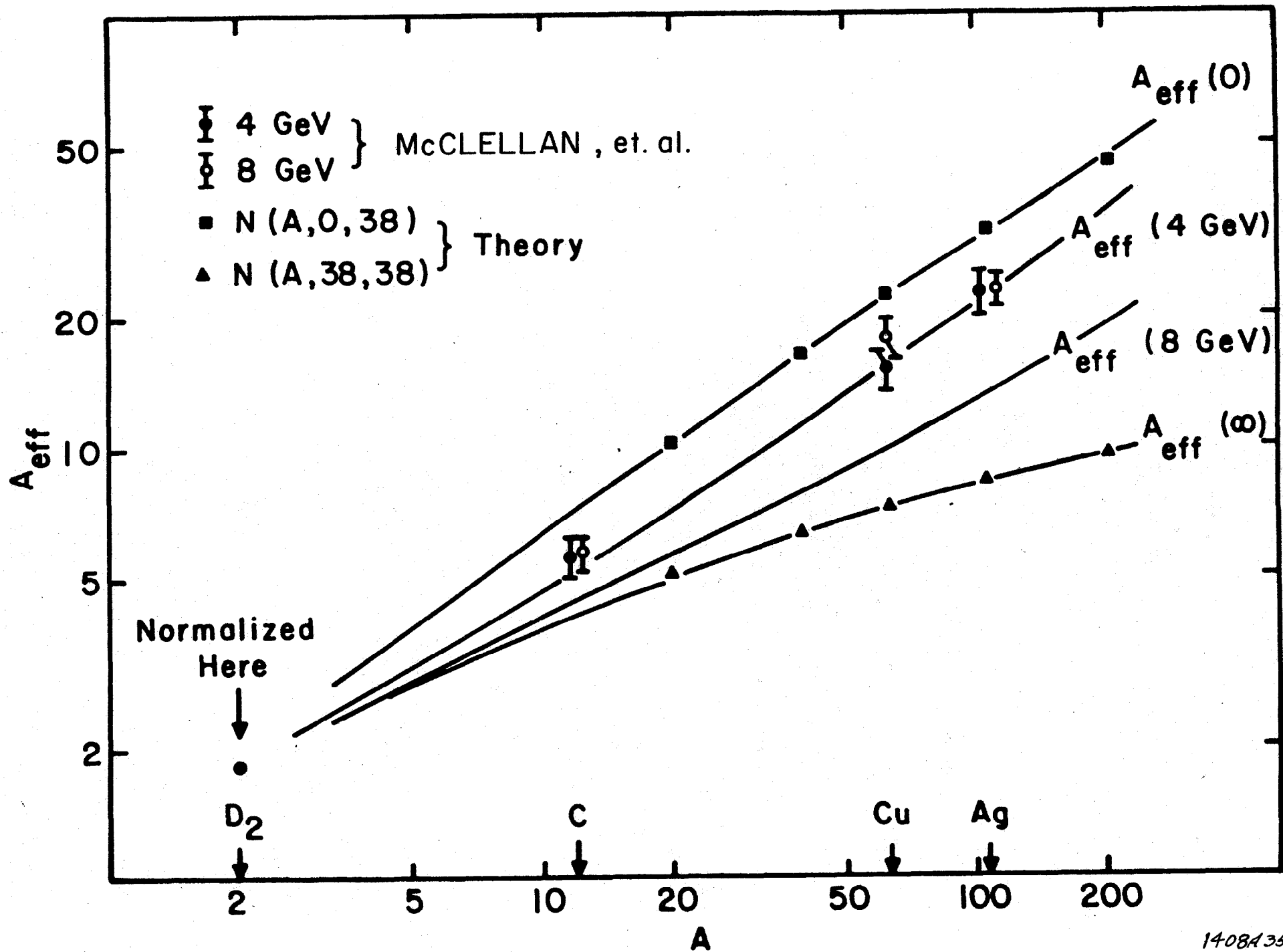
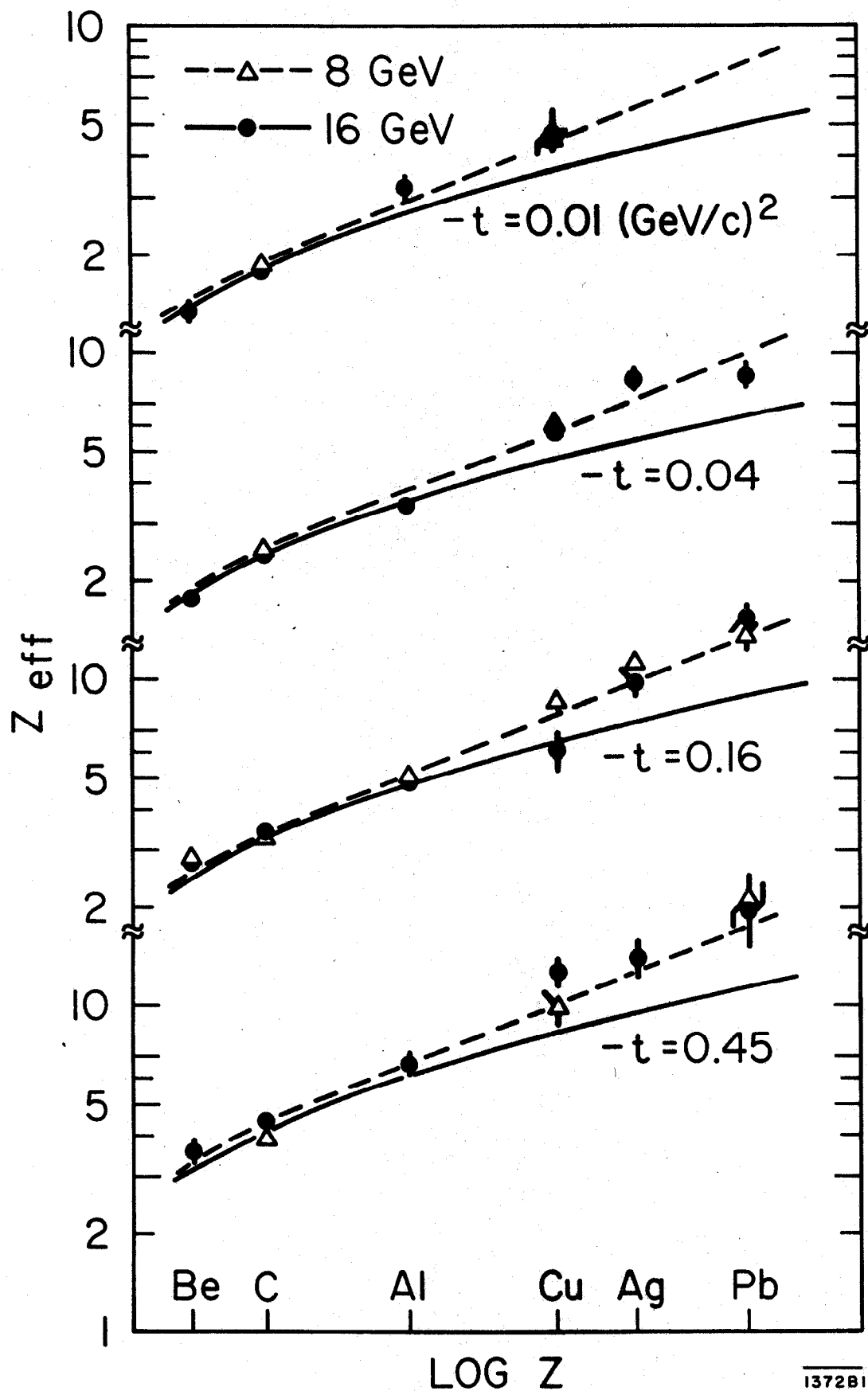


Fig. 44



1408A35

Fig. 45



LOG Z

1372B1

Fig. 46

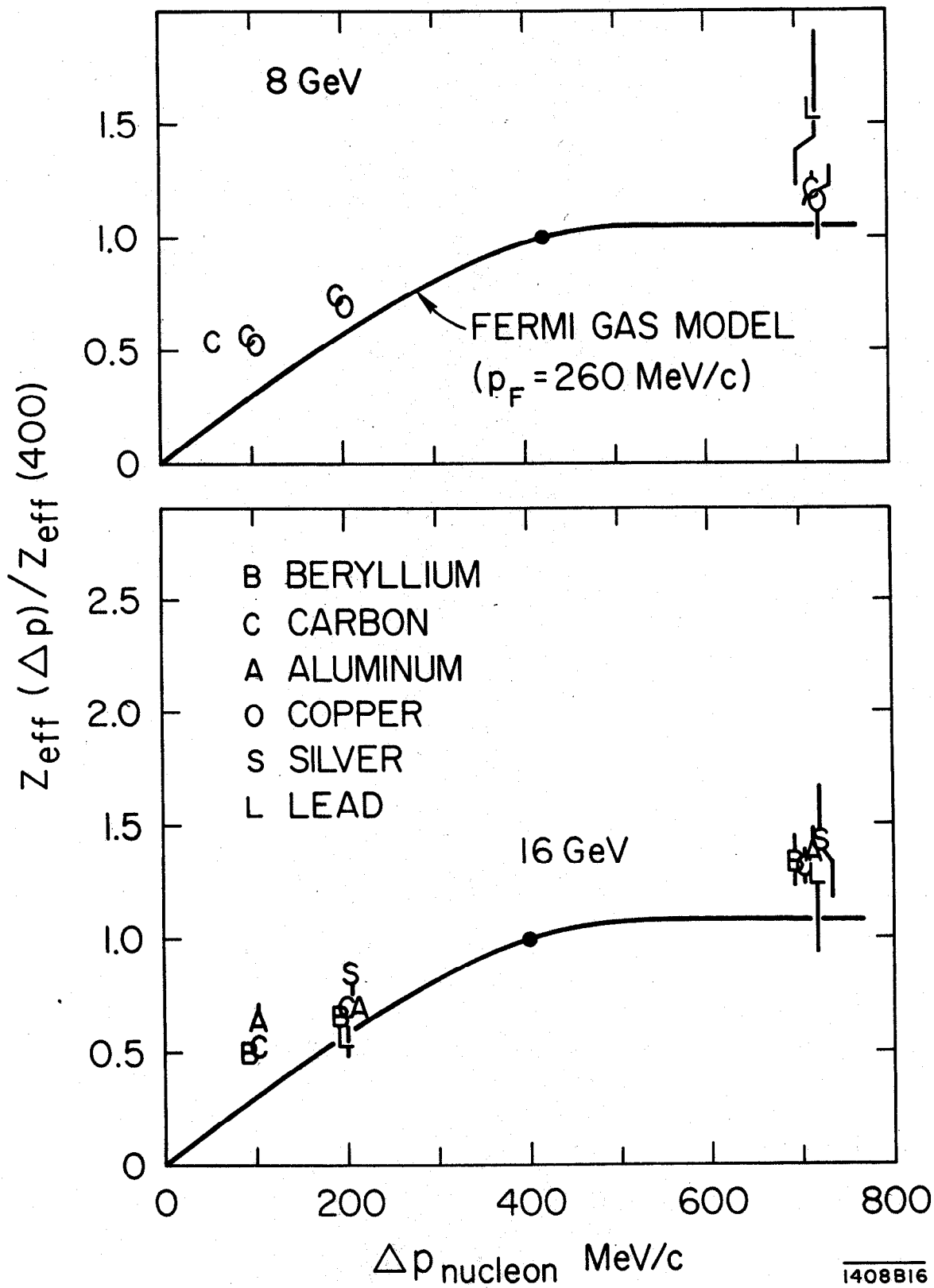


Fig. 47